Recent Advances in the Liquid-Phase Syntheses of Inorganic Nanoparticles

Brian L. Cushing,* Vladimir L. Kolesnichenko, and Charles J. O'Connor*

Advanced Materials Research Institute, University of New Orleans, New Orleans, Louisiana 70148-2820

Received October 28, 2003

Contents

* To whom correspondence should be addressed. B.L.C.: (504) 280-1385 (phone); (504) 280-3185 (fax); bcushing@uno.edu (e-mail). C.J.O.: (504) 280-6846 (phone); (504) 280−3185 (fax); coconnor@uno.edu (e-mail).

1. Introduction

The development of novel materials is a fundamental focal point of chemical research; and this interest is mandated by advancements in all areas of industry and technology. A good example of the synergism between scientific discovery and technological development is the electronics industry, where discoveries of new semiconducting materials resulted in the evolution from vacuum tubes to diodes and transistors, and eventually to miniature chips. The progression of this technology led to the development

10.1021/cr030027b CCC: $48.50
Published on Web 08/20/2004

Brian L. Cushing received his B.S. in Chemistry from the University of West Florida (1994) and his Ph.D. in Inorganic Chemistry from the University of New Orleans (1999). He previously held a postdoctoral research position at the University of Texas at Austin and is currently a Research Specialist at the Advanced Materials Research Institute at the University of New Orleans. His current research interests include interfacing magnetic nanoparticles with biologically active compounds.

Vladimir L. Kolesnichenko, born in Kiev (Kyiv), Ukraine, received his M.S. in Chemistry from Kiev State University and his Ph.D. in Inorganic Chemistry from the Palladin Institute of General and Inorganic Chemistry (Kiev, Ukraine). His research interests include transition metal cluster coordination chemistry and synthesis of functional nanocrystalline materials. He currently develops synthetic methodologies for magnetic nanoparticles and investigates their surface reactivities for different applications.

of smaller and smaller electronic elements, resulting in chips with a higher density of circuitry and greater computing power. The size of these electronic circuits and magnetic memory elements is approaching nanometer dimensions, and as this realm is entered, scientists have found that properties of materials with nanometer dimensions can differ from those of the bulk material.

Through the National Nanotechnology Initiative (http://www.nano.gov), a national strategic research plan focuses on the development of new materials at the atomic, molecular, or macromolecular levels, on the length scale of approximately 1−100 nm. These research efforts are expected to provide a fundamental understanding of phenomena and materials at the nanoscale and to create and use structures, devices, and systems that have novel properties and functions due to their small and/or intermediate size, typically under 100 nm.

Any researcher entering the nanoscience arena should read Feynman's 1959 "There's Plenty of Room at the Bottom" speech,[1] if only for its historical relevance. Several articles outlining the current applications and speculating on the future impact of nanotechnology are available.[2−4] Discipline-specific papers hypothesizing on the impact of nanotechnology in fields ranging from automotive technology[5] to medicine[6−8] to earth science[9] to chemistry[10−12] are also common.

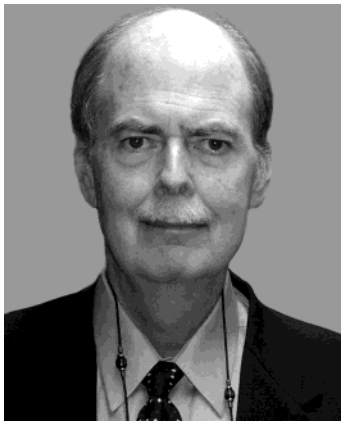

Dr. Charles J. O'Connor is Distinguished Professor of Chemistry and the Director of the Advanced Materials Research Institute (AMRI) at the University of New Orleans. He has been at the University of New Orleans for 25 years following his Ph.D. in Inorganic Chemistry from the University of Illinois in Chicago in 1976 and three years as an Instructor at the University of Virginia. Dr. O'Connor has over 300 publications in refereed scientific journals and has active research programs in solid state nanomaterials research, especially on magnetic nanomaterials.

While articles offering highly detailed reviews of specific synthesis techniques for preparing nanoparticles are commonplace, they are usually quite narrow in scope. For researchers entering the field, or for those already in the field but working with a very limited synthetic repertoire, developing a broad-based, working knowledge of the various state-of-the-art synthetic techniques constitutes an enormous undertaking, complicated in part by the sheer volume of available literature and the rapid pace of development. This survey is intended to address this gap by providing a relatively broad overview of synthetic techniques.

This survey focuses primarily on advances developed within the past five years in order to offer a critical review of state-of-the-art methodology. The various preparative techniques will be discussed first followed by a discussion of novel properties and applications that are likely to fuel research into the coming decades. This review will discuss nanoparticle syntheses by coprecipitation, sol-gel processing, microemulsions, hydrothermal/solvothermal methods, templated syntheses, and biomimetic syntheses. Where appropriate, considerable background material is presented to provide the uninitiated reader with sufficient understanding of the underlying principles and theories of the synthetic methodologies.

2. Nanoparticle Synthesis by Coprecipitation

Many of the earliest syntheses of nanoparticles were achieved by the coprecipitation of sparingly soluble products from aqueous solutions followed by thermal decomposition of those products to oxides.

Coprecipitation reactions involve the simultaneous occurrence of nucleation, growth, coarsening, and/or agglomeration processes. Due to the difficulties in isolating each process for independent study, the fundamental mechanisms of coprecipitation are still not thoroughly understood. The following discussion provides an overview of current coprecipitation theory.

2.1. Theory and Thermodynamics of Coprecipitation

The theory of coprecipitation is not a trivial subject. Numerous books[13,14] and review articles[15−19] cover the topic much more thoroughly than the discussion presented here. As a brief overview, coprecipitation reactions tend to exhibit the following characteristics: (i) The products of precipitation reactions are generally sparingly soluble species formed under conditions of high supersaturation. (ii) Such conditions dictate that nucleation will be a key step of the precipitation process and that a large number of small particles will be formed. (iii) Secondary processes, such as Ostwald ripening and aggregation, will dramatically affect the size, morphology, and properties of the products. (iv) The supersaturation conditions necessary to induce precipitation are usually the result of a chemical reaction. As such, any reaction conditions influencing the mixing process, such as rate of reactant addition and stirring rate, must be considered relevant to product size, morphology, and particle size distribution.

Although precipitation can be induced in any number of ways, chemical reactions are by far the most common method for the synthesis of nanoparticles. Generally, chemical reactions are chosen that result in products with low solubilities, such that the solution quickly reaches a supersaturated condition.

The chemical reactions used to induce coprecipitation can take numerous forms. For illustrative purposes, we consider the case of a simple addition reaction for the formation of an electrolyte, A_xB_y:

$$xA^{y+}(aq) + yB^{x-}(aq) \leftrightharpoons A_xB_y(s) \tag{1}$$

The equilibrium relationship between the product and its reactants is expressed as the solubility product constant, K_{sp}:

$$K_{sp} = (a_A)^x(a_B)^y \tag{2}$$

where a_A and a_B are the activities of cation A and anion B in aqueous solution. K_{sp} values (and therefore solubilities) tend to be very low for many hydroxides, carbonates, oxalates, and chalcogenides in aqueous solutions, and the precipitation reactions for several of these species are specifically discussed in later sections. Tables of K_{sp} values are widely available in reference volumes and in textbooks. Solubility data for compounds in solvents other than water are substantially more sparse.

Beyond simple addition/exchange reactions, precipitation can be induced by numerous other methods, such as chemical reduction, photoreduction, oxidation, and hydrolysis. Alternatively, precipitation can be induced by altering other parameters related to solubility, most notably temperature and concentration.

When the product contains only one or two elements (e.g. a metal, binary oxide, etc.), precipitation reactions are relatively straightforward. In more complicated ternary and quarternary systems, the process becomes more complex, as multiple species must be precipitated simultaneously (hence, the term *coprecipitation*).

Merely inducing precipitation of a compound, however, does not guarantee that the product will be nanoparticulate and/or monodispersed. The processes of nucleation and growth govern the particle size and morphology of products in precipitation reactions. When precipitation begins, numerous small crystallites initially form (nucleation), but they tend to quickly aggregate together to form larger, more thermodynamically stable particles (growth).

2.1.1. Nucleation

The key to any precipitation process is the degree of supersaturation, S, given by

$$S = \frac{a_A a_B}{K_{sp}} \tag{3}$$

where a_A and a_B are the activities of solutes A and B and K_{sp} is the solubility product constant, or alternatively by $S = C/C_{eq}$, where C and C_{eq} are the solute concentrations at saturation and at equilibrium, respectively. Indeed, the literature frequently refers to the difference in C and C_{eq}, $\Delta C = C - C_{eq}$, as the "driving force" for precipitation.[17]

As nucleation begins in a supersaturated solution, there exists an equilibrium critical radius, R^*:

$$R^* = \frac{\alpha}{\Delta C} \tag{4}$$

The term α is given by

$$\alpha = \left(\frac{2\sigma_{SL}}{kT \ln S}\right)\nu C_\infty \tag{5}$$

where σ_{SL} is the surface tension at the solid−liquid interface, ν is the atomic volume of solute, k is the Boltzmann constant, T is temperature, and S is the supersaturation as defined in eq 3. Nucleated particles with $R > R^*$ will continue to grow, while those with $R < R^*$ will dissolve. The activation energy of the cluster formation is given by[19]

$$\Delta G^* = \frac{4\pi\sigma_{SL}R^{*2}}{3} = \frac{16\pi\sigma_{SL}{}^3\nu^2}{3k^2T^2 \ln^2 S} \tag{6}$$

Thus, for stationary conditions, the homogeneous nucleation rate, R_N, is then

$$R_N = \left(\frac{dN}{dt}\right)\frac{1}{V} = A \exp\left[\frac{-(\Delta G^*)}{kT}\right] \tag{7}$$

where N is the number of nuclei formed per unit time per unit volume, V, and A is a pre-exponential factor typically ranging from 10^{25} to 10^{56} s^{-1} m^{-3}.

Combining eqs 6 and 7

$$R_N = A \exp\left(\frac{-16\pi {\sigma_{SL}}^3 \nu^2}{3k^3T^3 \ln^2 S}\right) \quad (8)$$

revealing that R_N is an exponential function of S. It follows that R_N remains negligible until a certain critical supersaturation, S^*, is reached.

2.1.2. Growth

The growth process of the precipitated particles is every bit as complicated as nucleation. The process can be either diffusion-limited or reaction-limited. Experimental evidence suggests, however, that the overwhelming majority of precipitation reactions are diffusion-limited. As such, concentration gradients and temperature become the predominant factors determining growth rate as new material is supplied to the particle surface via long-distance mass transfer. The balance of that material, as a monomer, crossing the surface of a spherical crystallite is given by

$$\frac{dr}{dt} = D\Omega\left(\frac{1}{\delta} + \frac{1}{r}\right)(C_b - C_i) \quad (9)$$

where r is the crystal radius, t is time, D is the diffusivity of the monomer, Ω is the molar volume, and δ_i is the thickness of the layer over which the concentration changes from C_b, the bulk solute concentration, to C_i, the solute concentration in the vicinity of the crystal surface.[20,21]

The relationship between monomer concentration and crystal size is established by the Gibbs−Thomson equation:[22]

$$C_e(r) \cong C_\infty\left(\frac{1 + 2\Omega\gamma}{R_G T R}\right) \quad (10)$$

where γ is the interfacial tension, R_G is the universal gas constant, T is the temperature, and C_∞ is a constant.

Finally, the relationship between the rate of growth, G, and the supersaturation ratio, S, can be expressed as a power-law equation:[17]

$$G = \frac{dL}{dt} = k_G S^g \quad (11)$$

where k_G is the growth rate constant and g is the growth order.

2.1.3. Ostwald Ripening

Ostwald ripening (also referred to as *coarsening*) is the phenomenon by which smaller particles are essentially consumed by larger particles during the growth process and is itself a topic of considerable investigation and postulation.[23−29] This behavior can, to some extent, be predicted by eq 10, which establishes that the solubility of particles increases with decreasing particle size. A detailed mathematical description of Ostwald ripening was first developed by Lifshitz and Slyozov and also independently by Wagner; their combined models are today referred to as *LSW theory*.[20,21] Some authors have taken exception to various approximations and assumptions of LSW theory, most notably the theory's failure to adequately account for cooperative effects between nuclei and the theory's assumption of a steady change in solute concentration with time.[30] Those authors' criticisms are justified, insofar as the assumptions in LSW theory have lead to frequent disagreements between theoretical and experimental results. Nonetheless, most competing or expanded theories of Ostwald ripening are still based on the original LSW model, and for the purposes of this discussion, the theory is adequate to make several important points concerning the precipitation of nanoparticles.

The mathematics involved in LSW theory are not rudimentary, and the reader is referred to the literature for details of the derivations. The principles of LSW theory, however, are summarized as follows:

(i) For a diffusion-controlled process, the average radius of the precipitate particles, $\bar{r}$, as a function of time, t, is[27]

$$\bar{r}(t) = \sqrt[3]{Kt} \quad (12)$$

where K is the coarsening rate, given by $4\alpha D/9$, and D is the diffusion current of solute across the grain boundary. Particle size is thus proportional to the cube-root of time.

(ii) During diffusion-controlled ripening, the number density N of nucleated particles decays as[27]

$$N(t) = \frac{0.22Q_0}{\bar{R}(t)^3} = \frac{0.22}{2D\alpha t} \quad (13)$$

where Q_0 is the total initial supersaturation. The number of solute particles therefore decreases as t^{-1} during ripening.

(iii) The size distribution of particles is given by

$$f(R,t) = \left[\frac{N(t)}{\bar{R}(t)}\right] p_0(\rho(t)) \quad (14)$$

where $\rho(t) \equiv R/\bar{R}(t)$ and $p_0(\rho)$ is a time-independent function of the absolute dimension of the grains, ρ.

Equations 1−14 provide several useful insights into the precipitation of nanoparticles. To produce nanoparticles, the nucleation process must be relatively fast while the growth process remains relatively slow. The formation of particles with a narrow size distribution further requires that the nuclei of all species present form simultaneously and without subsequent nucleation of smaller particles. Park et al. have recently published a study specifically addressing the coprecipitation of nanoparticles.[31]

2.1.4. Growth Termination and Nanoparticle Stabilization.

Due to the thermodynamics discussed in section 2.1 that favor the maximization of the surface/volume ratio, the agglomeration of small particles precipitated from solutions is practically inevitable in the absence of a stabilizer. For the purposes of this discussion, we are primarily interested in nanoparticles that can be prepared as stable colloids or isolated as powdered products. It should be pointed out, however, that agglomeration can occur at any

stage during synthesis; aggregation and agglomeration of particles during precipitation is itself a subject of investigation.[32]

There are generally two approaches to nanoparticle stabilization: (a) steric repulsion between particles caused by surfactants, polymers, or other organic species bound to the nanoparticles' surfaces (generically referred to as *capping ligands*) and (b) electrostatic (van der Waals) repulsions resulting from the chemisorption of charged species (usually, though not necessarily, H^+ or OH^-) at the surfaces. STM and TEM studies of Pd clusters capped with tetrabutylammonium bromide have shown that, at least in some cases, capping ligands indeed form monolayers at the particles' surfaces.[33]

The reader will find that steric stabilization is somewhat more common, probably due to issues concerning the chemical stability of the nanoparticles at very high or very low pH values, and the literature contains a dizzying variety of stabilizing agents used in nanoparticle syntheses. Consequently, our discussions of synthetic methods in section 2.2 include detailed accounts of the methods of nanoparticle stabilization where appropriate. A more thorough account of colloid stabilization is presented in section 8.

2.2. Coprecipitation Synthetic Methods

2.2.1. Synthesis of Metals from Aqueous Solutions

Due to their widespread application as catalysts,[34] metals precipitated from aqueous solutions continue to be a thoroughly investigated subject (the role of nanomaterials in catalysis is specifically discussed elsewhere[35,36]). The precipitation of metals from aqueous or nonaqueous solutions typically requires the chemical reduction of a metal cation. Reducing agents take many forms, the most common of which are gaseous H_2, solvated ABH_4 (A = alkali metal), hydrazine hydrate ($N_2H_4 \cdot H_2O$), and hydrazine dihydrochloride ($N_2H_4 \cdot 2HCl$).

For a typical reduction reaction of a transition metal cation,

$$M^{n+} + ne^- \rightarrow M^0 \qquad (15)$$

there must, of course, be a corresponding oxidation process of some species X, such that

$$X^m - ne^- \rightarrow X^{m-n} \qquad (16)$$

In order for the electron transfer to occur, the free energy change, ΔG, must be favorable. As a matter of convention, the favorability of oxidation−reduction processes is reflected in the standard electrode potential, $E°$, of the corresponding electrochemical half-reaction.

Since the $E°$ values of all reactions are stated relative to that of H_2, the half-reaction and $E°$ for H_2 are, by definition,

$$2H^+ + 2e^- \leftrightarrows H_2 \qquad E° = 0.00\ V \qquad (17)$$

at standard temperature and pressure (STP). Numerous metal ions can be reduced from aqueous solution to the metallic state in the presence of gaseous H_2 with proper adjustment of pH. These reactions are reviewed extensively elsewhere.[37,38]

The electrochemical half-reaction and $E°$ for borohydride ion are given by

$$B(OH)_3 + 7H^+ + 8e^- \leftrightarrows BH_4^- + 3H_2O \qquad E° = -0.481\ V \qquad (18)$$

Borohydride ions, however, should be employed judiciously, as they are known to reduce some cations to metal borides, particularly in aqueous systems.[39−42] The use of borohydride specifically for the precipitation of metal nanoparticles has recently been reviewed.[43]

Hydrazine hydrate is freely soluble in water, but since N_2H_4 is basic, the chemically active free-ion is normally represented as $N_2H_5^+$:

$$N_2H_4 \cdot H_2O \leftrightarrows N_2H_5^+ + OH^- \qquad (19)$$

or, in the case of hydrazine dihydrochloride,

$$N_2H_4 \cdot 2HCl \leftrightarrows N_2H_5^+ + H^+ + 2Cl^- \qquad (20)$$

The standard reduction potential for the hydrazinium ion, $N_2H_5^+$, is

$$N_2 + 5H^+ + 4e^- \leftrightarrows N_2H_5^+ \qquad E° = -0.23\ V \qquad (21)$$

In theory, the reduction of any metal with an $E°$ more positive than −0.481 V or −0.23 V, respectively, should be possible at room temperature, given a sufficient excess of reducing agent and proper control of pH. With respect to precipitating metals from solution, this would obviously include many first-row transition metal ions, such as Fe^{2+}, Fe^{3+}, Co^{2+}, Ni^{2+}, and Cu^{2+}, but also many second- and third-row transition metals, as well as most post-transition elements and a few nonmetals. A brief survey of nanoparticles prepared by reduction from aqueous solutions is provided in Table 1.

As a practical matter, the reduction of some metal ions with $E° > -0.481$ V is either not feasible or exceedingly difficult, but this is usually due to the instability of the cation in aqueous environments. However, in some instances, transition metal cations, such as Rh^{3+}, form stable complexes with hydrazine, thereby greatly limiting the available options for carrying out a reduction.[50] We should further emphasize that consideration of pH and relative redox potentials is, at best, only a guide for predicting which metals may or may not be prepared by this method.

The reduction of gold cations to gold metal is easily the single most thoroughly studied metal precipitation reaction. Gold cations, usually in the form of $AuCl_4^-$, are easily reduced by gaseous H_2

$$2AuCl_4^-(aq) + 3H_2(g) \leftrightarrows 2Au(s) + 6H^+(aq) + 8Cl^-(aq) \qquad (22)$$

although $AuCl_4^-$ is so strongly oxidizing ($E° = +1.002$ V) that weaker reducing agents such as carboxylates or alcohols are usually sufficient. Tan et al. have

Table 1. Representative Sampling of Nanoparticulate Metals Precipitated from Aqueous Solutions

metal	starting material	reducing agent	stabilizer[a]	notes	avg diam (nm)	ref
Co	$Co(OAc)_2$	$N_2H_4 \cdot H_2O$	none		~20	44
Ni	$NiCl_2$	$N_2H_4 \cdot H_2O$ + NaOH	CTAB	reaction performed at 60 °C	10−36	45
Ni	$Ni(OAc)_2$	$N_2H_4 \cdot H_2O$ + NaOH	none		(10−20) × (200−300) rods	44
Cu	$CuSO_4$	$N_2H_4 \cdot H_2O$	SDS		~35	44
Ag	$AgNO_3$	ascorbic acid	Daxad 19		15−26	46
Ag	$AgNO_3$	$NaBH_4$	TADDD		3−5	47
Pt	H_2PtCl_6	potassium bitartrate	TDPC	60 °C	<1.5	48
Au	$HAuCl_4$	trisodium citrate	S3MP	simultaneous addition of reductant and stabilizer	not stated	49

[a] CTAB = cetyltrimethylammonium bromide (see section 4); SDS = sodium dodecyl sulfate; Daxad 19 = sodium salt of high-molecular-weight naphthalene sulfonate formaldehyde condensate; TADDD = bis(11-trimethylammoniumdecanoylaminoethyl)-disulfide dibromide; TDPC = 3,3′-thiodipropionic acid; S3MP = sodium 3-mercaptopropionate

recently reported the synthesis of Au, Pt, Pd, and Ag nanoparticles by reduction with potassium bitartrate; all of the products formed stable colloids with the addition of a suitable stabilizing agent.[48]

In many cases, an organic capping agent that is normally used to prevent agglomeration can also serve as the reducing agent. This is the case in the well-known Turkevich process for the synthesis of gold colloids.[51] In their 1951 paper, Turkevich et al. described a synthetic method for colloidal gold prepared by boiling a mixture of dilute $HAuCl_4$ and sodium citrate.[52] This method is still widely used today and is the basis of a recently published laboratory experiment on Au monolayer self-assembly designed for undergraduate students.[53]

Normally, if thiol stabilizing agents are used, the reduction of $AuCl_4^-$ in aqueous solution must be performed with borohydride or similar reducing agents because the complexes formed between $AuCl_4^-$ and thiols are too stable to be reduced by citrate or other weak reducing agents. Yonezawa et al., however, have demonstrated that reduction of $AuCl_4^-$ with citrate in the presence of a thiol is possible, if the thiol and citrate are added to the gold solution simultaneously.[49] Gold colloids with 2−10 nm dimensions are achievable with this method, and narrow size distributions are possible at high [thiol]/[Au] ratios, as evidenced in Figure 1.

The reduction of metals with highly negative reduction potentials requires reducing agents with considerably stronger reducing ability than that afforded by most amines, hydroxycarboxylic acids, or alcohols. The reduction of ions such as Ni^{2+} ($E° = -0.257$ V), Co^{2+} ($E° = -0.28$ V), and Fe^{2+} ($E° = -0.447$ V) is therefore typically performed with borohydride salts (eq 18).

Silver can similarly be reduced with borohydride from aqueous Ag^+ in a solution containing bis(11-trimethylammoniumdecanoylaminoethyl)disulfide dibromide (TADDD), producing monodisperse nanoparticles as small as 3.3 nm.[47] In this case, the excess borohydride reduces the disulfide to a thiol that serves as a capping ligand. The particles are easily redispersed into stable colloids in slightly acidified water.

While nanoparticulate Fe and Cu are easily reduced individually with borohydride, Chow et al. prepared *fcc* $Fe_{1-x}Cu_x$ ($0.6 \leq x \leq 1$) alloys with 30−45 nm particle sizes by reduction of aqueous $FeCl_2$ + $CuCl_2$ mixtures.[54] The result is noteworthy in that

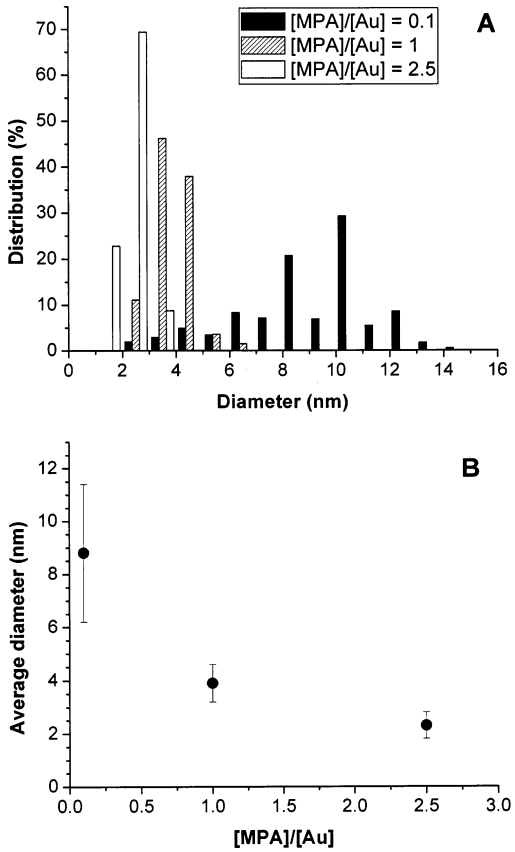

Figure 1. (A) Size distribution of Au nanoparticles capped with mercaptopropionate (MPA) at various [MPA]/[Au] ratios and (B) the relationship between average particle diameter and [MPA]/[Au], where the bars represent the standard deviations of the particle sizes. (Adapted with permission from ref 49. Copyright 1997 Chemical Society of Japan.)

Fe and Cu are not normally miscible in the equilibrium state. The formation of the alloy may, however, be facilitated by the incorporation of boron due to formation of Fe_2B, as is known to be the case with $Fe_{1-x}Co_x$ alloys prepared by reduction with KBH_4 in aqueous solution.[55]

Harris et al. heat-treated mixtures of CuO + CoO precipitated from aqueous solution to produce $Cu_{80}Co_{20}$ alloys. The samples were heated under flowing H_2 at temperatures ranging from 200 to 650 °C, resulting in alloy particles with 10−20 nm particle sizes with a broad size distribution. Heat treatment at 650 °C or above resulted in decomposition to the composite metals.[56]

2.2.2. Precipitation of Metals by Reduction from Nonaqueous Solutions

The stabilization of Au nanoparticles against agglomeration in aqueous solutions by capping ligands such as citrate is a well-documented process. Brust et al., however, reported the synthesis of alkanethiol-stabilized colloidal Au nanoparticles that are stable almost indefinitely in nonpolar solvents.[57,58] Moreover, the particles exhibited the rather unusual ability to be fully redispersed into colloids after being isolated as dry powders.

The synthesis method of Brust et al. is noteworthy in that a two-phase reaction mixture was used to carry out the gold reduction, similar to the technique of Faraday. Starting from an aqueous solution of $AuCl_4^-$, the tetrachloroaurate ions were transferred to an organic phase by vigorously mixing the aqueous solution with a solution of tetraoctylammonium bromide (TOAB) dissolved in toluene (TOAB is a well-known phase-transfer catalyst). After adding dodecanethiol to the organic phase, an aqueous solution of $NaBH_4$ was subsequently introduced into the mixture with rapid stirring. Colloidal gold (1−3 nm) was formed in the organic phase and subsequently isolated by vacuum evaporation or by precipitation with methanol. The authors found that once the products were isolated as dry powders, stable colloidal suspensions could be reconstituted in any number of nonpolar or weakly polar solvents, including toluene, pentane, and chloroform, but not alcohol or water. The authors further determined by IR and X-ray photoelectron spectroscopy (XPS) that the powder, even after washing, contains thiolate and that the gold is present as Au^0, which suggests that the thiol binds as RSH as opposed to RS^-.

The results of Brust et al. triggered a flurry of research into the thiol-based stabilization of colloidal nanoparticles. Among the more significant results from these investigations, numerous new thiol-, amine-, silane-, phosphine-, and disulfide-based capping ligands have been identified,[59−66] and several techniques have emerged for the exchange of capping ligands.[67−70] This effectively allows the functionality and chemical properties of the ligand shells to be tuned.[71,72] Stoeva et al. have modified Brust's method to allow the gram-scale synthesis of thiol-stabilized colloidal Au particles.[73]

Au nanoparticles reduced with borohydride and capped with mercaptosuccinic acid (MSA), $HOOCCH_2$-$CH(SH)COOH$, as reported by Chen et al., exhibit the additional benefit of being dispersable in water if the capped nanoparticles are precipitated as a sodium salt.[74] The sizes of the nanoparticles were controllable within the 1−3 nm range by variation of the [MSA]/[Au] ratio. The method was later adapted to the synthesis of 1.4−5.7 nm metallic Ag.[75]

Han et al. developed a method for reducing gold in nonaqueous solutions in which the solvent, in this case formamide ($HCONH_2$), also served as the reducing agent.[76] The reaction mechanism appears to involve a two-step process of ligand-exchange followed by reduction, and the reaction will not proceed in the presence of oxygen. The 30 nm particles were stabilized by poly(vinylpyrrolidone) (PVP) and exhibited a narrow size distribution. It is not clear, however, as to whether the particle size can be controlled, as the [PVP]/[Au] ratio did not appear to influence the particle size.

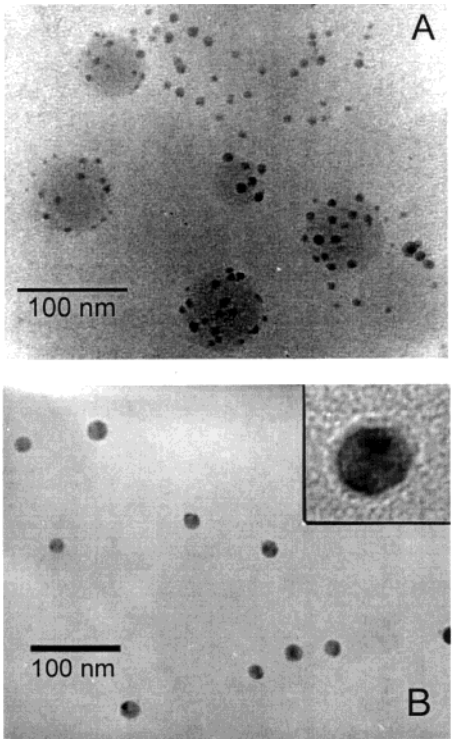

Figure 2. TEM image of Ag nanoparticles prepared in DMF (A) at room temperature and (B) under reflux conditions. Both samples are capped with 3-(aminopropyl)-trimethoxy silane that sometimes forms a thin silica shell, as demonstrated by the inset in image B. (Reprinted with permission from ref 77. Copyright 1999 American Chemical Society.)

In a similar reaction, silver nanoparticles have been prepared by reduction of $AgNO_3$ or $AgClO_4$ by *N*,*N*-dimethylformamide (DMF), where 3-(aminopropyl)trimethoxysilane served as the stabilizing agent.[77] The reaction probably involves the oxidation of DMF to a carboxylic acid:

$$HCONMe_2 + 2Ag^+ + H_2O \leftrightharpoons 2Ag^0 + Me_2NCOOH + 2H^+ \quad (23)$$

In this case, the size of the silver nanoparticles could be varied from 6 to 20 nm by adjustment of the temperature as well as the [DMF]/[Ag] molar ratio. The silane-based stabilizing agent is susceptible to hydrolysis and condensation, particularly at elevated temperatures and under acidic conditions, and some of the Ag particles exhibited thin SiO_2 coatings, although this apparently did not lead to agglomeration (Figure 2).

As previously mentioned, the ability of alcohols such as ethanol to act as reducing agents for strongly oxidizing cations is well-known. Particle aggregation in such reactions can, however, be problematic, even in the presence of stabilizing agents. Reactions carried out in polyalcohols such as ethylene glycol or 1,2-propanediol tend to yield more monodispersed products. Such polyols effectively act as bidentate chelating

agents for the solvated metal cations and, in some cases, also serve as reducing and/or stabilizing agents once the metal nanoparticles are precipitated. Viau et al., for example, prepared monodispersed 4 nm Ru particles by reduction of $RuCl_3$ in various polyols; the polyols served as the reducing agents, and the products were stabilized with dodecanethiol.[78] A similar technique has been used to successfully reduce Ni^{2+} to Ni^0 with hydrazine hydrate (eq 19) in ethylene glycol solution, resulting in monodispersed 9 nm particles.[79] By eq 21, hydrazinium ions do not normally exhibit sufficient reducing ability to reduce Ni^{2+} to Ni^0. In this case, excess NaOH was added to the reaction mixture, such that

$$2Ni^{2+} + N_2H_5^+ + 5OH^- \leftrightarrows 2Ni^0 + N_2 + 5H_2O \quad (24)$$

The elevated pH, along with the 60 °C reaction temperature, greatly enhanced the reducing ability of $N_2H_5^+$. This underscores the point that standard reduction potentials, which are, by definition, taken at room temperature and in aqueous solutions, should only be used as guides.

Similarly, Hou and Gao recently reported the synthesis of monodispersed 3.7 nm Ni particles by reducing a $Ni(acac)_2$ (acac = acetylacetonate) solution with $NaBH_4$ at 100 °C where hexadecylamine served as both stabilizer and solvent.[80] The particles could be redispersed in nonpolar solvents and did not exhibit indications of oxidation upon air exposure.

In cases where the $M^{n+} + ne^- \leftrightarrows M^0$ reduction necessary to produce metallic nanoparticles exhibits a substantially negative $E°$, the use of an aqueous solvent is precluded because the reducing agents capable of supplying electrons to the metal will reduce water, given that

$$2H_2O + 2e^- \leftrightarrows H_2 + 2OH^- \qquad E° = -0.8277\ V \quad (25)$$

In these cases, solvents that are more stable must be employed.

Thermodynamically, the strongest reducing agent possible in solution is the solvated electron (e_s^-), followed closely by the alkali-metal anion (A^-). Either species may be generated by the dissolution of an alkali metal in an aprotic solvent such as dimethyl ether or tetrahydrofuran (THF) in the presence of an alkali-metal complexing agent such as 15-crown-5 ether:

$$2A^0 + (15\text{-crown-}5) \leftrightarrows A^+(15\text{-crown-}5)A^- \quad (26)$$

The active reducing agent produced by eq 26 is commonly referred to as an *alkalide*. Given a sufficient excess of complexing agent,

$$A^0 + 2(15\text{-crown-}5) \leftrightarrows A^+(15\text{-crown-}5)_2e_s^- \quad (27)$$

and such products are called *electrides*. The above equilibrium is forced to the right by the extremely strong complex formed between the alkalis and chelate ethers.[81] Both electride and alkalide solutions, while powerful reducing agents, are not thermally stable and decompose in air; reactions involving such reagents must therefore be carried out at low temperatures and under inert atmosphere.

Dye et al. reported as early as 1991 the synthesis of numerous metal nanoparticles from alkalide and electride solutions, including Au, Pt, Cu, Te, Ni, Fe, Zn, Ga, Si, Mo, W, In, Sn, Sb, and Ti, as well as Au−Cu, Au−Zn, Cu−Te, and Zn−Te alloys.[82,83] The reactions were typically carried out at −50 °C and resulted in 3−15 nm products. With the exception of Au, Pt, Cu, and Te, however, all of the products exhibited strong tendencies to oxidize on washing with methanol, even under inert atmosphere. More recently, Kirkpatrick et al. used lithium metal dissolved in naphthalene for the synthesis of nanoparticulate mixed-phase Mg−Co composites.[84]

The trialkylborohydride reducing agents, $ABEt_3H$ (A = Li, Na, or K), and solvated magnesium, Mg*, also act as powerful reducing agents. Bönnemann et al. have demonstrated that these reagents reduce an impressive array of electropositive metals from their various salts in nonpolar organic solvents such as toluene, dioctyl ether, or THF:[85−87]

$$xMX_y + yABEt_3H \rightarrow xM + yAX + yBEt_3 + {}^{xy}/_2H_2 \quad (28)$$

where $M^{y+} = Cr^{3+}$, Mn^{2+}, Fe^{2+}, Fe^{3+}, Co^{2+}, Ni^{2+}, Cu^{2+}, Zn^{2+}, Ru^{3+}, Rh^{3+}, Pd^{2+}, Ag^+, Cd^{2+}, In^{3+}, Sn^{2+}, Re^{3+}, Os^{3+}, Ir^{3+}, Pt^{2+}, or Au^+; A = Li or Na; and X represents the counterion. Others later adapted the method to the reduction of Mo^{3+} and W^{4+}.[88] The reaction in eq 28 typically results in 1−5 nm metal colloids, though the products tend to exhibit poor crystallinity due to the relatively low reaction temperatures (T < 70 °C). Interestingly, the above reaction is sensitive to both the reducing agent and the solvent: substituting $LiBEt_3H$ for $NaBEt_3H$ and THF for toluene results in the formation of 1−5 nm colloidal metal carbides (M_2C).[88]

Sun and Murray et al. developed an analogous, convenient elevated-temperature method of synthesizing nanocrystalline cobalt and nickel and their alloys with tight size distributions ($\sigma = 7-10\%$).[89−91] Their method involved the reduction of metal salts, typically chlorides or acetates, in the presence of two types of capping ligands: strongly bound (carboxylic acid) and weakly bound (trialkyl phosphine and phosphine oxide). Injecting a solution of reducing agents, long-chain 1,2-diol or $LiBEt_3H$, into a preheated solution of metal salts and capping agents in a high-boiling solvent (dioctyl or diphenyl ether) resulted in fast nucleation followed by slower nanocrystal growth. Changing the ratio of the two capping ligands, as well as their chain length, allowed tuning of the nanocrystal sizes. The reaction products formed stable dispersions in nonpolar solvents due to the presence of carboxylic (oleic) acid groups covalently attached to the nanocrystal surfaces (Figure 3).

According to a recent report by Bönnemann et al., the reduction of metal salts, as well as the stabilization of colloids, can be performed by organoaluminum compounds:[92−96]

$$MX_n + nAlR_3 \rightarrow M + nR_2AlX + nR_2 \quad (29)$$

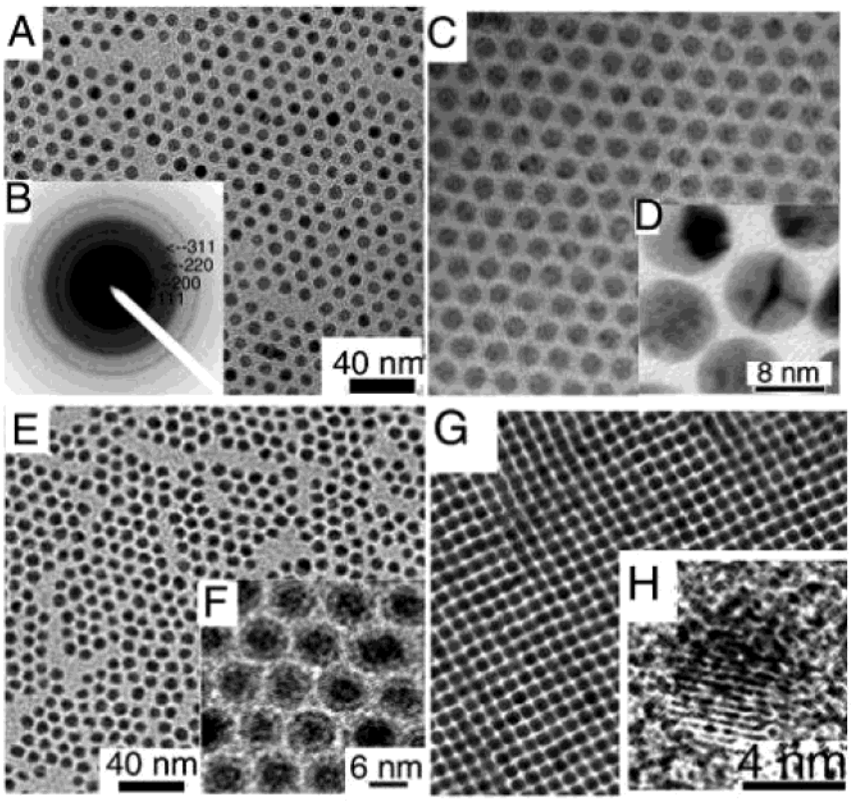

Figure 3. (A) Low-magnification TEM image of 8 nm Co−Ni alloy nanoparticles. (B, inset) Electron diffraction pattern from 8 nm Co−Ni nanoparticles confirming the predominantly *fcc* structure. (C) TEM image of an ensemble of 8 nm *fcc* Co nanoparticles. (D, inset) HRTEM image highlighting the multitwinned internal structure of Co nanoparticles. (E) TEM image of an ensemble of 6 nm Fe nanoparticles. (F, inset) TEM image at higher magnification, in which the surface oxide layer is clearly visible. (G) Image of an ensemble of 6 nm *fcc* FePt nanoparticles. (H, inset) HRTEM image of FePt nanocrystals after annealing and forming of the face-centered tetragonal (*fct*) phase. (Reprinted with permission from ref 91. Copyright 1999 Materials Research Society.)

Table 2. Survey of Nanoparticulate Metals and Alloys That Have Been Precipitated by Reduction from Nonaqueous Solutions

compd	starting material	solvent[a]	reductant[b]	stabilizer[c]	conditions	product size[d] (nm)	ref
Fe	$Fe(OEt)_2$	THF	$NaBEt_3H$	THF	16 h at 67 °C	10−100	85
Fe	$Fe(acac)_3$	THF	Mg*	THF		∼8[e]	87
$Fe_{20}Ni_{80}$	$Fe(OAc)_2$ $Ni(OAc)_2$	EG	EG	EG	reflux (150−160 °C)	6 (A)	98
Co	$Co(OH)_2$	THF	$NaBEt_3H$	THF	2 h at 23 °C	10−100	85
Co	$CoCl_2$	THF	Mg*	THF		∼12	87
$Co_{20}Ni_{80}$	$Co(OAc)_2$ $Ni(OAc)_2$	EG	EG	EG	reflux (150−160 °C)	18−22 (A)	98
Ni	$Ni(acac)_2$	HDA	$NaBH_4$	HDA	160 °C	3.7 (C)	80
Ni	$NiCl_2$	THF	Mg*	THF		∼94[e]	87
Ni	$Ni(OAc)_2$	EG	EG	EG	reflux (150−160 °C)	25 (A)	98
Ru	$RuCl_3$	1,2-PD	1,2-PD	Na(OAc) and DT	170 °C	1−6 (C)	78
Ag	$AgNO_3$	methanol	$NaBH_4$	MSA	room temp	1−6 (C)	75
Ag	$AgClO_4$	DMF	DMF	3-APTMS	20−156 °C	7−20 (C)	77
Au	$AuCl_3$	THF	$K^+(15C5)_2K^-$	THF	−50 °C	6−11 (C)	83
Au	$HAuCl_4$	formamide	formamide	PVP	30 °C	30 (C)	76

[a] EG = ethylene glycol; DMF = dimethylformamide; HAD = hexadecylamine; THF = tetrahydrofuran; 1,2-PD = 1,2-propanediol. [b] See text for descriptions of reducing agents. [c] MSA = mercaptosuccinic acid; 3-APTMS = 3-(aminopropyl)trimethoxysilane; PVP = poly(vinylpyrrolidone); DT = dodecanethiol. [d] (A) = agglomerated; (C) = colloidal/monodispersed [e] Estimated from BET surface area assuming spherical shape.

where M = metals of groups 6−11 and X = acetylacetonate. Nanoparticles of metal remain surrounded by organoaluminum species that enable control of their growth. Slow oxidation and derivatization of these core−shell species allows the tailoring of their solubility and colloidal stability in different media. The specific chemical reactivities of the organoaluminum-coated nanoparticles open new pathways to the design and synthesis of heterogeneous catalysts.

The techniques involving organoaluminum reagents have recently been extended by the same authors to include the metal carbonyl decomposition route.[97] This resulted in the synthesis of 10 nm Co

nanoparticles with a narrow size distribution (±1.1 nm) surrounded by organoaluminum species. Slow air oxidation and peptization with suitable surfactants lead to air-stable magnetic fluids.

Table 2 provides a summary of metals that have been reported in the literature as being precipitated from nonaqueous solutions.

2.2.3. Precipitation of Metals by Electrochemical Reduction

Although the method is not widely used, the synthesis of powdered metallic nanoparticles is possible by electrochemical reduction. The method developed by Reetz et al. involves the anodic dissolution of a metal and the reduction of the intermediate metallic salt at the cathode (usually Pt foil).[99] The reaction must be carried out in the presence of a stabilizer, such as a tetraalkylammonium salt, to prevent all of the particles from simply depositing (plating) at the cathode's surface.

In Reetz's initial experiments, Pd metal was deposited from a 0.1 M solution of tetraoctylammonium bromide dissolved in a 4:1 mixture of acetonitrile−THF by applying a 0.1 mA/cm^2 current at 1 V using a potentiostat. The monodispersed 4.8 nm particles were collected by decantation/drying and were redispersable in THF or toluene (Figure 4). The authors also noted that increasing the current density resulted in a substantial decrease in particle size, such that 1.4 nm particles were obtained at 5.0 mA/cm^2.

Rodríguez-Sánchez et al. adapted the method to the precipitation of 2−7 nm silver nanoparticles by cycling a Ag|0.1 M tetrabutylammonium bromide in acetonitrile|Pt cell from 1.35 V to −0.15 V at 500 mV/s for 5 min.[100] The authors noted a similar relationship between current density and particle size as reported by Reetz. In a variation of this method, Mohamed et al. were able to deposit Au nanorods by adding Ag^+ to the supporting electrolyte.[101]

Asenjo et al. have recently developed an analogous method for the preparation of nanoparticulate strontium ferrites by electrolyzing acidic aqueous solutions of Sr^{2+} and Fe^{2+} chlorides and nitrates in a 40−80 °C temperature range.[102] The spherical products were typically on the order of ∼50 nm, although trace impurities were detected in their lattices resulting from the electrolysis.

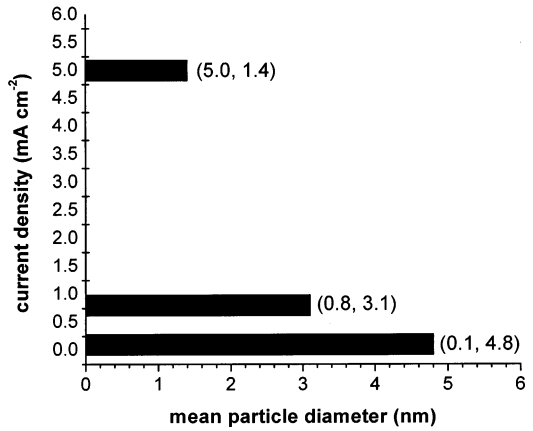

Figure 4. Mean particle diameter as a function of current density for Pd clusters precipitated electrochemically from acetonitrile−THF solution. (Adapted with permission from from ref 99. Copyright 1994 American Chemical Society.)

2.2.4. Precipitation of Metals by Radiation-Assisted Reduction

The most obvious example of radiation-assisted reduction is the photoreduction of aqueous $AgNO_3$ solutions upon exposure to UV light. Huang et al. adapted this method to the synthesis of Ag nanoparticles by exposing a solution of $AgNO_3$ to 243 nm radiation in the presence of poly(*N*-vinylpyrrolidone) (PVP) as stabilizer.[103] The average particle size could be varied from 15 to 22 nm by adjusting the [PVP]/[Ag^+] ratio.

At the extreme end of radiation-assisted reductions, all of the noble metals, as well as many other electronegative metals, can be reduced in aqueous solutions by exposure to γ-radiation. γ-rays decompose H_2O to H_2, H_2O_2, $^\bullet$OH and $^\bullet$H radicals, and aqueous, solvated electrons:[104]

$$H_2O \xrightarrow{\gamma\text{-rays}} {}^\bullet OH\ (2.8),\ e_{aq}^-\ (2.7),\ H_2O_2\ (0.71),\ {}^\bullet H\ (0.55),\ H_2\ (0.45) \quad (30)$$

where the numbers in parentheses represent the radical chemical yields expressed as the number of species per 100 eV of energy absorbed.

The reactions are usually performed under a nitrous oxide atmosphere that acts as a scavenger for the hydrated electrons (e_{aq}^-):

$$N_2O + e_{aq}^- + H_2O \rightarrow N_2 + OH^- + {}^\bullet OH \quad (31)$$

The $^\bullet$OH and $^\bullet$H radicals are subsequently scavenged by short-chain alcohols such as methanol:

$$^\bullet OH + CH_3OH \rightarrow H_2O + {}^\bullet CH_2OH \quad (32)$$

$$^\bullet H + CH_3OH \rightarrow H_2 + {}^\bullet CH_2OH \quad (33)$$

The $^\bullet CH_2OH$ radical then serves as a reducing agent for the metal accompanied by oxidation of the radical to an aldehyde:

$$M^{n+} + n\,{}^\bullet CH_2OH \rightarrow M^0 + nCH_2O + nH^+ \quad (34)$$

In instances where the strong reducing power of e_{aq}^- is necessary to perform the reduction, the nitrous oxide atmosphere can be foregone, thereby allowing some degree of control over the strength of the active reducing agent.

The nanoparticle metals produced by radiolytic reduction include Au (2 nm, stabilized in poly(vinyl alcohol) or poly(vinylpyrrolidone)),[105] Co (2−4 nm, stabilized by polyacrylate),[106] and Cu (20−100 nm in poly(vinyl sulfate).[107] 20 nm particles of Ag stabilized with sodium dodecyl sulfate have also been reported, but the resulting colloidal suspensions were not stable against agglomeration.[108]

The radiolytic reduction method is perhaps most useful when enlarging colloidal metals or layering dissimilar metals over one another, forming core−shell type arrangements. In these reactions, a metal colloid is usually prepared by a conventional chemical

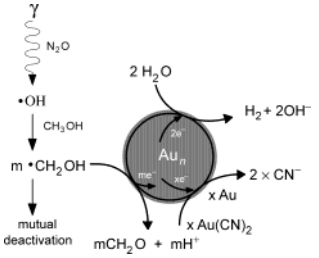

Figure 5. Mechanism of Au nanoparticle enlargement using γ irradiation. (Reprinted with permission from ref 110. Copyright 2000 American Chemical Society.)

route such as the Turkevich (citrate) method discussed in section 2.2.1. The metal colloids are then essentially used as seed particles for subsequent growth of the same or a different metal from aqueous solutions. For instance, starting from a solution of 15 nm Au prepared by the citrate method, Henglein et al. enlarged the Au particles sequentially up to diameters of 120 nm by adding aqueous $Au(CN)_2^-$ and methanol to the colloidal solution and irradiating with a ^{60}Co source.[109] The size distribution and monodispersity of the nanoparticles do not appear to be adversely affected throughout the process.

In Henglein's method, rather than the organic radicals directly reducing the metal cations, they instead charge the colloidal Au particles that subsequently act as reducing agents for the aqueous $Au(CN)_2^-$ ions:[110]

$$^{\bullet}CH_2OH + Au_n^{x-} \rightarrow Au_n^{(x+1)-} + CH_2O + H^+ \quad (35)$$

$$Au_n^{(x+1)-} + Au(CN)_2^-(aq) \rightarrow Au_{(n+1)}^{x-} + 2\,CN^- \quad (36)$$

This mechanism is demonstrated schematically in Figure 5. There is, of course, no requirement that the nanoparticle seeds and aqueous metal ions consist of the same metals. A dissimilar metal cation dissolved in the aqueous solution would essentially coat the surfaces of the existing metal colloid particles, creating a core−shell type composite. Henglein et al. have published extensively on this method, and their successes include nanocomposites of $Au_{core}Pt_{shell}$,[111] $Pt_{core}Au_{shell}$,[111] $Au_{core}Hg_{shell}$,[112] $Au_{core}Pb_{shell}$,[113] Pd_{core}-$Au_{shell}Ag_{shell}$,[114] and the $Au_{core}Ag_{shell}$ material shown in Figure 6.[110]

Very recently, Lee et al. have reduced aqueous solutions of Ni^{2+} and $NaPH_2O_2 \cdot H_2O$ to 100−300 nm Ni−P nanocomposites with synchrotron X-rays.[115] The particle sizes could be controlled by adjusting the temperature of the solution, although considerable aggregation of the products was observed. Nonetheless, this appears to be the first report of nanoparticles prepared by irradiation with synchrotron X-rays.

Yeh et al. have reported the synthesis of Au−Ag, Au−Pd, Ag−Pd, and Au−Ag−Pd nanoparticles by irradiating the appropriate mixtures of metal colloids with an Nd:YAG laser.[116−118] Although this method cannot be classified as a precipitation reaction, since the metals were already in colloidal form prior to irradiation, it is nonetheless noted here as a potentially very useful method of preparing bi- and trimetallic nanoparticles.

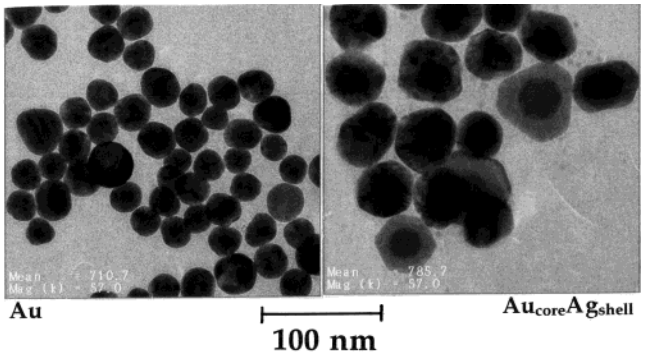

Figure 6. TEM image of 20 nm Au nanoparticles (left) produced by the Turkevich method and (right) after coating with Ag by a radiation-assisted reduction method. (Reprinted with permission from ref 110. Copyright 2000 American Chemical Society.)

2.2.5. Precipitation of Metals by Decomposition of Metallorganic Precursors

The thermolysis of organometallic precursors in the presence of a polymer is one of the older methods of preparing colloidal metals. Typically, a metal complex such as $Co_2(CO)_8$ is decomposed at 130−170 °C under inert atmosphere in Decalin or ethylene glycol solvents:

$$Co_2(CO)_8 \rightarrow 2Co(s) + 8CO\uparrow \quad (37)$$

45 nm Co particles capped with PVP have been prepared by this approach.[119] Originally, the polymers were thought to function as simple stabilizing agents.[120] Later, in their study of the thermolysis of $Fe(CO)_5$, Smith and Wychick observed catalytic activity by copolymers such as copoly(styrene-4-vinylpyridine) and copoly(styrene-*N*-vinylpyrolidone).[121] The nitrogen-containing polymer chains were found to effectively serve as nucleophiles (Nu), leading to the formation of ligated metal-cluster macromolecules:

$$(n+1)Fe(CO)_5 + xNu \rightarrow [Fe(Nu)_x][Fe_n(CO)_m] \quad (38)$$

$$x \equiv 2-6$$
$$n = 2,\ m = 8$$
$$n = 3,\ m = 11$$
$$n = 4,\ m = 13$$

Polymers such as polystyrene, which do not contain nitrogen and therefore do not function as nucleophiles, react only with $[Fe(CO)_4]$ intermediates generated by thermolysis. In either case, the polymers effectively serve as nucleation sites for Fe. Because the polymers serve as catalysts,[121] the functionality of the polymers profoundly influences the kinetics of the carbonyl decomposition reactions. It follows that particle size can be controlled by varying polymer functionality, as well as reactant concentration. Smith and Wychick were able to selectively prepare 5−15 nm colloidal Fe particles in this manner.[121]

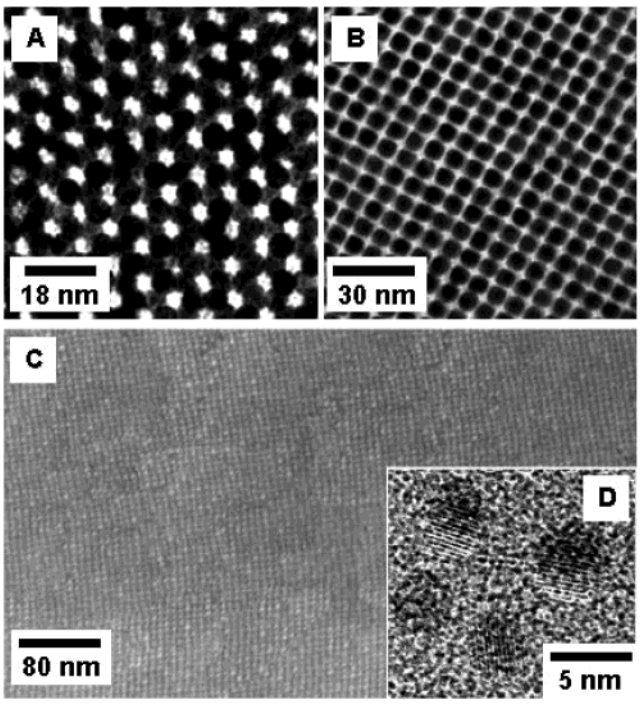

Figure 7. (A) TEM micrograph of a 3-D assembly of 6 nm as-synthesized $Fe_{50}Pt_{50}$ particles. (B) TEM micrograph of a 3-D assembly of 6 nm $Fe_{50}Pt_{50}$ particles after replacing oleic acid−oleylamine with hexanoic acid−hexylamine. (C) HRSEM image of a ∼180 nm thick, 4 nm $Fe_{52}Pt_{48}$ nanocrystal assembly annealed at 560 °C for 30 min under 1 atm of N_2 gas. (D) HRTEM image of 4 nm $Fe_{52}Pt_{48}$ nanocrystals annealed at 560 °C for 30 min. (Reprinted with permission from ref 128. Copyright 2000 American Association for the Advancement of Science.)

Van Wonterghem et al. substituted a surfactant (Sarkosyl-0) for the polymers and carried out the thermolysis of $Fe(CO)_5$ in Decalin at $T < 187$ °C.[122,123] Their method resulted in a ferrofluid of 8.5 nm Fe with a 1.0 nm standard deviation. Ni, Cr, W, and Mo nanoparticles prepared by the thermolysis of metal carbonyls have also been reported. Ge et al. later adapted the method to the synthesis of 10 nm γ-$(Fe_{44}Ni_{56})$ alloy particles.[124]

Further development of the metal carbonyl decomposition method led to the use of capping ligands instead of polymers for controlling the nanocrystal growth and protecting the products from oxidation and aggregation. Dinega et al. reported the discovery of a new crystalline phase of metallic cobalt (ϵ-Co) related to the β phase of manganese.[125] This metastable phase appeared as a kinetically controlled product of the thermal decomposition of $Co_2(CO)_8$ in hot toluene in the presence of trioctylphosphine oxide (TOPO); the same reaction performed in the absence of TOPO resulted in formation of a pure *fcc* Co phase.

More detailed study of this system performed by Puntes et al. under a wide range of conditions revealed the stepwise character of the crystal growth.[126,127] Rapid injection of cobalt carbonyl solution into a hot *o*-dichlorobenzene solution containing both the labile ligand TOPO and the stronger ligand oleic acid, followed by quenching of the reaction, resulted in formation of different products. The initial product is *hcp*-Co with a nanodisk shape with dimensions that are tunable from 4 × 25 to 4 × 75 nm. At a fixed concentration of oleic acid, the length of the nanodisks was directly proportional to the concentration of TOPO. As time progressed, the nanorods dissolved and spherical 8 nm nanocrystals of ϵ-Co with a tight size distribution appeared within a few minutes as the final product. When the decomposition of $Co_2(CO)_8$ was performed in the presence of the long-chain aliphatic amines instead of, or in addition to, TOPO, the lifetime of nanodisks in solution increased, which facilitated their preparation.[127] Varying the reaction time and [capping ligand]/[precursor] ratio allowed the synthesis of *hcp*-Co nanodisks with sizes ranging from 2 × 4 to 4 × 90 nm, although the narrowest size distribution was obtained for medium sized (4 × 35 nm) disks.

Thermal decomposition of $Fe(CO)_5$ combined with the polyol reduction of $Pt(acac)_2$ in the same pot resulted in formation of intermetallic FePt nanoparticles.[128] Their composition was controllable by adjusting the molar ratio of Fe and Pt precursors. Particle size could be tuned by growing seed particles followed by addition of additional reagents to enlarge them in the range 3−10 nm (Figure 7).

The reaction between $Co_2(CO)_8$ and $Pt(hfacac)_2$ (hfacac = hexafluoroacetylacetonate) resulted in the formation of bimetallic $CoPt_3$ and CoPt nanoparticles.[129] This reaction was performed under reflux in a toluene solution containing oleic acid as stabilizing agent:

$$Co_2(CO)_8 + Pt(hfacac)_2 \rightarrow CoPt + Co(hfacac)_2 + 8CO \quad (39)$$

In contrast, when presynthesized Co nanoparticles were reacted with $Pt(hfacac)_2$, the transmetalation redox reaction led to core−shell structured nanoparticles of Co@Pt:

$$2Co + Pt(hfacac)_2 \rightarrow Co/Pt + Co(hfacac)_2 \quad (40)$$

The resulting nanoparticles were coated with dodecyl isocyanide capping ligands and exhibited diameters of 6.27 nm ($\sigma = 0.58$ nm). They were air-stable and dispersible in nonpolar solvents.

Alkene (olefin) complexes are similar to metal carbonyls in that they usually contain zerovalent or low-oxidation-state metals. Like carbonyls, alkene complexes decompose easily, liberating pure metal and olefin ligands. This characteristic has been used advantageously for the development of new synthetic methods for colloidal transition metals. The most commonly used ligands include 1,5-cyclooctadiene (COD), 1,3,5-cyclooctatriene (COT), and dibenzylidene acetone (DBA), in addition to the π-allyl ligands, such as cyclooctenyl ($C_8H_{13}^-$).

Chaudret et al. have applied this method extensively to the synthesis of Co, Ni, Ru, Pd, Pt, CoPt, CoRu, CoRh, and RuPt nanoparticles[130−149] in addition to Co and Ni nanorods.[150,151] Solution syntheses were typically performed in the presence of H_2 or CO at room or slightly elevated temperature, yielding 1−2 nm particles with clean surfaces. The authors have determined that the stabilizing agent poly(vinylpyrrolidone) (PVP) that is frequently used in this method exhibits practically no influence on the

saturation magnetization of Co and Ni nanoparticles compared to the pure, bulk metals.[133,140]

Recently this method was used for the synthesis of colloidal Pt in 1-butyl-3-methylimidazolium hexafluorophosphate ionic liquid.[152] The isolated nanoparticles could be redispersed in the ionic liquid or in acetone or used under solventless conditions for liquid−liquid biphasic, homogeneous, or heterogeneous hydrogenation of alkenes and arenes under mild reaction conditions.

The cyclopentadiene complex of indium has been used for the synthesis of 15 nm uniform particles of In metal protected with PVP or other capping ligands.[153,154] Performing this reaction in the presence of long-chain amines yielded nanowires of In and In_3Sn alloy with high aspect ratios.[155] Similarly, colloidal 5 nm Cu has been obtained from the organometallic complex $CpCu(^tBuNC)$ in the presence of CO and PVP (3.5 nm) or polydimethylphenylene oxide (5 nm) in solutions of CH_2Cl_2 or anisole at room temperature.[156]

2.2.6. Precipitation of Oxides from Aqueous Solutions

The precipitation of oxides, from both aqueous and nonaqueous solutions, is somewhat less straightforward than the precipitation of metals. Reactions for the synthesis of oxides can generally be broken into two categories: those that produce an oxide directly and those that produce what is best termed a precursor that must be subjected to further processing (drying, calcination, etc.). In either case, monodispersed nanoparticles of oxides, like those of metals, frequently require a capping ligand or other surface-bound stabilizer to prevent agglomeration of the particles.

In those cases where calcination or annealing of the samples is necessary, some agglomeration will be unavoidable. Nanoparticles can nonetheless be so obtained, but there is little chance of the particles being monodispersed. For many of the reported syntheses of oxides, monodispersity of the products was neither a requirement nor a priority for the researchers involved.

The products of coprecipitation reactions, particularly those performed at or near room temperature, are usually amorphous. In those cases where hydroxides or carbonates of mixed metals are precipitated from solution and subjected to a calcination or postannealing process, it is extremely difficult to experimentally determine whether the as-prepared precursor is a single-phase solid solution or a multiphase, nearly-homogeneous mixture of the constituent metal hydroxides−carbonates−oxides that react to form a single-phase mixed-metal oxide when heated.

Many nanoparticulate metal oxides are prepared by calcining hydroxide coprecipitation products. Albuquerque et al. prepared spinel-structured $Ni_{0.5}Zn_{0.5}Fe_2O_4$ by precipitating a mixture of Fe, Ni, and Zn nitrates with NaOH and calcining at 300 °C or higher.[157] Particle sizes ranged from 9 to 90 nm, depending on the calcination temperature. $MgFe_2O_4$[158] and $Sm_{1-x}Sr_xFeO_{3-\delta}$[159] have been prepared by nearly identical methods.

The coprecipitation of metal cations as carbonates, bicarbonates, or oxalates, followed by their subsequent calcination and decomposition, is a common method for producing crystalline nanoparticulate oxides. The calcination will, however, almost invariably lead to agglomeration or, at high temperatures, aggregation and sintering. Fortunately, nanoparticulate hydroxide, carbonate, and oxalate precursors tend to decompose at relatively low temperatures (<400 °C) due to their high surface areas, thereby minimizing agglomeration and aggregation. As an example, $Ce_{0.8}Y_{0.2}O_{1.9}$ (a fluorite-structured, oxide-ion conducting electrolyte for solid oxide fuel cells) was precipitated by the addition of oxalic acid to an aqueous solution of $Ce(NO_3)_3$ and $Y(NO_3)_3$, followed by calcination.[160] Calcining at 500 °C yielded 10 nm, slightly agglomerated, roughly spherical particles. Calcining at 1000 °C resulted in 100 nm aggregates with irregular shapes, although lower calcination temperatures reduced aggregation considerably. CeO_2 nanopowders, by contrast, have been prepared by calcining the product of the precipitation between $Ce(NO_3)_3$ and $(NH_4)_2CO_3$, resulting in crystalline, 6 nm particles of CeO_2 at calcination temperatures as low as 300 °C.[161] 10−15 nm particles of NiO have been similarly prepared by precipitating aqueous Ni^{2+} solutions with $(NH_4)_2CO_3$ and calcining the products at 400 °C.[162]

Du et al. were able to prepare the $Bi_4Ti_3O_{12}$ ferroelectric by calcining the product from the reaction between a basic solution of TiO_2 and $Bi(NO_3)_3$ performed in acidic solution.[163] Agglomerate sizes ranged from 16 to 48 nm after calcining between 500 and 800 °C. When the calcination temperature was kept at 500 °C or below, $Bi_4Ti_3O_{12}$ appeared to crystallize in a metastable tetragonal phase previously thought to be stable only at high temperatures.

In some rare instances, crystalline oxides can be precipitated from aqueous solution, eliminating the need for a calcination step and greatly reducing the risk of agglomeration. This approach is most common for simple binary oxides. 50−60 nm aggregates of 4 nm rutile-structured TiO_2, for instance, can be prepared by precipitating aqueous $TiCl_3$ with NH_4OH under ambient conditions and stabilizing the products with poly(methyl methacrylate).[164]

The direct coprecipitation of more complex ternary oxides, while somewhat uncommon, is nonetheless possible, particularly when the product assumes a very thermodynamically favorable structure such as spinel. In such cases, the precipitation reactions are normally carried out at elevated temperatures (50−100 °C), such that the hydroxide intermediates are condensed into oxides in the same reaction vessel as where coprecipitation was induced. Such "one-pot" synthesis techniques render calcination steps unnecessary. Fe_3O_4, for example, has been prepared as an oxide by the simple coprecipitation of (Fe^{2+} + 2 Fe^{3+}) with NaOH at temperatures above 70 °C.[165] 5−25 nm particles of $MnFe_2O_4$ were similarly prepared from aqueous Mn^{2+} and Fe^{2+} at temperatures up to 100 °C.[166] Pr^{3+}-doped ceria has likewise been precipitated by aging aqueous solutions of $Ce(NO_3)_3$ and $PrCl_3$ at 100 °C in the presence of a hexameth-

Table 3. Summary of Reactions for the Precipitation of Oxides from Aqueous Solutions

compd	starting material	ppt agent	stabilizer	conditions	product size (nm)	ref
$VO_2(B)$	NH_4VO_3	$N_2H_4 \cdot H_2O$	none	calcined 300 °C	35	44
Cr_2O_3	$K_2Cr_2O_7$	$N_2H_4 \cdot H_2O$	none	calcined 500 °C	30	44
γ-Mn_2O_3	$KMnO_4$	$N_2H_4 \cdot H_2O$	none		8	44
$MnFe_2O_4$	$MnCl_2$ $FeCl_3$	NaOH	none	100 °C	5−25	172
Fe_3O_4	$FeCl_2$ $FeCl_3$	NH_4OH	H^+	N_2 atm	8−50	173
NiO	$NiCl_2$	NH_4OH	CTAB	annealed 500 °C	22−28	174
ZnO	$ZnCl_2$	NH_4OH	CTAB	annealed 500 °C	40−60	174
SnO_2	$SnCl_4$	NH_4OH	CTAB	annealed 500 °C	11−18	174
Sb_2O_3	$SbCl_3$	NaOH	PVA	annealed 350 °C	10−80	175

ylenetetramine stabilizer to yield monodispersed 13 nm particles.[167] In this case, the stabilizer indirectly serves as the precipitating agent by raising the pH high enough to induce precipitation of the metal hydroxides.

Chinnasamy et al. reported an extensive series of experiments for the spinel-structured $CoFe_2O_4$ designed to determine the influence of reaction temperature, reactant concentration, and reactant addition rate on the size of the products.[168] In each case, aqueous solutions of Fe^{3+} and Co^{2+} were precipitated with dilute NaOH. The results were predominantly in line with expectations based on the considerations outlined in section 2.1: Increasing the temperature from 70 °C to 98 °C increased the average particle size from 14 to 18 nm. Increasing the NaOH concentration from 0.73 to 1.13 M increased particle size from 16 to 19 nm. NaOH concentrations of 1.5 M or greater resulted in the formation of a secondary FeOOH phase, and slowing the NaOH addition rate appeared to broaden the particle size distribution.

Li et al. prepared 12 nm $CoFe_2O_4$ by a similar route but stabilized the product by acidification with dilute nitric acid.[169] The electrostatic repulsion of the particles created by the adsorption of H^+ at the particle surfaces resulted in an indefinitely stable colloid of ferromagnetic particles (a *ferrofluid*). By contrast, Fe_3O_4 ferrofluids, which tend to not be stable under acidic solutions, have been sterically stabilized by coating Fe_3O_4 nanoparticles with oleic acid, poly(vinyl alcohol), or starch.[170,171]

A summary of oxides precipitated from aqueous solutions, including the relevant reaction conditions, is given in Table 3.

2.2.7. Precipitation of Oxides from Nonaqueous Solutions

Simple precipitation reactions are sometimes carried out in nonaqueous solvents. This method can be particularly advantageous when precipitating dissimilar metals that cannot be simultaneously precipitated from aqueous solution due to large variations in the pH values necessary to induce precipitation of the constituent cations. Such is the case with $LiCoO_2$, a well-known cathode material for rechargeable lithium batteries.[176] LiOH cannot be precipitated from aqueous solution, but its solubility in alcohols is greatly diminished. Hagenmuller et al. induced nearly simultaneous coprecipitation of ($LiOH + Co(OH)_2$) by dripping a mixture of $LiNO_3$ and $Co(NO_3)_2$ dissolved in ethanol into a stirred 3 M KOH ethanol solution.[177] The hydroxide mixture was then calcined at 400−700 °C in air to yield 12−41 nm $LiCoO_2$.

Similar procedures have been adapted to the hydroxide precipitation of other transition metals. Amorphous $RuO_{2-\delta} \cdot nH_2O$ can be precipitated by addition of tetramethylammonium hydroxide to $RuNO(NO_3)_3$ dissolved in alcohol at 90 °C.[178] Subsequent annealing of the product at 400 °C in air resulted in 14 nm crystalline RuO_2. By contrast, precipitation of $RuO_{2-\delta} \cdot nH_2O$ from aqueous solution required over 2 weeks at 90 °C and ultimately resulted in products containing about 5% metallic Ru.

There is at least one account of a nanoparticle oxide synthesis in which the solvent also served as the precipitating agent. Deb et al. prepared 5−20 nm γ-Fe_2O_3 by melting a mixture of stearic acid ($CH_3(CH_2)_{16}COOH$) and hydrated $Fe(NO_3)_3$ at 125 °C and calcining the product in air at 200 °C.[179] The product underwent the γ (maghemite) → α (hematite) phase transition on prolonged heating at 200 °C, well below the transition temperature of bulk γ-Fe_2O_3. The results of Ennas et al., however, suggest that the phase transition temperature of γ-Fe_2O_3 is not strictly a function of particle size, as they observed a transition starting at ∼250 °C for 5 nm γ-Fe_2O_3.[180]

In other cases, the use of aqueous solvents is avoided specifically to prevent the premature precipitation of metal hydroxides/oxides. Premature precipitation tends to be problematic with high-valence, electropositive metals such as Ti^{4+}, Zr^{4+}, and so forth. This can, to some extent, be circumvented by using metal chloride or metal alkoxide precursors in nonaqueous solvents. The hydrolysis reactions can consequently be controlled to limit particle growth and prevent agglomeration. Ferroelectric $BaTiO_3$, for instance, has been prepared by precipitating a mixed-metal alkoxide precursor, $BaTi(O_2C(CH_3)_6CH_3)[OCH(CH_3)_2]_5$ (that is highly susceptible to hydrolysis) with H_2O_2 in diphenyl ether solution with oleic acid as stabilizer.[181] The addition of H_2O_2 effectively initiates an hydrolysis reaction. Condensation occurred as the solution was heated at 100 °C, resulting in Ba−O−Ti linkages, but with particle growth constrained by the presence of the oleic acid stabilizer. This method resulted in 6−12 nm monodisperse, crystalline particles that did not require calcination. These reactions are similar in many respects to the sol-gel reactions discussed in section 3.

The method of Caruntu et al. for the synthesis of colloidal ferrites is similar in that a metal chelate precursor formed between a metal chloride and

diethylene glycol was subsequently subjected to controlled hydrolysis:[182]

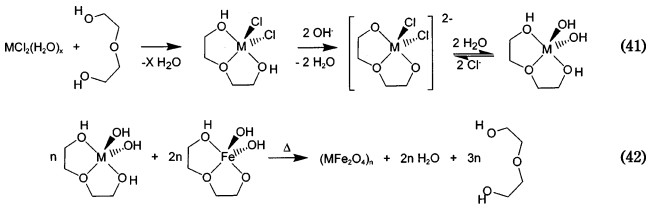

Here, the diethylene glycol served as both solvent and stabilizing agent, although the glycol was usually exchanged for oleic or myristic acid to ensure growth termination. The authors have prepared a series of monodispersed MFe_2O_4 ferrites by this method, where M = Mn, Fe, Co, Ni, or Zn, exhibiting sizes in the 3−7 nm range with the standard deviation of particle sizes typically on the order of 15% (Figure 8).

Using a somewhat more conventional route, Sun et al. prepared 4 nm Fe_3O_4 by dissolving $Fe(acac)_3$, 1,2-hexadecanediol, oleic acid, and oleylamine in diphenyl ether and refluxing for 30 min.[183] Precipitation was induced when ethanol was added under air atmosphere after the solution had cooled to room temperature. It is uncertain in this method at what point or by what reagent Fe^{3+} is reduced to Fe^{2+}.

Rockenberger et al. developed a method for preparing surfactant-capped oxide nanoparticles by decomposition of metal-Cupferron complexes, M^xCup_x (Cup = $C_6H_5N(NO)O^-$).[184] The reactions involved injecting a solution of $FeCup_3$, $MnCup_2$, or $CuCup_2$ dissolved in octylamine into a solution of trioctylamine under inert atmosphere at 300 °C, well above the decomposition temperatures of the Cupferron complexes. The resulting precipitates were found to consist of 4−10 nm nanoparticles of either γ-Fe_2O_3, MnO, or Cu and were easily dispersed in toluene.

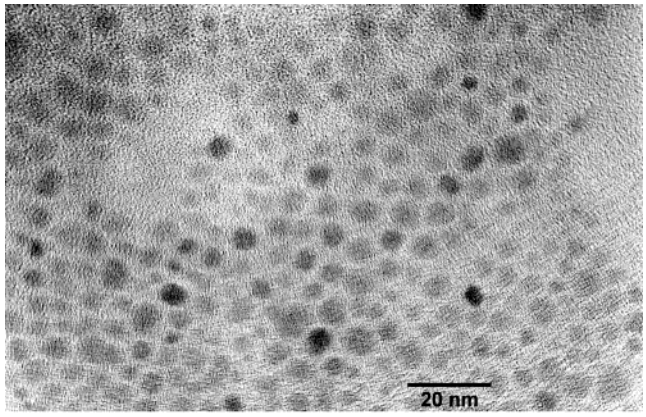

Figure 8. TEM images of $MnFe_2O_4$ nanoparticles prepared by the hydrolysis and condensation of metal chelates in nonaqueous solutions. (Reprinted with permission from ref 182. Copyright 2002 American Chemical Society.)

2.2.8. Coprecipitation of Metal Chalconides by Reactions of Molecular Precursors

Interest in chalcogenide nanoparticles has grown dramatically in recent years, primarily due to the potential applications of quantum dots (semiconducting nanoparticles with band gaps that are particle-size dependent and therefore tunable).[185−187] Because experimental and theoretical considerations for the syntheses of nanoparticulate semiconductors have recently been reviewed,[188,189] we present only a brief overview here, with emphasis on the most recent developments.

Early studies on the physical and optical properties of quantum dots were severely hampered by a lack of synthetic routes to monodisperse products. Demand for nanocrystalline semiconductors with uniform size and shape stimulated research into synthetic methods based on reactions with easily tunable rates. Classic metathesis reactions between metal and chalcogenide ions that occur instantaneously upon mixing usually produce precipitates consisting of agglomerated crystallites with widely disparate sizes and shapes. A successful method of controlling the precipitation process lies in performing the reactions in heterogeneous media (reverse micelles, solid templates, etc.; see section 4) where the rate is controlled by diffusion restrictions.

Alternative methods may be based on nucleophilic or other reactions between neutral molecules that are readily kinetically controlled. The reaction between metal- and chalcogen-containing covalent compounds can have a significant potential energy barrier and can be driven by thermal energy. Changing the amount of supplied heat therefore allows tuning of the reaction kinetics. This approach was systematically developed at AT&T Bell Labs by M. L. Steigerwald and L. E. Brus in the mid-1980s to mid-1990s.[190−196] Their novel strategy of using organic chalcogenides, metal molecular carriers, and organic coordinating solvents as the reaction media resulted in the preparation and characterization of a variety of nanoscale II−VI and III−V semiconductors.

The approach of temporal separation of nucleation and crystal growth resulted in processable, highly crystalline nanoparticles with unprecedentedly narrow size distributions. This method was developed for cadmium chalcogenides,[197−200] as well as for Ga and In pnictides.[201−203] For the synthesis of cadmium chalcogenides, the Cd-precursor was $Cd(CH_3)_2$, and the chalcogen source molecules were $[(CH_3)_3Si]_2S$, $[(CH_3)_3Si]_2Se$, R_3PSe, and R_3PTe (R = C_4−C_8 *n*-alkyl). Rapid injection of a room-temperature solution containing both precursors into the preheated (340−360 °C) solvents resulted in rapid nucleation, and ma-

nipulation of the temperature allowed the time-scale separation of nucleation and growth of the nanocrystals. Typically, the temperature was lowered to 280−300 °C and the relatively slow nanocrystal growth takes place until the reactants are consumed. Adding another portion of reagents allowed further growth of the nanocrystals, thus expanding the size tunability to 1.2−12 nm. The reaction medium was a high-boiling mixture of trioctylphosphine (TOP) and trioctylphosphine oxide (TOPO) that acts not only as a solvent but also as a passivating agent and stabilizer. Molecules of TOP and TOPO compounds readily coordinate to metal and chalcogen intermediates and bind to the surface of growing nanocrystals, thereby reducing their surface energy. Nanocrystals grown with their surfaces protected with these capping ligands do not agglomerate but remain in reaction solution as long as necessary in the experiments.

Detailed study of the evolution of nanocrystals' sizes and size distributions revealed some key processes.[203] Depending on the concentration of mononuclear species (reagents) and the sizes of the nanocrystals, two distinct processes were found to be occurring. When the concentration of the monomer is higher than the solubility of the nanocrystals, the "focusing" phase occurs when all nanocrystals grow, and the smaller crystals grow faster than the larger crystals. As a result, the size distribution of the nanocrystals is narrowed. When the concentration of the monomer becomes lower than the solubility of nanocrystals at their critical size, the Ostwald ripening mechanism is engaged, whereby larger crystals grow at the expense of smaller ones. This is a "defocusing" phase when size distribution broadens. Properly manipulating the kinetics of the reaction while keeping the monomer concentration higher than the critical threshold provides a versatile tool for synthesizing monodispersed, variable-sized nanocrystals of presumably the entire class of II−VI and III−V semiconductors.

Further modification of this method led to the development of a three-component coordinating solvent system containing TOP, TOPO, and hexadecylamine for the synthesis of CdSe.[204] Introducing the additional complexing agent resulted in the elimination of the defocusing step from the nanocrystals' growth phase. The resulting nanoparticles exhibited nearly spherical shapes with exceptionally narrow size distributions without the need for size-selective fractionation. Substituting trialkylphosphine and trialkylphosphine oxide for the amine capping ligands resulted in an increase in the photoluminescence quantum efficiency from 10−25% to 40−50%. Depositing a shell of ZnS around a CdSe core further improved the room-temperature values of quantum efficiency to 50−60%.

In addition to their hexagonal and cubic modifications, cadmium chalcogenides can assume the highly anisotropic wurtzite structure with a unique *c*-axis. Consequently, an uneven crystal growth under kinetic conditions is expected. This was recently observed experimentally for the synthesis of CdSe by the same organometallic reaction described above but under modified conditions.[205−207] At a monomer concentration higher than was used for spherical nanocrystals, nanorods were formed instead of nanoparticles (Figure 9). At these high concentrations, the rate of reaction is very high and nanocrystals grow in all directions, although faster along the *c*-axis. Introducing an additional reagent that acts as a strong ligand for Cd, such as alkylphosphonic acid ($R = C_6$ or C_{14}), enables control of the reaction rate and tuning of the morphology of the product. Soluble and processable nanorods with a high aspect ratio (30:1) and arrow-, teardrop- and tetrapod-shaped CdSe nanocrystals have been reported.[206]

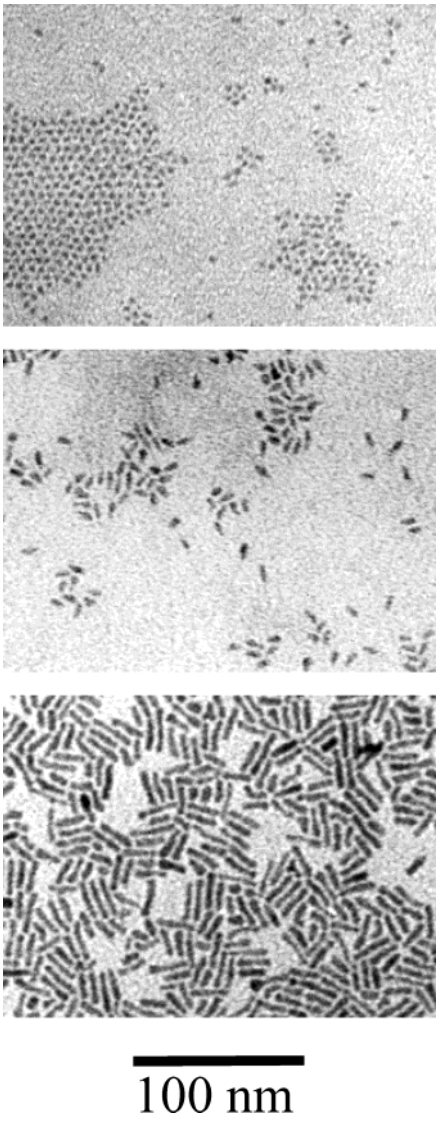

Figure 9. (Top) CdSe dots formed in 13% tetradecylphosphonic acid at 360 °C for injection and 250 °C for growth. (Middle and bottom) Quantum rods grown from the dots in the top image by a secondary injection and subsequent growth for 23 h. (Reprinted with permission from ref 207. Copyright 2001 American Chemical Society).

There are three distinctive diffusion-controlled phases of the process: one-dimensional growth, three-dimensional growth, and one-to-two-dimensional ripening.[207] The first phase occurs when the monomer concentration at the beginning of the reaction is at its highest and results in nanorods with high aspect ratios and uniform thicknesses. The second phase occurs when the concentration of the

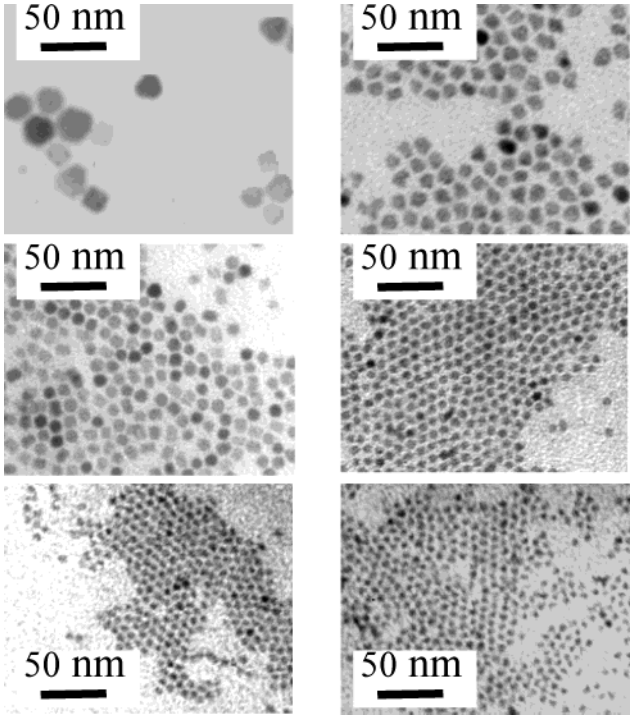

Figure 10. TEM micrographs of different sized wurtzite CdSe nanocrystals (as-prepared) synthesized in stearic acid related solvents. (Reprinted with permission from ref 209. Copyright 2001 American Chemical Society.)

monomer is intermediate and nanorods grow in all three dimensions. Finally, the last phase of intraparticle ripening at low monomer concentrations results in mass transport from long to short dimensions of nanorods that reduces their aspect ratio.

Evaluation of the possible pathways of the initial reaction involving dimethylcadmium resulted in the development of more practical methods of synthesizing nanocrystalline cadmium chalcogenides.[208,209] In this method, CdO was used instead of $Cd(CH_3)_2$ and was predissolved in a solution of alkylphosphonic acid ($R = C_6H_{13}$ or $C_{14}H_{29}$) in TOPO. A solution of chalcogen precursor $[(CH_3)_3Si]_2S$, $[(CH_3)_3Si]_2Se$, R_3PSe, or R_3PTe ($R = C_4-C_8$ *n*-alkyl) in TOPO was injected into the hot Cd-containing solution, resulting in the formation of colloidal nanoparticles. Cadmium carboxylates, such as acetate, laurate, and stearate have been successfully substituted as cadmium precursors that facilitate the nanocrystals' growth (Figure 10).[209] Tuning the concentrations of the reagents and reaction temperature enabled the control of the nanocrystals' sizes and shapes, analogous with the systems where dimethylcadmium was employed. This new one-pot method represents a significant step toward the industrial-scale production of semiconductor quantum dots, since the expensive, flammable, and toxic dimethylcadmium has now been eliminated.

The synthesis of monodispersed nanocrystals of PbSe capped with oleic acid has been successfully performed by combining lead oleate with trioctylphosphine selenide.[210] Rapid injection of a solution of the precursors (in TOPO) into preheated (150 °C) diphenyl ether, followed by controlled annealing of the solutions at lower temperatures, allowed the separation of the nucleation and growth processes, similar to the cases of the systems described above for cadmium chalcogenides.

Semiconductor quantum dots of CdSe and PbSe doped with paramagnetic Mn^{2+} ions have been prepared by modification of the above methods, in that $Mn_2(\mu\text{-SeMe})_2(CO)_8$ was added as a manganese-containing precursor.[211,212] Nanocrystals of these diluted magnetic semiconductors may be useful as materials for spin applications.

2.2.9. Microwave-Assisted Coprecipitation

The microwave processing of nanoparticles results in rapid heating of the reaction mixtures, particularly those containing water. As a consequence, the precipitation of particles from such solutions tends to be rapid and nearly simultaneous. As outlined in section 2.1, this leads to very small particle sizes and narrow size distributions within the products. The method offers the additional benefit of requiring very short reaction times.

Pastoriza-Santos and Liz-Marzán were able to make a direct comparison of colloidal Ag and Au nanoparticles prepared by both reflux-induced precipitation and microwave-assisted precipitation. In both cases, the metals were reduced by the solvent, DMF.[213] They found that, generally, the microwave method offered better control of particle size and morphology.

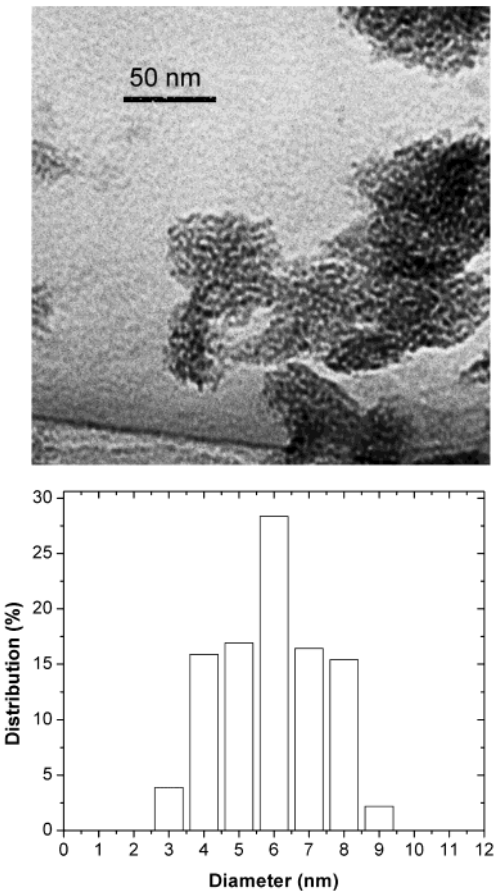

Figure 11. TEM image (top) and size distribution (bottom) of Ni nanoparticles prepared under microwave irradiation and stabilized with PVP. (Reprinted with permission from ref 216. Copyright 2002 Chemical Society of Japan.)

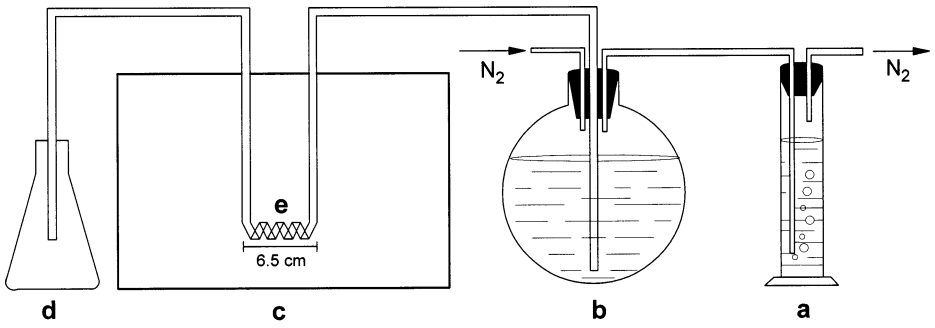

Figure 12. Schematic of a continuous-flow microwave reactor consisting of (a) a liquid column as a pressure regulator, (b) a metal salt solution container, (c) a microwave oven cavity, (d) a metal cluster dispersion receiver, and (e) a spiral tube reactor. (Reprinted with permission from ref 217. Copyright 2000 American Chemical Society.)

Table 4. Representative Sample of Nanoparticulate Compounds That Have Been Prepared by Microwave-Assisted Coprecipitation

compd	starting material	solvent	stabilizer	microwave conditions	product size (nm)	ref
α-Fe_2O_3	$Fe(NO_3)_3$	H_2O	none	reflux, 2.4 GHz, 850 W	50−100	224
Ni	$Ni(OH)_2$	EG	PVP	2.5 GHz, 200 W	5−8	225
Ni	$Ni(OH)_2$ H_2SO_4	50% EG−H_2O	PVP	2.5 GHz, 200 W	3−9	216
Bi_2S_3	$Bi(NO_3)_3$ $CS(NH_2)_2$	40% CHCO−H_2O	none	reflux	10 × 300 rods	226

Many colloidal metals can be prepared by microwaving mixtures of metal salts and polyalcohols. This method, originally developed by Fiévet et al.,[214] is now referred to as the *microwave-polyol process*. Recently, Yu et al. prepared 2−4 nm colloidal Pt particles by irradiating a mixture of poly(*N*-vinyl-2-pyrrolidone), aqueous H_2PtCl_6, ethylene glycol, and NaOH with 2450 MHz microwaves in an open beaker for 30 s.[215] Tsuji et al. have prepared PVP-stabilized, nanoparticulate Ni in ethylene glycol by a similar method; a TEM image and size distribution chart for their products are presented in Figure 11.[216] Tu et al. adapted the method to a continuous-flow reactor; their apparatus is depicted in Figure 12.[217] This method can reportedly produce colloidal ∼1.5 nm Pt at 0.8 L/h.

Microwave methods have similarly been used for the synthesis of chalcogenides. Gedanken et al. prepared CdSe, PbSe, and $Cu_{2-x}Se$ nanoparticles by microwave-refluxing[218] solutions containing aqueous Cd^{2+}, Pb^{2+}, or Cu^{2+} and Na_2SeSO_3 in the presence of an amine-based stabilizer.[219] In the case of CdSe, increased irradiation time influenced the structure of the product. Interestingly, as-prepared CdSe samples consisted of well-dispersed 4−5 nm particles, whereas the PbSe and $Cu_{2-x}Se$ formed aggregates. Gedanken's group has published extensively on various oxides and chalcogenides prepared by microwave-assisted irradiation.[220−223]

A brief survey of compounds prepared by microwave-assisted coprecipitation is given in Table 4.

2.2.10. Sonication-Assisted Coprecipitation

Like microwave-induced heating, sonication of a liquid also results in rapid heating, although the mechanism is fundamentally different. The sonication of a liquid results in cavitation (the implosive collapse of bubbles) that creates localized "hot spots" with effective temperatures of 5000 K and lifetimes on the order of a few nanoseconds or less.[227−229] As such, the chemical reactions largely take place inside the bubbles.[230] The extremely rapid cooling rates encountered in this process, however, strongly favor the formation of amorphous products.

Many of the methods reported in the literature for sonochemical syntheses of nanoparticles involve the decomposition of carbonyl precursors, as discussed in section 2.2.5. Suslick et al., who have published extensively on the use of ultrasound in chemical syntheses, have prepared amorphous, nanoparticulate Fe, Co, and several Fe−Co alloys.[231−233] Typically, the corresponding metal carbonyls were dissolved in decane and irradiated at 20 kHz for ∼3 h under an inert atmosphere to produce well-dispersed ∼8 nm particles (Figure 13). Others have reported the synthesis of 40 nm particles of M50 steel by a similar process.[234]

Oxides can be prepared by similar methods if the sonication is performed under an oxygen atmosphere. Shafi et al. prepared amorphous nanoparticles of $NiFe_2O_4$ by sonicating a solution of $Fe(CO)_5$ and $Ni(CO)_4$ in Decalin under a 1−1.5 atm pressure of O_2, although the products were agglomerated.[235]

In some cases, the use of carbonyl precursors is not necessary. ZrO_2, for instance, has been precipitated by ultrasonic irradiation of an aqueous solution containing $Zr(NO_3)_4$ and NH_4OH, followed by calcination at 300−1200 °C to improve the crystallinity or, for temperatures of 800 °C and above, to induce a tetragonal → monoclinic phase transition.[236] Nanoparticulate, perovskite-structured $La_{1-x}Sr_xMnO_3$ has been similarly prepared.[237]

Zheng et al. have developed an interesting variation of this method, in which 100−200 nm hollow

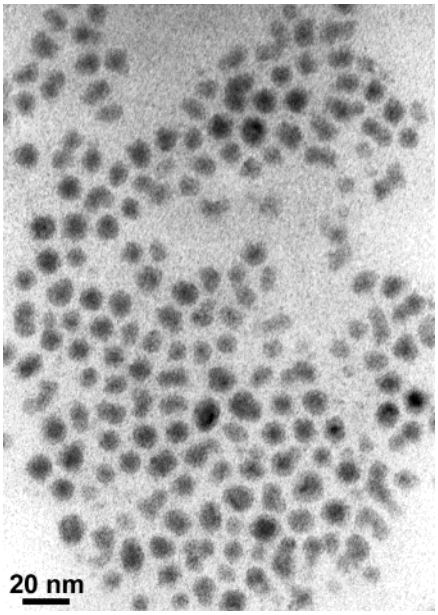

Figure 13. TEM image of colloidal Fe particles prepared by the sonochemical decomposition of $Fe(CO)_5$ in octanol. The particles are stabilized by oleic acid. (Reprinted with permission from ref 232. Copyright 1996 American Chemical Society.)

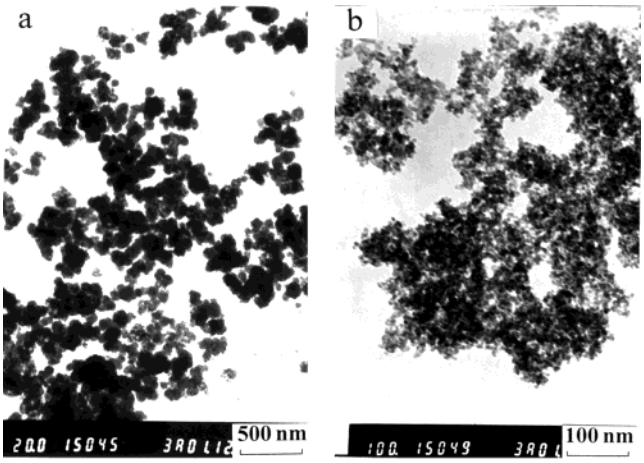

Figure 14. TEM image of CdSe nanoparticles synthesized in supramolecular vesicle templates. (Reprinted with permission from ref 238. Copyright 2002 Elsevier.)

spheres of CdSe have been precipitated by ultrasonic irradiation of a solution of Na_2SeO_3 and $CdCl_2$ in the presence of sodium dodecyl sulfate (SDS), an anionic surfactant that serves as a vesicle template (Figure 14).[238]

3. Sol-Gel Processing

3.1. Fundamentals of the Sol-Gel Process

Traditionally, sol-gel processing refers to the hydrolysis and condensation of alkoxide-based precursors such as $Si(OEt)_4$ (tetraethyl orthosilicate, or TEOS). The earliest examples of such reactions date to the work of Ebelmen in 1846.[239] Sol-gel processing did not garner wide attention until Geffcken and Berger devised a method of preparing oxide films from sol-gel precursors in the late 1930s, which proved useful in the manufacturing of stained glass.[240]

The versatility and general usefulness of modern sol-gel processing is reflected in the sheer volume of available literature. Since this review is limited to discussing those aspects of sol-gel processing relevant only to the synthesis of nanoparticles, the reader is referred to the literature for more detailed discussions of the broader applications of the method. Though somewhat dated, the review article by Hench and West provides an excellent overview of the theory concerning each step of the sol-gel process.[241] Several textbooks and reference works devoted entirely to the application and theory of sol-gel science are also available.[242−249]

Disregarding the nature of the precursors, which are discussed in sections 3.1.1−3.1.4, the sol-gel process can be characterized by a series of distinct steps.

Step 1: Formation of stable solutions of the alkoxide or solvated metal precursor (the *sol*).

Step 2: Gelation resulting from the formation of an oxide- or alcohol-bridged network (the *gel*) by a polycondensation or polyesterification reaction that results in a dramatic increase in the viscosity of the solution. If so desired, the gel may be cast into a mold during this step.

Step 3: Aging of the gel (*syneresis*), during which the polycondensation reactions continue until the gel transforms into a solid mass, accompanied by contraction of the gel network and expulsion of solvent from the gel pores. Ostwald ripening and phase transformations may occur concurrently with syneresis. The aging process of gels can exceed 7 days and is critical to the prevention of cracks in gels that have been cast.

Step 4: Drying of the gel, when water and other volatile liquids are removed from the gel network. This process is complicated due to fundamental changes in the structure of the gel. The drying process has itself been broken into four distinct steps:[241] (i) the constant rate period, (ii) the critical point, (iii) the first falling rate period, and (iv) the second falling rate period. If isolated by thermal evaporation, the resulting monolith is termed a *xerogel*. If the solvent is extracted under supercritical or near-supercritical conditions, the product is an *aerogel*.

Step 5: Dehydration, during which surface-bound M−OH groups are removed, thereby stabilizing the gel against rehydration. This is normally achieved by calcining the monolith at temperatures up to 800 °C.

Step 6: Densification and decomposition of the gels at high temperatures (T > 800 °C). The pores of the gel network are collapsed, and remaining organic species are volatilized. This step is normally reserved for the preparation of dense ceramics or glasses.

3.1.1. Precursors and the Partial-Charge Model

While the above steps are common to most sol-gel processes, the natures of the specific reactions involved in hydrolysis and condensation differ substantially between the various types of possible precursors. The processing of metal alkoxides, solvated metal cations, and organometallic precursors are discussed separately to avoid confusion.

Understanding of the formation, stability, and reactivity of alkoxides and solvated metal cations is greatly enhanced by a cursory understanding of the partial-charge model of Livage et al., in which the partial charge, δ, on an atom, i, is given by

$$\delta_i = \frac{(\bar{\chi} - \chi_i^0)}{k\sqrt{\chi_i^0}} \tag{43}$$

where χ_i^0 is the electronegativity of the atom, k is a constant (1.36 in the Pauling scale of electronegativity) and $\bar{\chi}$ is the mean electronegativity of the system. $\bar{\chi}$ is given by

$$\bar{\chi} = \frac{\sum_i p_i\sqrt{\chi_i} + kz}{\sum_i (p_i/\sqrt{\chi_i})} \tag{44}$$

where p_i is the stoichiometry of atom i, χ_i is the electronegativity of atom i, and z is the net charge of the ionic species. Though cumbersome to perform, calculations of partial charge provide meaningful insight into the chemistry of sol-gel precursors, and the partial-charge model is frequently invoked in the literature.

3.1.2. Sol-Gel Chemistry of Metal Alkoxides

Ebelmen's early work[239] involving the hydrolysis of $SiCl_4$ complexed with alcohols formed the basis of modern sol-gel processing. Although silicon alkoxide chemistry exhibits a number of peculiarities, the reaction mechanisms for the hydrolysis and condensation of $Si(OR)_4$, where R is an alkyl group, are analogous to those for many other metal alkoxides. $Si(OR)_4$ is discussed extensively here as an illustrative example. Detailed descriptions of the alkoxide chemistry of numerous elements are available elsewhere.[250]

$Si(OR)_4$ is easily prepared from $SiCl_4$ and the appropriate alcohol, as was reported in the original work of Ebelmen:[239]

$$SiCl_4 + ROH \rightarrow Si(OR)_4 + 4HCl \tag{45}$$

where R = CH_3, C_2H_5, or C_3H_7. The resulting products, in the absence of water, form a stable solution of $Si(OR)_4$ particles. The introduction of water into the system initiates hydrolysis. In acidic solution

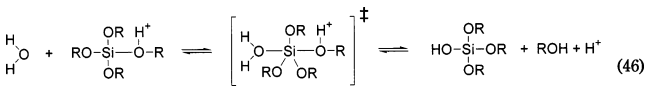

(46)

And in basic solution

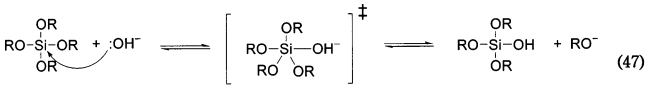

(47)

Note that eqs 46 and 47 are both nucleophilic substitution (S_N2) reactions, characterized by the pentacoordinate transition state of Si. Depending on the Si/H_2O ratio, more than one alkoxy group may be substituted:

$$Si(OR)_4 + nH_2O \rightarrow Si(OR)_{4-n}(OH)_n + nROH \tag{48}$$

Variation and control of n has profound consequences for the morphology and structure of the resulting gel.[251]

The relatively high electronegativity of Si weakens the O−H bonds to the extent that condensation can occur. Like hydrolysis, condensation of $Si(OR)_{1-n}(OH)_n$ can be catalyzed by either acid or base. Under acidic conditions

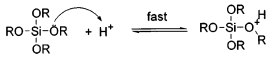

(49)

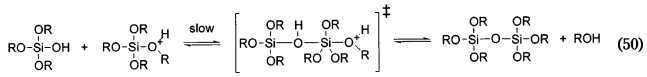

(50)

or

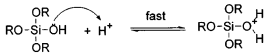

(51)

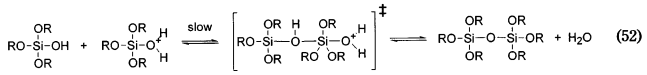

(52)

And under basic conditions

(53)

or

(54)

followed by

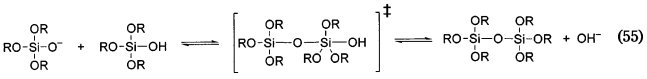

(55)

As noted previously, the degree of hydrolysis of the alkoxide precursor (n in $Si(OR)_{4-n}(OH)_n$) strongly influences the structure of the Si−O−Si network. Because OH^- is a marginally better leaving group than −OR, the condensation process can be tailored to favor the formation of dimers, chains, or 3-D agglomerates (Figure 15).

A similar effect has been demonstrated with titanium(IV) isopropoxide, $Ti(O^iPr)_4$, by substituting one or two of the O^iPr^- ligands with bidentate acetylacetonate (acac) (Figure 16). Condensation of $Ti(O^iPr)_4$ resulted in 10−20 nm particles. In comparison, condensation of the precursor in Figure 16a resulted in spherical, 5 nm particles, and condensation of the precursor in Figure 16b produced polymer chains.

Whether the hydrolysis is acid or base catalyzed also has important consequences for the structure of the resulting gel network. For $Si(OR)_{4-n}(OH)_n$ under acidic conditions (pH < 4), the rate of hydrolysis will always exhibit faster kinetics than the rate of condensation due to the ability of −OR groups to better stabilize the transition states in eqs 46 and 47. Moreover, the rate of condensation decreases with

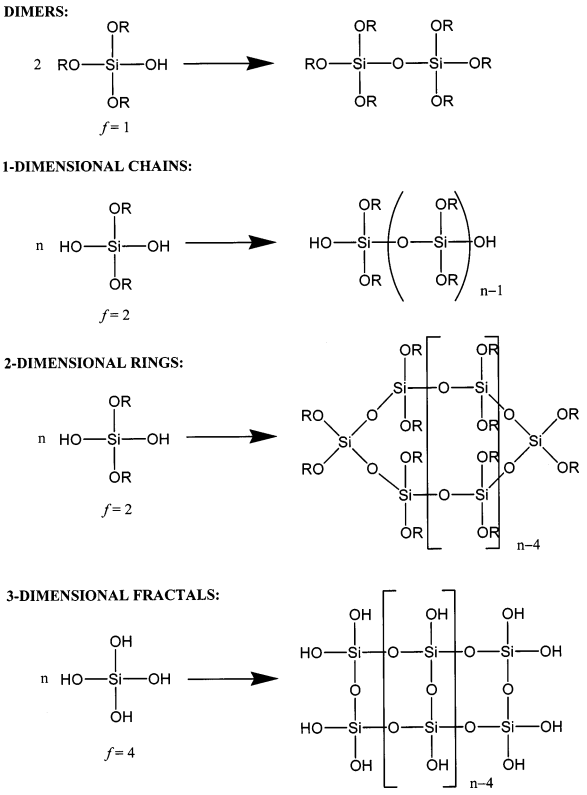

Figure 15. Precursors favoring the formation of dimers and 2-D and 3-D structural moeities in sol-gel processing of silicon alkoxides.

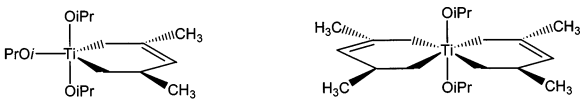

A B

Figure 16. Partial substitution of $(TiO^iPr)_4$ precursors. Condensation of precursor A results in spherical particles. Condensation of B results in polymer-like chains.

increasing *n*. As a result, Si−O−Si chains tend to preferentially form in the early stages of the polymerization process, followed by subsequent branching and cross-linking of the chains during aging. Under basic conditions, the stability of the transition states in eqs 46 and 47, and consequently the rate of hydrolysis, increases with increasing *n*. Under these conditions, the silica products tend to form large agglomerates that eventually cross-link. The differences between acid and base catalyzed reactions and the consequences for particle morphology are conceptually represented in Figure 17.[252]

3.1.3. Sol-Gel Chemistry of Aqueous Metal Cations

The tendency of transition metals to exhibit substantially lower electronegativities than Si greatly diminishes the stability of their alkoxide complexes against hydrolysis. This is reflected in the partial-charge model: the partial charge, δ, on the metal of a four-coordinate tetraethoxy complex ($M(OEt)_4$) is +0.32 for Si, +0.63 for Ti, and +0.74 for Zr. High positive charges on the metal tend to stabilize the transition state during hydrolysis. Consequently, the rate of hydrolysis for the titanium and zirconium

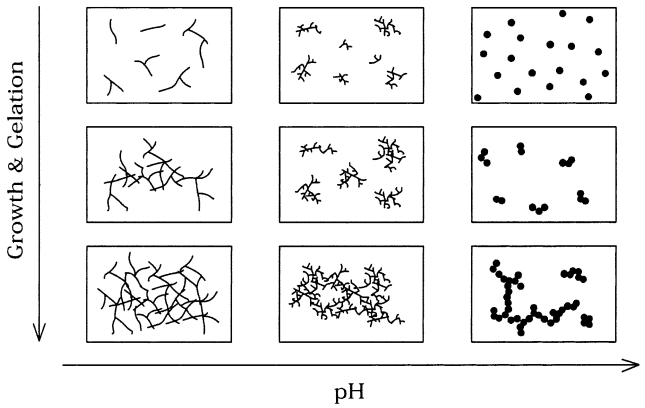

Figure 17. Effects of pH on particle morphology in sol-gel reactions. (Reprinted with permission from ref 252. Copyright 1996 Swiss Chemical Society.)

complexes is rapid, to the extent that special handling precautions must be taken to protect the complexes from water and oxygen. Likewise, the partial charges on the metals in alkali-metal alkoxides are so positive that their hydrolysis reactions are notoriously violent.

The hydrolysis and condensation of alkali-metal and alkaline-earth alkoxides in sol-gel type reactions can be achieved provided that one or more hydroxo ligands can be bound to the metal. For a transition metal M of charge *z*+ in aqueous solution, water molecules coordinate to the metal by transferring electrons from their bonding orbitals to empty d-orbitals on the metal:

$$M^{z+} + hH_2O \rightarrow [M(OH_2)_h]^{z+} \qquad (56)$$

where *h* is the coordination number of the cation. The electron-transfer weakens the O−H interactions of bound water, and depending on the pH of the solution, various degrees of hydrolysis (deprotonation) can be induced:

$$[M(OH_2)]^{z+} \leftrightarrows [M{-}OH]^{(z-1)+} + H^+ \leftrightarrows [M{=}O]^{(z-2)+} + 2H^+ \qquad (57)$$

Any solvated metal may then be generally represented as $[MO_NH_{2N-h}]^{(2-h)+}$ where *N* is the coordination number of the metal and *h* represents the molar ratio of hydrolysis. In the case of highly reactive compounds, controlling the hydrolysis ratio may necessitate the use of nonaqueous solvents, where hydrolysis is controlled by strict control of water in the system rather than by pH. Diao et al. have recently demonstrated the effectiveness of this approach in the preparation of gels from $Mg(OEt)_2$ in methanol and methanol−toluene solvents.[253]

In reactions involving less-reactive metal alkoxides, where aqueous solvents can be employed, the significance of pH in eq 57 is evident: acidic conditions force the equilibria to the left and favor the formation of hydroxo ligands, whereas basic conditions will force the equilibria to the right and favor oxo ligands. The charge on the metal, however, also plays a significant role in the above equilibria with respect to pH, given that highly positive charges on the metals tend to substantially weaken the O−H bonds and favor the

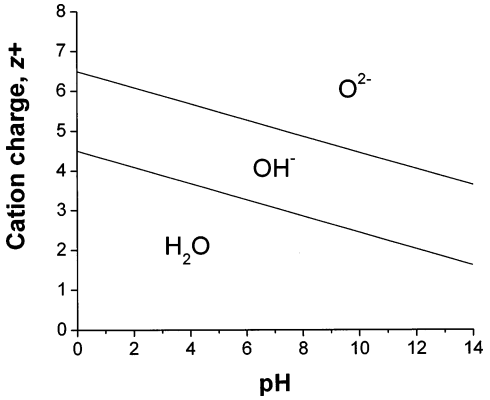

Figure 18. Relationship between charge, pH, and hydrolysis equilibrium of cations. (Reprinted with permission from ref 254. Copyright 1972 David Kepert.)

formation of oxo ligands. The relationships between charge, pH, and the position of the hydrolysis equilibria are represented in Figure 18.[254]

3.1.4. Condensation Reactions of Hydrolyzed Metals

When the cation of a metal-alkoxide complex is coordinatively unsaturated (when the coordination number N is equal to the cation's charge, z), condensation occurs via an S_N2 reaction:

$$M_1{-}OX + M_2{-}OY \rightleftharpoons M_1{-}\overset{X}{O}{-}M_2 + OY \quad (58)$$

When, however, the metal is coordinatively saturated ($N - z > 0$), nucleophilic addition occurs:

$$M_1{-}OX + M_2{-}OY \rightleftharpoons M_1{-}\overset{X}{O}{-}M_2{-}OY \quad (59)$$

The three types of ligands that are possibly formed during hydrolysis differ significantly with respect to their partial charges. As a consequence, the reactivity of the metal cation will vary, as well. Because the condensation of hydrolyzed metals occurs via nucleophilic substitution and nucleophilic addition mechanisms, the most important characteristics of the ligands are their nucleophilicity and leaving group behavior. As evident in eqs 58 and 59, the condensation of hydrolyzed metals requires that the metal be bound to at least one good nucleophile and one good leaving group. High nucleophilicity requires that the partial charge of the ligand be less than zero, and the more negative the better. The partial charges of the ligands vary as $\delta(O^{2-}) < \delta(OH^-) < \delta(OH_2)$, irrespective of the metal they are bound to. Thus, in general, oxo ligands are good nucleophiles but poor leaving groups, aquo ligands are good leaving groups but poor nucleophiles, and hydroxo ligands can serve as either nucleophiles or leaving groups. Since at least one hydroxo ligand is usually necessary for condensation to occur, operation in the hydroxo region of Figure 18 becomes paramount.

3.1.5. Xerogel and Aerogel Formation

As a gel is evaporated to dryness, either by thermal evaporation or supercritical solvent extraction, the gel structure changes—in some cases substantially. During thermal drying or room-temperature evaporation, capillary forces induce stresses on the gel that increase the coordination numbers of the particles and induce collapse of the network. The increase in particle coordination numbers results in the formation of additional linkages that strengthen the structure against further collapse and eventually lead to the formation of a rigid pore structure. The structure of the resulting xerogel can therefore be considered a collapsed, highly distorted form of the original gel network.

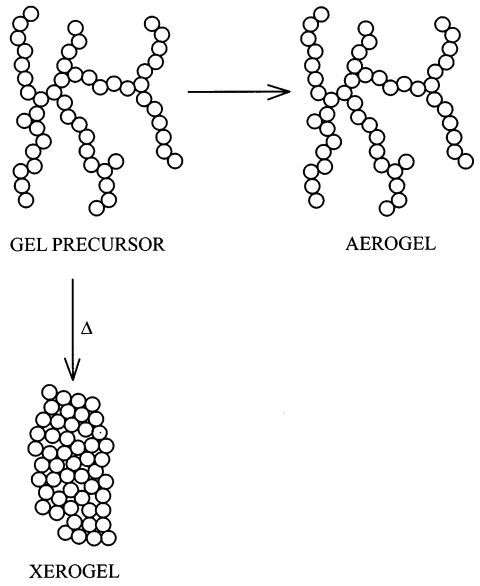

Figure 19. Structural relationship between a sol-gel precursor, a xerogel, and an aerogel.

The supercritical extraction of solvent from a gel does not induce capillary stresses due to the lack of solvent−vapor interfaces. As a result, the compressive forces exerted on the gel network are significantly diminished relative to those created during formation of a xerogel. Aerogels consequently retain a much stronger resemblance to their original gel network structure than do xerogels (Figure 19). Detailed investigations of the structural evolution of sol gels during aging and drying have been published.[255]

3.1.6. Gel Sintering

The sintering of gels, where the pore network is collapsed and organic species are volatilized, is a critical factor in determining the size and morphology of the sol-gel product. Due to the amorphous structure of the gels, the sintering process is governed primarily by viscous flow. The rate of contraction of the gel networks, ϵ, is given by[256]

$$\epsilon = \frac{\gamma_{SV}\sqrt[3]{N}}{\eta} \quad (60)$$

where γ_{SV} is the gel's surface energy, η is the viscosity, and N is the number of pores per unit volume. At least one topical review on the viscous sintering of gels is available, although it pertains primarily to the preparation of glasses.[257]

3.1.7. Controlling Particle Size and Morphology

As discussed in section 3.1.2, the gel network structure formed by acid- or base-catalyzed hydrolysis of metal alkoxides can be tailored to favor the formation of polymeric chains with extensive cross-linking and branching or the formation of discrete spherical particles with minimal cross-linking. For the purpose of preparing nanoparticles, base-catalyzed hydrolysis is clearly preferred, though not always necessary. In any event, experimental evidence suggests that precursor structure is at least as important as control of pH in directing the size and morphology of sol-gel products.[258]

In the case of hydrolyzed cations, controlling the hydrolysis equilibrium can be particularly effective for directing the structure of the product. The sol-gel processing of V_2O_5 is a vivid example. When $NaVO_3$ is solvated in water, cyclic $[V_4O_{13}]^{4-}$ results. When passed through an ion exchange column, $[V_4O_{13}]^{4-}$ is converted to vanadic acid, H_3VO_4, which in aqueous solution coordinates two water molecules to bring the coordination number of vanadium to six.[259] Because the V=O and one of the $V(OH_2)$ groups lie along the *z*-axis, condensation is restricted to two dimensions along the $x-y$ direction. Condensation (olation) along the *y*-axis, producing corner-sharing octahedral chains, is fast due to the H_2O ligand being a good leaving group. Condensation along the *x*-axis (oxolation), resulting in edge-sharing octahedral chains, is comparatively slow. Consequently, the resulting product consists of ribbonlike chains.

3.2. Sol-Gel Synthetic Methods

3.2.1. Sol-Gel Syntheses of Oxides

Although the 1988 review by Livage et al. on the sol-gel chemistry of transition metal oxides is somewhat dated and does not specifically address the synthesis of nanoparticles, the paper still ranks as one of the more comprehensive and authoritative articles written on sol-gel processing.[260] The discussion here focuses on recent advances in the sol-gel processing of nanoparticulate oxides.

An important distinction should be made between processes in which a xerogel or aerogel is the end product and those in which the xerogel or aerogel serves as a precursor that is subsequently calcined, sintered, and so forth. Despite supercritical drying, in the absence of a calcination step, many aerogel reactions will yield amorphous, although nanoparticulate, products. Condensation and supercritical drying of a $Zr(NO_3)_4 \cdot 5H_2O$ or $ZrO(NO_3)_2 \cdot 2H_2O$ precursor in alcohol, for instance, produced amorphous, ~1 nm particles of ZrO_2.[261,262] Calcination of the product at 400 °C resulted in 2−3 nm agglomerated particles with a mixed tetragonal/monoclinic phase composition.

Calcining an aerogel or xerogel will improve the crystallinity of the sample but normally leads to agglomeration. This can be limited, however, if the calcination conditions are kept moderate. Hamdeh et al. have prepared spinel-structured $Ge_{0.5}Fe_{2.5}O_y$ nanoparticles by initiating hydrolysis of a mixture containing $Ge(OMe)_4$, $Fe(OAc)_2$, and methanol and drying the product supercritically.[263] Despite annealing at 500 °C, only slight agglomeration of the nanoparticles was observed.

Neiderberger et al. have developed an interesting variation of the sol-gel method that produces nanocrystalline products without a calcination step.[264] The method involves a nonhydrolytic sol-gel type reaction between a metal chloride and benzyl alcohol that presumably forms a $MCl_{4-x}(OCH_2Ph)_x$ or similar intermediate that undergoes acid-catalyzed hydrolysis by eqs 49 and 50. Particle size was controllable in the range 4−8 nm by variation of temperature and reactant concentrations. The process has since been extended to vanadium and tungsten oxides.[265]

Other authors have demonstrated that titania nanoparticles are easily prepared by controlled hydrolysis and condensation of $Ti(O^iPr)$ in an alcohol solution acidified with HCl followed by supercritical drying.[266,267] Recently, several groups have published rather elaborate studies on the factors influencing the particle sizes and particle size distributions resulting from this reaction. Zhu et al. have detailed the morphology of the products by electron microscopy and small-angle neutron scattering.[268,269] Hsu et al. studied the effects of varying the alkoxide/water ratio, HCl concentration, reactant feed rate, and temperature.[270] Their results indicate that the alkoxide/water (hydrolysis) ratio and HCl concentration are the most influential parameters governing both mean size and size distribution. Liu et al. investigated the influence of UV radiation on the hydrolysis and condensation of $Ti(O^iPr)_4$ in propyl alcohol.[271] They found that UV radiation increased the oxygen defect concentration in the as-prepared amorphous TiO_2, thereby allowing conversion to crystalline anatase at temperatures as low as 100 °C.

Oliveria et al. have adapted the sol-gel synthesis route for titania nanoparticles described above to the synthesis of $Ti_xSn_{1-x}O_2$ solid solutions.[272] While rutile-structured $Ti_xSn_{1-x}O_2$ solid solutions are well documented, this appears to be the first report of an anatase-structured $Ti_xSn_{1-x}O_2$ solid solution.

In an excellent demonstration of the tailoring of precursors to create a homogeneous network of mixed-metal cations, Yu et al. prepared 60 nm particles of phase-pure $PbTiO_3$ by the hydrolysis and condensation of a precursor consisting of lead lactate ($Pb(CH_3CHOHCOO)_2$) and $Ti(OBu)_4$ followed by calcinations of the product at 420 °C or higher.[273]

Similarly, Gun'ko et al. prepared precursors specifically tailored to the hydrolysis/condensation chemistry of the sol-gel process.[274] The precursors, in this case, were substituted metal alkoxides, such as

$$FeBr_2 + 2NaO^tBu + THF\ (\text{excess}) \rightarrow Fe(O^tBu)_2(THF)_2 \quad (61)$$

The precursor formed in eq 61 was subsequently decomposed by ultrasonic irradiation, and the resulting precipitate was dried at 300 °C to yield ~15 nm Fe_3O_4 (Figure 20). Starting from precursors of $Fe[NC(C_6H_4)C(NSiMe_3)_2]_2Cl$ or $Fe_2(OSiPh_2)_3$ resulted in nanoparticulate γ-Fe_2O_3 or $Fe_2O_3-SiO_2$ composites, respectively.

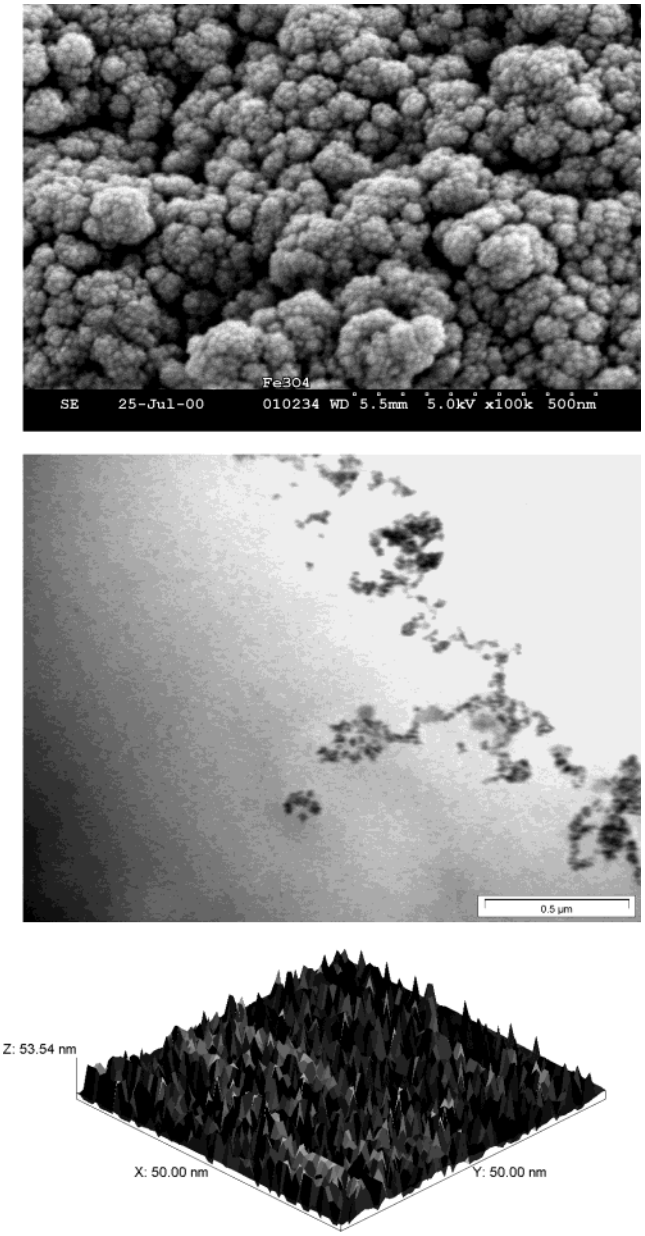

Figure 20. SEM (top), TEM (middle), and AFM (bottom) images of Fe_3O_4 nanoparticles prepared by the hydrolysis/condensation of a metallorganic precursor. (Reprinted with permission from ref 274. Copyright 2001 Kluwer Academic Publishers.)

As an example of the variety of materials that can be prepared by the condensation of hydrolyzed metals, Cerda et al. prepared 200−500 nm $BaSnO_3$ by calcining a gel formed between $Ba(OH)_2$ and K_2SnO_3 at pH ∼ 11.[275] The product contained a $BaCO_3$ impurity unless calcined above 1000 °C, which led to substantial aggregation of the particles.

In recent years, the application of xerogels and aerogels in electrochemical energy storage has gained increased attention. The high surface areas and mesoporous structures of xerogels and aerogels appear to allow the storage of substantially more energy than the same compounds prepared as dense, crystalline powders.[276−278] Unfortunately, only a handful of elements exhibit metal-alkoxide chemistries amenable to sol-gel type syntheses. Investigations have therefore been limited primarily to V_2O_5,[279,280] MoO_3,[279,281] and MnO_2[282,283] aerogels in batteries and RuO_2-TiO_2[284] nanocomposites in supercapacitors. A recent review on the application of aerogels in electrochemical energy conversion and storage has been published by Rolison and Dunn[285,286] and is also covered in the review by Livage et al.[260]

3.2.2. Sol-Gel Syntheses of Other Inorganics

Though sol-gel methods are most commonly used to synthesize oxides, the syntheses of carbides, nitrides, and sulfides by sol-gel processes are also known. In these instances, hydrolysis reactions, which invariably produce hydroxides and oxides, were avoided by performing the reactions in aprotic solvents under inert atmospheres.

Kim et al. have recently reported the synthesis of TiN by thermal decomposition of a titanium alkoxy hydrazide precursor.[287] The precursor was prepared by addition of anhydrous hydrazine to titanium(IV) isopropoxide in anhydrous acetonitrile to yield a complex of composition $Ti(O^iPr)_{0.83}(N_2H_3)_{1.17}(NH)_2 \cdot 3CH_3CN$. Subsequent decomposition of the precursor under nitrogen at 1000 °C resulted in 10−20 nm TiN. The lack of oxides in the product is surprising, given the presence of O^iPr^- in the precursor. The authors attributed this to the presence of carbon (from CH_3CN) inhibiting the crystallization of an oxide phase. The same authors have reported the syntheses of ∼10 nm AlN[288] and AlON[289] powders by similar routes.[249]

Nanoparticulate agglomerates of TiS_2 and NbS_2 have been prepared by reaction of $Ti(O^iPr)_4$ or $Nb(OEt)_5$ with H_2S in benzene and acetonitrile solutions, respectively, to yield metal alkoxysulfide intermediates.[249,290] In these cases, the metal alkoxides undergo thiolysis that is mechanistically similar to hydrolysis in many respects. The alkoxysulfides were decomposed at 600−800 °C under flowing H_2S to yield the metal sulfides.

3.2.3. Sol-Gel Processing of Nanocomposites

The sol-gel processing of silicon alkoxides allows the low-temperature preparation of amorphous phases. When metal oxides or metal chalcogenides are hydrolyzed and condensed simultaneously with silicon alkoxides, the metal-containing nanoparticles become dispersed in an amorphous silica matrix. The nanoparticles embedded in the silica tend to exhibit extremely narrow size distributions, and if the metal nanoparticle concentration is kept low, the particles tend to be very well dispersed. Furthermore, the silica matrix tends to exhibit mesoporous structural features, giving the composites high porosities and allowing for rapid mass exchange with liquids and gases. As such, nanoparticles dispersed in glass matrixes are very useful as heterogeneous catalysts[291−294] and chemical sensors.[295−297] The highly dispersed imbedded particles also greatly facilitate investigations of magnetic properties, since interparticle interactions can be minimized. Furthermore, imbedding nanoparticles in an amorphous matrix can have profound consequences for the nonlinear optical properties of materials, particularly when the nanocomposite is prepared as a thin film.[298−300]

Most sol-gel-based nanocomposite syntheses can be categorized as involving either (a) the mixing of a preformed colloidal metal (or oxide) with a sol containing the matrix-forming species followed by gelation, (b) the direct precipitation of metal, metal oxide, and so forth nanoparticles within a prehydrolyzed silica sol, or (c) complexing the metal to a functionalized silane and reducing the metal prior to hydrolysis/condensation. Bronstein et al. have recently published a comprehensive review of these techniques.[301]

With respect to the first approach described above, the colloidal metal or metal oxide nanoparticles will normally contain a stabilizing agent at the particles' surfaces (see section 2.1.4). Consequently, the size and size distribution of the individual colloidal particles are largely determined by their method of synthesis, before they are ever introduced into the sol. If the resulting gel is heated to even moderately high temperatures, however, the stabilizing agent may decompose, leaving the colloidal particles subject to aggregation unless the colloid concentration within the sol is very low. Nanocomposites consisting of gold imbedded in silica matrixes are a common target with this approach, which is not surprising given the well-developed methods of preparing Au colloids and the potential applications of gold nanoparticles in heterogeneous catalysis. Anderson et al. prepared such a composite by adding a sol of colloidal Au (prepared by the citrate method) to a silica sol, casting the sol into a mold, and drying the composite supercritically to form an aerogel.[302] They were able to demonstrate the porosity of the silica matrix by adsorbing methyl orange on the surfaces of the Au nanoparticles after the composite had been cast and dried. Others have prepared similar composites starting from Au nanoparticles passivated with dodecanethiol.[303] Wallace et al. have adapted such $Au-SiO_2$ composites to allow the Au nanoparticles to act as nucleating agents for self-organized protein superstructures that are subsequently encapsulated in the silica matrix after supercritical drying.[304]

Morris et al. developed an intriguing variation of this technique in which the colloidal solid is added to a silica sol just prior to gelation.[305] By minimizing the time of interaction between the colloidal particles and the silica network, the colloids were not fully encapsulated by the silica network, which may be significant in terms of preserving the properties of the guest species (catalytic activity, optical properties, etc.). Colloidal particles of Pt, Au, carbon black, titania, and Fe^{II}(bpy) imbedded in zeolite have been successfully incorporated into SiO_2 matrixes in this manner.

Richard-Plouet et al. modified this technique such that Co^{2+} ions were complexed to PVA-based polymeric "microcapsules" prior to addition to a silica sol.[306] Thermal treatments of the resulting gels under a reducing atmosphere resulted in the formation of Co nanoparticles with an average diameter of ~50 nm. The silica matrix appeared to stabilize the Co particles against oxidation.

Zhang et al. have adapted this technique to the synthesis of luminescent $Si-SiO_2$ nanocomposites.[307] The Si nanoparticles were stabilized with amino acids prior to addition to a TEOS solution at low pH. The gels were aged and dried at room temperature to form xerogels. The photoluminescences of the composites were found to vary significantly, depending primarily on the capping ligand.

With respect to the second approach, precipitation of metal or metal oxide particles from their precursors is carried out within the silica sol, usually by a low-temperature heat treatment. This in-situ nucleation/growth approach is generally used for the preparation of thin films,[308] but solid monoliths may also be prepared this way.

Liz-Marzán et al. developed a technique to apply SiO_2 coatings to colloidal Au, forming an $Au@SiO_2$ core−shell arrangement.[309] The Au sol was prepared by the citrate method and a solution containing (3-aminopropyl)trimethoxysilane (3-APTMS) was added to it, followed by a solution of sodium silicate. The amino functional groups of the 3-APTMS were effectively bound to the Au surfaces. The Si−O−Si network was formed by addition of the silicate ions under basic conditions:

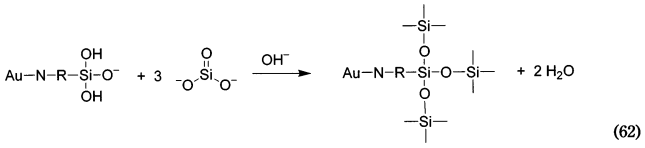

(62)

After deposition of the initial SiO_2 shell, the thickness of the SiO_2 layer could be increased by mixing the product with TEOS dissolved in an ethanol solution; SiO_2 shells as thick as 83 nm have been successfully grown (Figure 21). Lu et al. were able to prepare $Au-SiO_2$ with shells as thick as 80 nm by a similar method in which the shells were deposited on Au colloids from TEOS solutions and the thickness was controlled by adjusting the reaction time.[310] $Ag@SiO_2$,[311] $Fe_2O_3@SiO_2$,[312] $Fe_3O_4@SiO_2$,[313] and $CdTe@SiO_2$[314] nanoparticles have been prepared by similar schemes.

Cheng et al. prepared $Au-SiO_2$ by combining colloidal gold with a prehydrolyzed TEOS solution in the presence of a dibenzoyltartaric acid stabilizer.[315] After aging and drying, the resulting aerogel was calcined at 550 °C to produce 2−8 nm Au particles homogeneously distributed in amorphous silica with 3−4 nm pores. Others have achieved similar results with Au imbedded in borosilicate glass.[316]

Fonseca et al. prepared $Ni-SiO_2$ nanocomposites by adding a mixture of $Ni(NO_3)_2$ and TEOS to a solution of citric acid dissolved in ethanol.[317] Polyesterification was induced by addition of ethylene glycol to the reaction mixture, and pyrolysis was carried out at 500 °C under inert atmosphere. The nickel ions were reduced by CO generated from pyrolysis of the organic matrix. The resulting $Ni-SiO_2$ nanocomposite contained 1.5−5 wt % of ~3 nm Ni particles dispersed in amorphous SiO_2. The embedded Ni particles exhibited no signs of oxidation, suggesting that the SiO_2 matrix protects the embedded particles.

Corrias et al. have reported $FeCo-SiO_2$ composites prepared in a similar manner.[318,319] Interestingly, the nature of the counterion in the metal salts was observed to influence the structure of the resulting

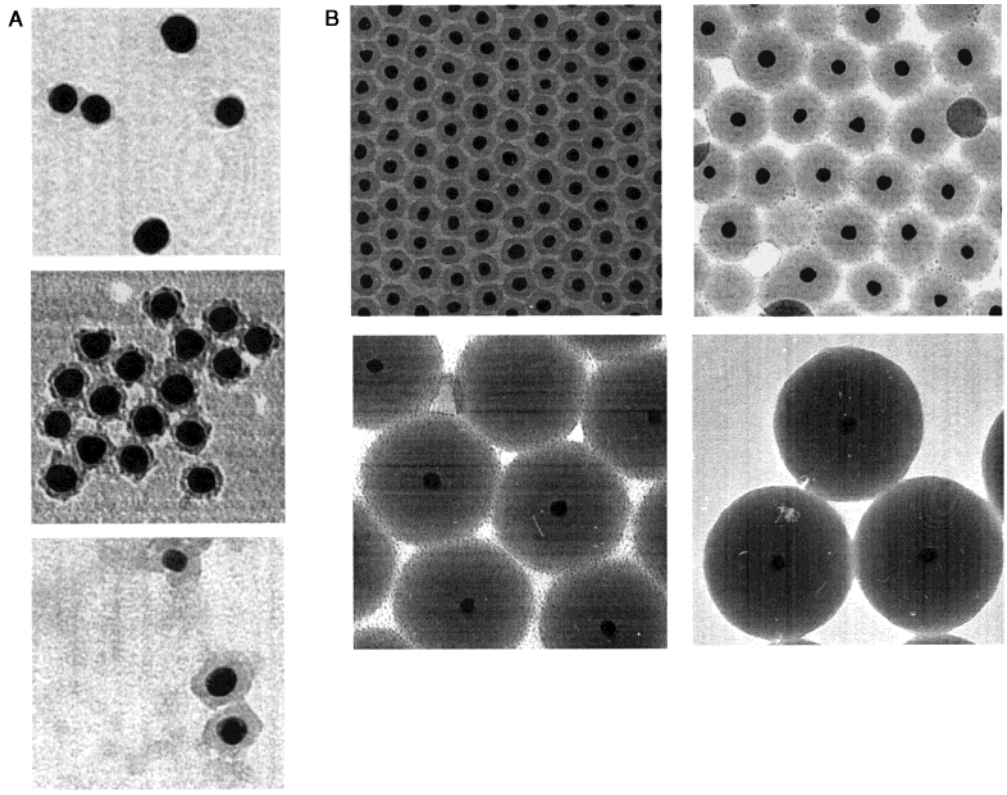

Figure 21. (A) TEM images of 15 nm Au particles coated with thin silica layers: (top) 18 h after addition of active silica; (center) 42 h after addition; (bottom) 5 days after addition. (B) The silica shell keeps growing, but eventually small SiO_2 particles nucleate from solution. (Reprinted with permission from ref 309. Copyright 1996 American Chemical Society.)

nanocomposite, in that metal nitrates favored the formation of low-density aerogels via a ferrihydrite + Co_3O_4 intermediate,[320] whereas metal acetates favored higher-density xerogels via a $CoFe_2O_4$ intermediate.[321]

The technique of precipitating a metal in a prehydrolyzed silica sol has also recently been employed by Wu et al. for the preparation of $Ag-SiO_2$ nanocomposites.[322] Aqueous $AgNO_3$ solutions were added to prehydrolyzed TMOS sols prior to gelation. When the condensation reaction was catalyzed by HCl, reduction of Ag^+ occurred via the photodecomposition of an AgCl intermediate. When catalyzed by HNO_3, the Ag^+ reduction was explained as the likely result of photodecomposition of a complex formed between Ag^+ and methanol radicals resulting from TMOS hydrolysis. Morley et al. have prepared similar $Ag-SiO_2$ nanocomposites by thermal decomposition of Ag^+ complexes in silica sols in $scCO_2$.[323]

Casas et al. have precipitated iron oxides in silica sols by combining $Fe(NO_3)_3 \cdot 9H_2O$ with TEOS in ethanol.[324] The hydrated iron salt provided sufficient water to induce hydrolysis of the orthosilicate. When dried supercritically, their method resulted in ~5 nm particles of $Fe_5HO_8 \cdot 4H_2O$ imbedded in a porous silica matrix. No phase change was observed when the samples were calcined. When prepared as a xerogel, however, the iron nanoparticles were amorphous and crystallized as a mixed γ/α-Fe_2O_3 phase when calcined at 400 °C or pure α-Fe_2O_3 when calcined at 600 °C. Others have prepared $NiO-SiO_2$ and $Ni-SiO_2$ nanocomposites by similar methods.[325,326]

With respect to the third approach of preparing metal−silica nanocomposites, where metal−silane complexes are reduced to form metal nanoparticles prior to hydrolysis/condensation of the sol, Bharathi prepared $Au-SiO_2$ by complexing an amino-functionalized silane to $HAuCl_4$, inducing gelation, and reducing the metal cations with sodium borohydride.[327] By binding to the gold surfaces, the aminosilane groups ensured good homogeneity of the Au particles. Subsequent hydrolysis and condensation of the silanes resulted in the formation of the Si−O−Si network in which the Au particles were dispersed. The resulting gels could be dried into monoliths or deposited as thin films. An interesting variation of this experiment involves initiating hydrolysis/condensation of the silane prior to reduction of the metal, which yields 4−6 nm $Au-SiO_2$, $Pt-SiO_2$, or $Pd-SiO_2$, but 2−20 nm $Ag-SiO_2$ particles.[328]

Kobayashi et al. took a somewhat different approach to the synthesis of $Au-SiO_2$ composites by first preparing $Au@SiO_2$ core−shell particles and subsequently imbedding them in an amorphous SiO_2 matrix.[329] The $Au@SiO_2$ was prepared by addition of an aminosilane and sodium silicate to colloidal Au prepared by the Turkevich method, resulting in Au nanoparticles with 5−7 nm thick SiO_2 shells in a stable dispersion.[309] The $Au@SiO_2$ particles were imbedded in a SiO_2 matrix by adding sodium silicate or TMOS to the $Au@SiO_2$ dispersion, lowering the pH, and inducing hydrolysis/condensation of the Si−O−Si network. As such, the possibility of the colloidal particles agglomerating prior to gel formation was greatly diminished and the $Au@SiO_2$ exhibited excellent dispersion in the silica matrix.

Nanocomposites formed by sol-gel processing are not limited to metal nanoparticles or to silica ma-

trixes. Claus et al. developed a similar method for imbedding gold nanoparticles in a TiO_2 matrix by substituting $Ti(OBu)_4$ for TEOS, adding colloidal gold by dropwise addition, and calcining the dried gel at 450 °C. The resulting $Au-TiO_2$ composite contained Au particles with a mean diameter of 1.1 nm. Others have prepared $Au@ZrO_2$ core−shell particles by a similar method.[330]

Caizer et al. have reported a series of $Zn_xNi_{1-x}Fe_2O_4$ ($x = 0.15, 0.35, 0.65$) nanoparticles imbedded in SiO_2 by simply adding TEOS to a water−ethanol solution containing the proper stoichiometric ratios of dissolved metal nitrates.[331] After drying, the gels were annealed at 1100 °C. The products consisted of amorphous silica containing a near-homogeneous dispersion of 8−20 nm oxide particles. $Ni-SiO_2$, γ-$Fe_2O_3-SiO_2$, and $ZnO-SiO_2$ nanocomposites have been prepared by almost identical methods, but usually with lower calcinination temperatures, or calcination under an H_2 atmosphere in the case of Ni.[332]

Xing et al. prepared ZnO−BN and TiO_2−BN assemblies by combining ZnO or TiO_2 sols suspended in ethanol with a mixture of boric acid and urea, also dissolved in ethanol.[333] The BN is formed by

$$H_3BO_3 + CO(NH_2)_2 \rightarrow BN + H_2O + CO\uparrow \quad (63)$$

and the resulting gels were calcined at 200−700 °C after drying. The products consisted of 10 nm ZnO or 17 nm TiO_2 encapsulated in concentric BN sheets.

3.3. The Pechini Method

In 1967, Pechini developed a modified sol-gel process for metals that are not suitable for traditional sol-gel type reactions due to their unfavorable hydrolysis equilibria.[334] Although Pechini's original method was developed specifically for the preparation of thin films, it was later adapted to the synthesis of powdered products.

The Pechini method, as it is now referred to, relies on the formation of complexes of alkali metals, alkaline earths, transition metals, or even nonmetals with bi- and tridendate organic chelating agents such as citric acid. A polyalcohol such as ethylene glycol is added to establish linkages between the chelates by a polyesterification reaction, resulting in gelation of the reaction mixture. This process is represented schematically in Figure 22. ^{13}C and ^{87}Sr NMR studies of some gelled precursors have recently been published.[335−337] After drying, the gel is heated to initiate pyrolysis of the organic species, resulting in agglomerated submicron oxide particles.

The advantage of the Pechini method lies in the elimination of the requirement that the metals involved form suitable hydroxo complexes. Chelating agents tend to form stable complexes with a variety of metals over fairly wide pH ranges, allowing for the relatively easy synthesis of oxides of considerable complexity. Review articles covering the Pechini process are available, although rare.[338,339]

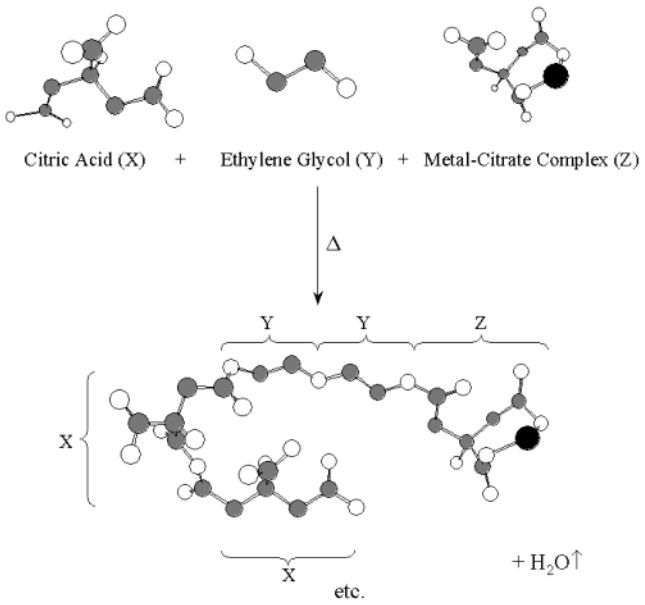

Figure 22. Conceptual representation of the condensation between a metal cation, citric acid, and a polyol: the early stages of the Pechini method. (Adapted from ref 338 with permission from the American Ceramic Society, www.ceramics.org. Copyright 1999. All rights reserved.)

3.3.1. Chelate Selection and Complex Formation

The literature contains numerous variations of the Pechini method, most involving alternative chelating agents. Ethylenediaminetetraacetic acid (EDTA) is occasionally substituted for citric acid.[340,341] EDTA is widely used as a complexing agent for quantitative complexometric titrations due to its ability to bind almost any cation. The four carboxylate groups allow the molecule to behave as either a bi-, tri-, tetra-, penta-, or hexadendate ligand, depending on the pH of its solution. Although EDTA's binding ability tends to increase with increasing pH, the polyesterification reaction between carboxylic acids and polyalcohols that is necessary for gelation is acid catalyzed. Fortunately, due to its zwitterionic character, EDTA will still bind many metals as a bidentate ligand, even under highly acidic ($pH < 4$) conditions.

Oxalic acid and polymeric alcohols such as poly(vinyl alcohol) (PVA) have also been used as chelating agents for Pechini type syntheses.[342,343] In the case of polymer alcohols, given the 3-D network provided by the polymer, addition of a polyol and subsequent esterification are not necessary. The polymer is simply combined with the metal cations in solution to form a precursor that is subsequently calcined to pyrolyze the organic species. These reactions are sometimes referred to as *polymer combustion syntheses*.

There are a number of syntheses reported in the literature that, while similar to the Pechini method in their use of carboxylic acid-based chelating agents and pyrolysis of the resulting precursors, forego the use of a polyol or similar reagent to induce polymerization.[344,345] As such, it is unclear whether these solutions are in fact forming gels or simply contain precipitated metal−citrate complexes. We have noted that the products of such reactions tend to exhibit relatively large crystallite sizes with irregular morphologies.[346,347]

Table 5. Representative Sampling of Oxides Prepared by the Pechini Method

compd	starting material	chelating agent	polymerization agent	calcination temp (°C)	product size (nm)	ref
$ZnTiO_3$	$Zn(OAc)_2$ $Ti(OBu)_4$	CA	EG	500−1000	18−31	348
$SrTiO_3$	$Ti(OBu)_4$	CA + PAA	EG	550−700	<500	349
$YNi_{0.33}Mn_{0.67}O_3$	$Y(NO_3)_3$ $Ni(NO_3)_2$ $Mn(NO_3)_2$	CA	EG	750−800	17	350
$YBa_2Cu_3O_{7-\delta}$	$Y(NO_3)_3$ $BaCO_3$ $CuCO_3$	CA	EG	920	not stated	351
$Y_xZr_{1-x}O_{2-x/2}$	$Y(NO_3)_3$ $ZrCl_4$	CA	EG	600−1000	∼20	352
$Zr_xCe_{1-x}O_2$ ($x = 0.35$)	$ZrOCl_2$ $(NH_4)_2Ce(NO_3)_6$	glycine	none	600	13	353
$BaTiO_3$	$BaCO_3$ $Ti(O^iPr)_4$	CA	EG	700−1100	50−340	354
$BaCeO_3$	$BaCO_3$ $Ce(NO_3)_3$	CA	EG	800−1000	∼100	355
$LaCoO_3$	$La(NO_3)_3$ $Co(NO_3)_2$	glycine	none	800	35	356
$RE_xLi_{1-x}NbO_3$ (RE = La, Pr, Sm, Er)	Li_2CO_3 Nb-ammonium complex La_2O_3 $Pr_2(CO_3)_3$ $Sm_2(CO_3)_3$ $Er_2(CO_3)_3$	CA	EG	500−900	40−60	357
$La_{1.85}Sr_{0.15}CuO_4$	$La(NO_3)_3$ $SrCO_3$ $Cu(NO_3)_2$	CA	EG	900	<1 μm	351
$Pb_3MgNb_2O_9$	$PbCO_3$ $MgCO_3$ $Nb(OEt)_5$	CA	EG	400−800	∼50	358
$Bi_2Sr_2Ca_{n-1}Cu_nO_{4+2n+\delta}$ ($n = 1, 2, 3$)	$Bi(NO_3)_3$	EDTA	none	700	not stated	359

3.3.2. Limitations of the Pechini Method

The primary disadvantage of the Pechini method lies in the lack of control over particle size, shape, and morphology. Unlike traditional sol-gel processes, where the metal itself becomes an integral part of the gel network, the gel network in the Pechini method is formed by the esterification of the chelating agent and polyalcohol. The metal ions are essentially trapped in the organic matrix, to which they are weakly bound. As such, the Pechini method cannot easily produce specific structural moieties such as 2-D chains and ribbons. The particles obtained after calcination are virtually always spherical or nearly spherical, and at least some aggregation from sintering should be expected.

The Pechini method does afford some control over particle size, but this is primarily achieved by variation of the calcination temperatures. If a pure product (free of organic contaminants) is to be obtained, calcination temperatures of at least 300 °C are usually necessary, and some chelating agents require substantially higher decomposition temperatures. Furthermore, although the Pechini method could, in theory, be adapted to the synthesis of sulfides, carbides, or nitrides, to our knowledge, no such synthesis has ever been reported. The method should therefore be considered limited to the synthesis of oxides.

Given the above limitations, it is not surprising that the Pechini method is frequently used to prepare fine particles that are subsequently compacted and sintered into dense ceramic pellets. This is particularly useful for materials used as electrodes in devices such as the solid-oxide fuel cell (SOFC), where the electrodes must be sufficiently dense as to not allow permeation of gases through cracks or pores.

3.3.3. Oxide Syntheses with the Pechini Method

The number of oxides prepared by the Pechini method now stretches into the hundreds. A representative sampling demonstrating the flexibility of the method is given in Table 5. The discussion here should be considered an overview of recent developments and representative examples.

Most syntheses involving the Pechini method still use citric acid as the metal chelating agent and ethylene glycol as the polyol. Among the more recent oxides prepared this way are 25 nm Y_2O_3,[360] 500 nm $Bi_2Ru_2O_7$,[361] sub-100 nm lanthanide-doped $Y_3Al_5O_{12}$ (YAG),[362] $LiMn_2O_4$,[363] $BaFe_{12}O_{19}$,[364] and numerous perovskite-structured materials, such as $LaCoO_3$[365] and $Ba(In_{0.67}Mo_{0.33})O_3$.[366]

Oxides prepared using EDTA as chelating agent include $Ba_2Ti_9O_{20}$. The substitution of EDTA for citric acid substantially reduced the amount of time the sample had to be calcined at 1200 °C in order to obtain a single-phase product.[341] Similarly, Sen and Pramanik prepared a series of nanocrystalline molybdates by complexing the ions with EDTA in the presence of PVA and sucrose and heat-treating the precursor at 500 °C.[367]

Among the oxides prepared using oxalic acid as a chelating agent are two $(Tl_{0.6}Pb_{0.2}Bi_{0.2})Sr_{4-x}Ca_xCu_3O_y$

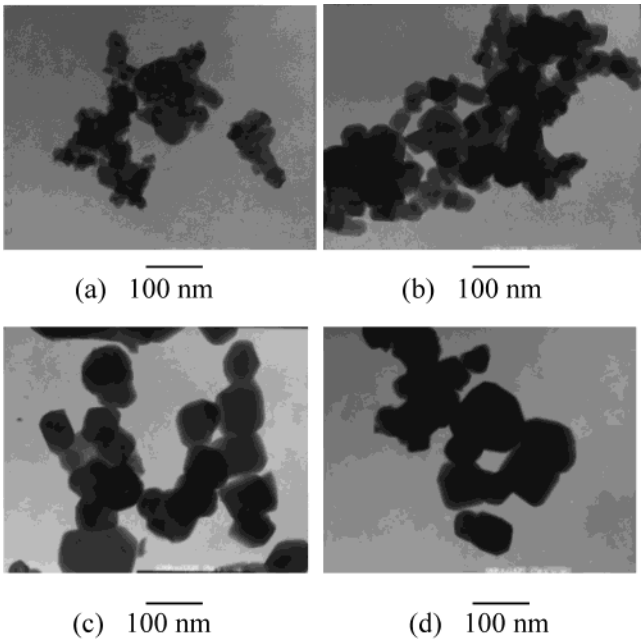

Figure 23. TEM micrographs of $LiMn_{1.9}Cr_{0.1}O_4$ powders prepared by the Pechini method and calcined at (a) 500 °C, (b) 600 °C, (c) 700 °C, and (d) 800 °C. (Reprinted with permission from ref 368. Copyright 2003 Kluwer Academic Publishers.)

($x = 2$, 2.4) superconductors.[342] The oxide gels were prepared by dissolving the metal nitrates in water, adding an excess of oxalic acid, adjusting the pH to ~7, and heating at 100−120 °C. The dried precursor was subsequently annealed at temperatures up to 940 °C under oxygen. Oxalic acid was substituted for citric acid in order to lower the decomposition temperature of the chelate and improve the purity of the final product.

$LiMn_{2-x}Cr_xO_4$, which is of interest as a lithium-ion battery cathode material, has been prepared by a modified Pechini method using PVA as a chelating agent.[368] The metal nitrates were dissolved in aqueous solution to which PVA was added. After drying at 80 °C, the precursors were calcined at 500−900 °C. Agglomerates ranged from 25 to 90 nm in diameter depending on the calcination temperature (Figure 23). 33 nm average diameter Co_3O_4 particles were prepared by a similar route with decomposition at 350 °C,[369] and 5−30 nm $NiFe_2O_4$ has been prepared using poly(acrylic acid) (PAA) as the complexing agent, followed by heating at 300 °C.[370]

Very recently, Tan et al. prepared $LaCo_xMn_{1-x}O_3$ perovskites with average diameters of 14 nm ($x = 0.4$) and 18 nm ($x = 0.3$) by complexing mixtures of the metal cations (preprecipitated as hydroxides) with diethylenetriaminepentaacetic acid (H_5DTPA).[371] The complex was calcined at 500 °C with relatively little sintering observed.

4. Microemulsions

4.1. Fundamentals of Microemulsions

Hoar and Schulman noted in 1943 that certain combinations of water, oil, surfactant, and an alcohol- or amine-based cosurfactant produced clear, seemingly homogeneous solutions that Schulman termed "micro emulsions."[372] The oil phases, in this case, were simple long-chain hydrocarbons, and the surfactants were long-chain organic molecules with a hydrophilic head (usually an ionic sulfate or quaternary amine) and lipophilic tail. The surfactant in Schulman's study was cetyltrimethylammonium bromide (CTAB), which is still used extensively today (Figure 24).

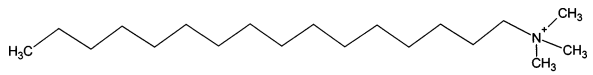

CTAB

Figure 24. Structure of cetyltrimethylammonium bromide (CTAB), a common surfactant used in microemulsions.

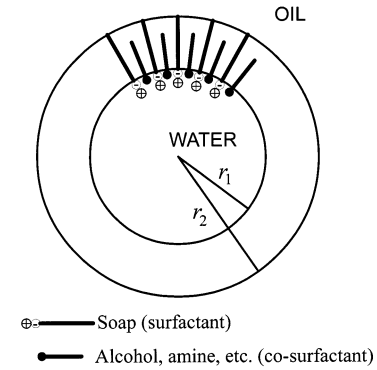

Figure 25. Schulman's model of the reverse micelle, as published in 1943. (Reprinted with permission from *Nature* (http://www.nature.com), ref 372. Copyright 1943 Nature Publishing Group.)

The amphiphilic nature of the surfactants such as CTAB makes them miscible in both hydrocarbons and water, but when the surfactant is mixed with a hydrocarbon, the resulting mixture, although optically isotropic, cannot be properly described as a solution. As noted by Schulman, the orientation of the surfactant molecules is not random.[373] Instead, the surfactant, through ion−dipole interactions with the polar cosurfactant, forms spherical aggregates in which the polar (ionic) ends of the surfactant molecules orient toward the center. The cosurfactant acts as an electronegative "spacer" that minimizes repulsions between the positively charged surfactant heads. The addition of water to the system will cause the aggregates to expand from the center as the water molecules (again as a result of ion−dipole and dipole−dipole interactions) situate at the center of the sphere (Figure 25).

Later, Friberg demonstrated through a series of NMR and IR experiments that the orientation of the molecules in the microemulsions minimizes interfacial tension between aggregates, and as such, microemulsions are thermodynamically stable.[374] This stability distinguishes microemulsions from traditional macroemulsions, which are, by definition, thermodynamically unstable.

The following discussion will be brief, given the abundance of review articles both on the general characteristics of microemulsions[375−382] and on their extensive use as micro- and nanoreactors.[380,383−388] The review article by Winsor, though outdated, stands out among the review papers concerning

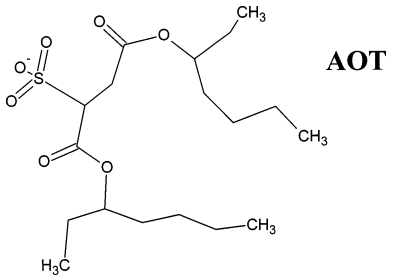

Figure 26. Structure of AOT (sodium bis(2-ethylhexyl)-sulfosuccinate).

microemulsion phase behavior, and much of the theory discussed therein is still valid.[389] The more recent paper by Silber et al., that comprehensively reviews the methodologies for probing the physical and chemical properties of microemulsions, is also noteworthy.[390]

4.1.1. Common Surfactants

The CTAB surfactant investigated by Schulman in 1943 has since been more thoroughly investigated.[391] More recently, other surfactants have emerged, most notably sodium bis(2-ethylhexyl)sulfosuccinate (generally referred to by its trade name, Aerosol OT or AOT) (Figure 26).[392] Like CTAB, AOT is ionic, but in this case the amphiphile is an anion. The fundamental properties of AOT and AOT-based microemulsions have been investigated rather extensively.[393−410] Somewhat less commonly used are nonionic surfactants, most based on polyethylene ethers such as pentaethylene glycol dodecyl ether (PEGDE), $CH_3(CH_2)_{11}-O-(CH_2-CH_2-O-)_5-H$,[50] or Triton-X:[411,412]

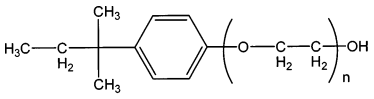

(64)

where $n \approx 10$. Reviews detailing the phase behaviors of numerous nonionic surfactants are available.[413,414]

4.1.2. Reverse Micelle Formation and Phase Equilibria

The spherical aggregates described by Schulman and represented in Figure 25 are commonly referred to as reverse micelles and are generally characterized by ω_0, the molar ratio of water to surfactant, S:

$$\omega_0 = [H_2O]/[S] \tag{65}$$

To establish the relationship between ω_0 and the micellar radius, R_M, we first consider the micellar molar volume, V_M, given by

$$V_M = \frac{4\pi R_M^3}{3} = n_s V_s + n_w V_w \tag{66}$$

where n_s and n_w are the moles of surfactant and water per micelle, respectively, and V_w is the volume of water in the micelle.[380] Assuming that the surface area of a micelle, Σ_M, is determined solely by the surfactant, then

$$\Sigma_M = 4\pi R_M^2 = n_s \Sigma_s \tag{67}$$

where Σ_s is the molar interfacial area at the surfactant−oil boundary. Since the volume in this model is fixed, then

$$\omega_0 = \frac{[H_2O]}{[S]} = \frac{n_w}{n_s} \tag{68}$$

Combining eqs 66−68 gives

$$R_M = \frac{3V_s}{\Sigma_s} + \frac{3V_w\omega_0}{\Sigma_s} \tag{69}$$

Experimentally, R_M has been shown to vary linearly with water content in various AOT and CTAB reverse micellar systems above a critical ω_0 of about 10, below which V_s, V_w, and Σ_s also increase with increasing ω_0.[391,392] As such, the size of the water pool at the reverse micelle core can be carefully controlled by adjusting the $[H_2O]/[S]$ ratio, provided $\omega_0 \geq 10$. However, controlling the size of the reverse micelles does not address the issue of micelle formation. As a four-component mixture of oil−water−surfactant−cosurfactant, the phase equilibria of reverse micelle systems are inherently complex.[415,416] Friberg noted early on that microemulsions tend to form over fairly limited oil/water/surfactant ratios.[374] Such phase relationships are normally depicted with Gibbs triangles; a representative example is given in Figure 27, where Om (oil−continuous micelle phase) represents the region of interest.[393] Note that solutions containing low volume fractions of oil form liquid crystalline (LC) phases and that solutions containing more than 50% H_2O versus AOT tend to contain both an Om and a water phase.

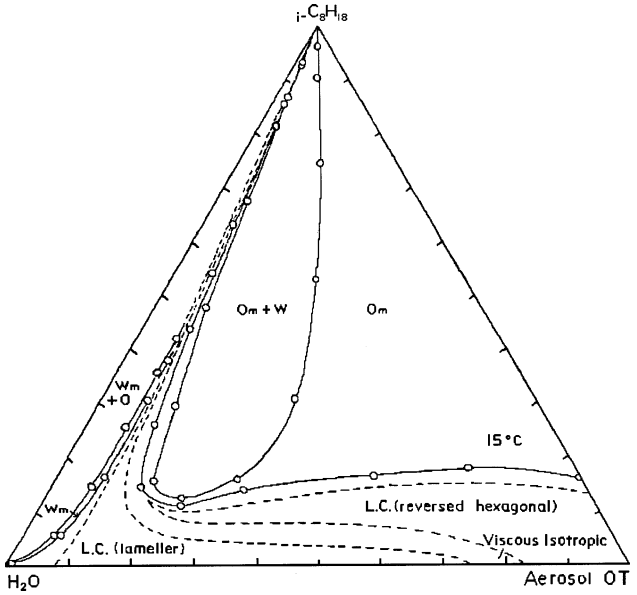

Figure 27. Phase diagram for the H_2O−AOT−isooctane microemulsion system at 15 °C. Om denotes the reverse micellar region. (Reprinted with permission from ref 393. Copyright 1979 Elsevier.)

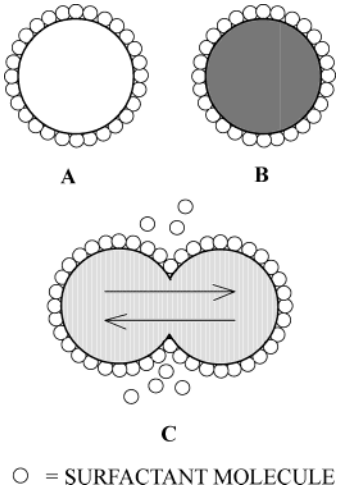

Figure 28. Schematic of a collision between two reverse micelles with dissimilar cores. The micelles form a short-lived dimer, as some surfactant molecules are released into the oil phase and the contents of the micellar cores are exchanged.

4.1.3. Reaction Dynamics in Reverse Micelles

The small size of reverse micelles subjects them to continuous Brownian motion, even at room temperature. Collisions between micelles are frequent, and approximately one collision in every thousand results in the formation of a short-lived dimer, formed by the expulsion of some surfactant molecules into the bulk oil phase (Figure 28).[400,417] During the ~100 ns lifetime of the dimer, two reverse micelles will exchange the contents of their aqueous cores before decoalescing, resulting in the eventual equilibrium distribution of all contents.[396]

Given the above model of reverse micelle interaction, the suitability of reverse micelles as nanoreactors becomes evident. Since the size of the water pools in reverse micelles can be controlled by adjusting ω_0, and the Brownian motion of the particles allows the distribution of reactants, then not only can reactions be performed inside the micellar cores, but also the products will have nearly uniform size and shape. The earliest reports of syntheses inside reverse micelle cores involved the preparation of colloidal metals in the early 1980s,[50] although the reaction dynamics of microemulsions were still not fully understood at the time.

The complexity of reverse micelle systems should not be underestimated, especially after ionic salts have been dissociated in the aqueous cores. Equilibrium constants and reaction rates frequently vary by more than an order of magnitude compared to the cases of similar systems in bulk aqueous solution.[407] Solvated ions tend to affect both the stability of reverse micelles and the phase equilibria.[401,418] In particular, solvated ions in reverse micelles formed from ionic surfactants cause a contraction of R_M, due to interactions with the charged surfactant heads, and tend to make the micelles more spherical.[399] Moreover, the influence of solvated ions on R_M tends to increase with increasing concentration and charge.[394] Predictably, interactions with the surfactant also change the physicochemical properties of the solvated ions.[408,419]

Experiments focusing on the interfacial water of reverse micelles have confirmed that the water molecules in close proximity to the surfactant are greatly influenced by dipole−dipole and ion−dipole interactions with the ionic surfactants and polar cosurfactants, and are largely immobilized.[397,404] The water at the reverse micelle core is affected to a lesser extent, but the immobilization of the interfacial water reduces the effective radius, R_E, of the core water pool (that which is available for solvation, transport, etc. of dissolved salts) to $R_E \approx {}^1/_2\omega_0$.

Last, the presence of the surfactant molecules in the reverse micelles, which to some extent act as capping agents, may serve to prevent flocculation of the products but does not alleviate the issue of Ostwald ripening (section 2.1.3).[420]

4.1.4. Factors Influencing Surfactant Selection

Careful consideration of a number of factors is advisable when selecting a suitable surfactant, starting with the reactants and reaction conditions. The surfactant should be chemically inert with respect to all other components of the microemulsion. This is particularly relevant when the system contains oxidizing or reducing agents. On this matter, both CTAB and AOT are stable against mild oxidizers, like dilute H_2O_2, and mild reducing agents, such as hydrazine. However, stronger reducing agents such as borohydride ions can be problematic.[421]

The possible interference of the counterions of ionic surfactants should likewise be carefully considered. In a reaction involving Ag^+, for instance, the dissociated Br^- ions of CTAB would cause immediate precipitation of AgBr. The Na^+ ions of AOT could similarly interfere with an intended precipitation reaction, that is, resulting in $NaMnF_3$ instead of $KMnF_3$.[422] Fortunately, at least in the case of AOT, Na^+ can be exchanged for ions more compatible with the synthesis prior to incorporation into reverse micelles.[423]

4.2. Microemulsion Synthetic Methods

4.2.1. Synthesis of Metals by Reduction

When a reverse micelle solution contains a dissolved metal salt and a second reverse micelle solution containing a suitable reducing agent is added, the metal cations can be reduced to the metallic state. Such reactions are, for all practical purposes, identical to those discussed in section 2.1 for the precipitation of metals from aqueous solutions. Although the number of metals that can be prepared this way is somewhat limited by the aqueous nature of the reactions, this approach has garnered much attention due to the potential application of the products as catalysts.[50] Table 6 provides a partial list of the metals prepared by this method.

The reducing agent must be stable in an aqueous environment and not react with the other components of the reverse micelle system. This immediately excludes all nonaqueous reducing agents, such as those discussed in section 2.2.2. Since bubbled H_2 gas results in slow reduction kinetics for many metals, particularly at room temperature,[50] sodium borohy-

Table 6. Representative Examples of Nanoparticulate Metals Prepared by Reduction in Microemulsions

metal	starting material	surfactant	reducing agent	reaction conditions	product size (nm)	ref
Co	$CoCl_2$	AOT	$NaBH_4$		<1	424
Ni	$NiCl_2$	CTAB	$N_2H_4 \cdot H_2O$	pH ~ 13	4	370
Cu	$Cu(AOT)_2$	AOT	N_2H_4		2−10	425, 426
	$Cu(AOT)_2$	AOT	$NaBH_4$		20−28	425, 426
Se	H_2SeO_3	AOT	$N_2H_4 \cdot 2HCl$		4−300	427
Rh	$RhCl_3$	PEGDE	H_2		3	50
Pd	$PdCl_2$	PEGDE	$N_2H_4 \cdot H_2O$	pH ~ 7	4	50
Ag	$AgNO_3$	PEGDE	$NaBH_4$		3−9	421
Ir	$IrCl_3$	PEGDE	H_2	70 °C	3	50
Pt	H_2PtCl_6	PEGDE	$N_2H_4 \cdot H_2O$		3	50
Bi	$BiOClO_4$	AOT	$NaBH_4$	Ar atm	2−10	428

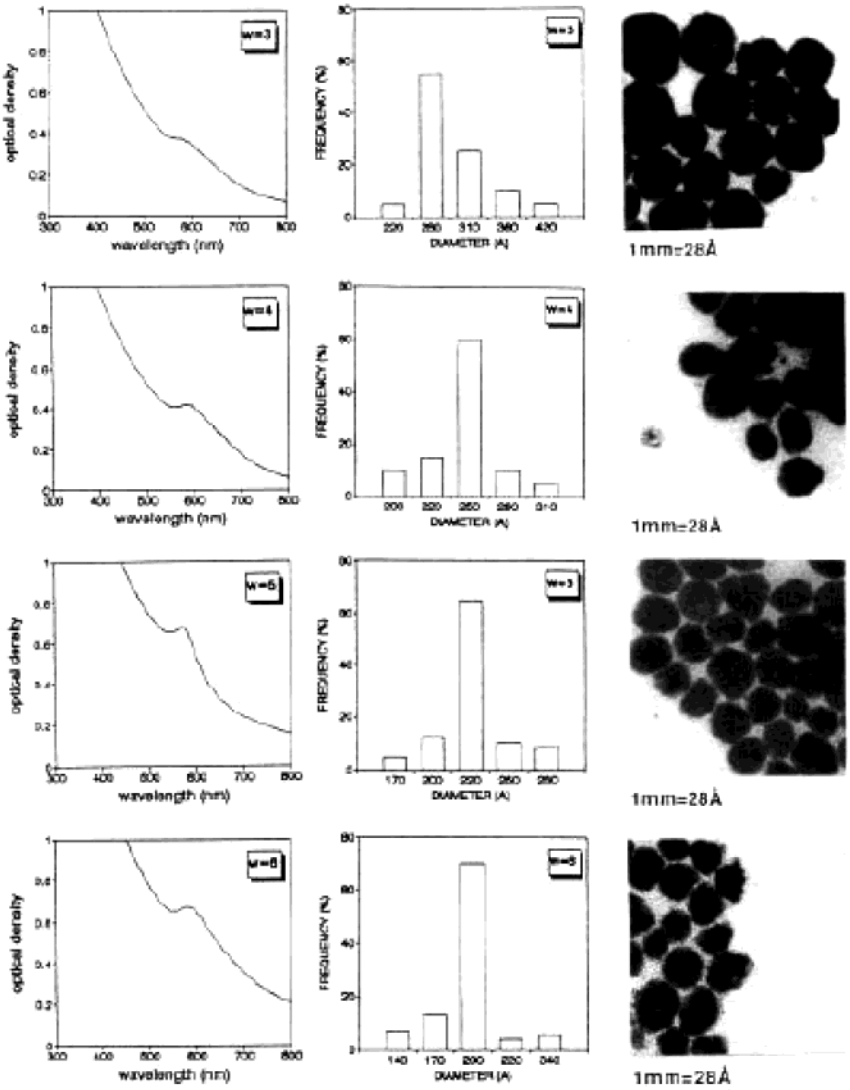

Figure 29. Absorption spectra, size-distribution histograms, and TEM images of Cu nanoparticles reduced with $NaBH_4$ at various $\omega = [H_2O]/[AOT]$ ratios. (Reprinted with permission from ref 425. Copyright 1993 American Chemical Society.)

dride and hydrazine (usually in the form of water-soluble $N_2H_4 \cdot 2HCl$ or $N_2H_4 \cdot H_2O$) are most commonly employed in such reactions.

The reduction of most metals is straightforward. One of the earliest reported reduction reactions in reverse micelles was that of H_2PtCl_6 with hydrazine via a $PtCl_4^{2-}$ intermediate:[50]

$$2PtCl_6^{2-} + N_2H_5^{+} \leftrightarrows 4PtCl_4^{2-} + N_2\uparrow + 5H^{+} + 4Cl^{-} \quad (70)$$

$$2PtCl_4^{2-} + N_2H_5^{+} \leftrightarrows Pt + N_2\uparrow + 5H^{+} + 8Cl^{-} \quad (71)$$

This reaction, performed in a PEGDE−hexane−water microemulsion, resulted in stable suspensions of 3 nm Pt particles.

Lisiecki and Pileni adapted the technique to the reduction of Cu^{2+} with hydrazine and $NaBH_4$, but they started from a $Cu(AOT)_2$ precursor:[425,426]

$$Cu(NO_3)_2 + 2Na^{+}AOT \leftrightarrows Cu(AOT)_2 + 2NaNO_3 \quad (72)$$

This technique is advantageous in that the NO_3^- counterions can be removed from the precursor, thereby avoiding any potential interferences, as discussed in section 4.1.3. Using hydrazine as the reducing agent, Lisiecki and Pileni obtained 2−10 nm Cu particles, whereas borohydride resulted in particles of 20−28 nm (Figure 29).

The reduction of oxo ions is somewhat more complicated and provides an example of where the control of pH is particularly important. In the case of H_2SeO_3, for example:[427]

$$\begin{array}{lll} H_2SeO_3 + 4\,H^+ + 4\,e^- & \leftrightarrows\ Se + 3\,H_2O & E^0 = 0.74\ V \\ N_2H_5^+ + H^+ & \leftrightarrows\ N_2 + 6\,H^+ + 4\,e^- & E^0 = -0.23\ V \\ \hline H_2SeO_3 + N_2H_5^+ & \leftrightarrows\ Se + N_2 + 3\,H_2O + H^+ & \end{array} \quad (73)$$

Both BH_4^- and $N_2H_4{\cdot}H_2O$ would have failed in the above example barring the addition of acid, since the presence of H^+ is required to initiate the reduction process.

The dispersities and size distributions of metal nanoparticles precipitated in microemulsions are typically very good. The TEM image and size distribution chart for Ni nanoparticles precipitated from a water−CTAB−*n*-hexanol system by Chen et al.[370]

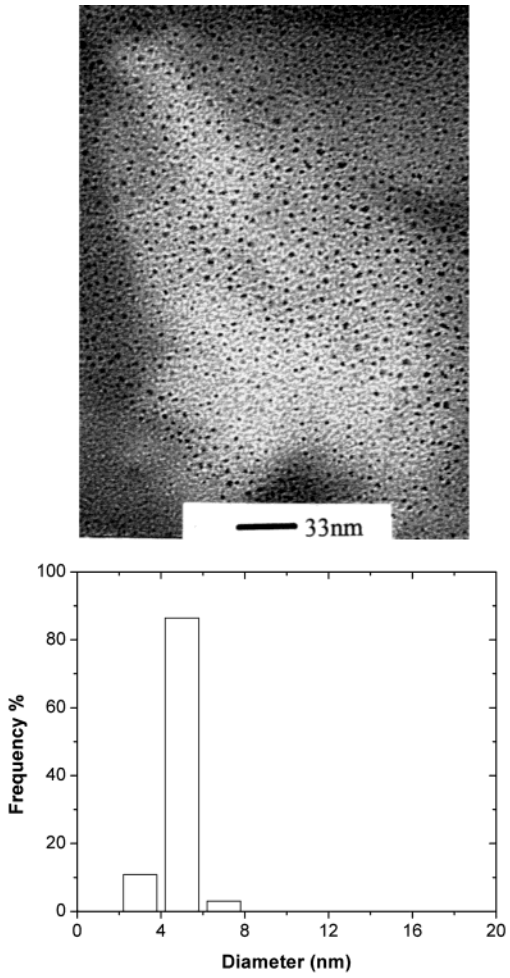

Figure 30. TEM micrograph and size distribution of nickel nanoparticles prepared in a water-in-oil microemulsion. [$NiCl_2$] = 0.05 M; [N_2H_4OH] = 1.0 M; water/CTAB/*n*-hexanol = 22/33/45; 73 °C. (Reprinted with permission from ref 370. Copyright 2000 American Chemical Society.)

are presented in Figure 30 and are typical for products of these types of reactions.

4.2.2. Synthesis of Alloys by Reduction

Substitutional alloys can similarly be prepared if salts of different metals are dissolved in the reverse micelle solution prior to reduction, provided the two metals are miscible in the metallic state. Reverse micelle solutions containing both Fe^{2+} and Pt^{2+}, for example, have been reported as being simultaneously reduced with BH_4^-.[429] Variation of the Fe/Pt ratio resulted in FePt, Fe_2Pt, disordered $FePt_3$, or ordered $FePt_3$.[429,430]

4.2.3. Synthesis of Metal Oxides

The synthesis of oxides from reverse micelles relies on the coprecipitation of one or more metal ions and is similar in most respects to the precipitation of oxides from aqueous solutions (section 2.2.5). Typically, precipitation of hydroxides is induced by addition of a reverse micelle solution containing dilute NH_4OH to a reverse micelle solution containing aqueous metal ions at the micellar cores. Alternatively, dilute NH_4OH can simply be added directly to a micelle solution of the metal ions. The precipitation of the metal hydroxides is typically followed by centrifugation and heating to remove water and/or improve crystallinity. This technique has proven particularly useful in preparing mixed-metal ferrites:[431]

$$M^{2+} + 2Fe^{2+} + OH^- \text{ (excess)} \xrightarrow{\Delta,\ O_2} MFe_2O_4 + xH_2O\uparrow \quad (74)$$

where M = Fe, Mn, or Co. The oxidation of $Fe^{2+} \rightarrow Fe^{3+}$ results from the reaction being performed under air, although other authors prefer to use Fe^{3+} as a starting material.[432] The products were typically on the order of 10−20 nm in diameter. Zhang et al. have recently demonstrated that, at least in the case of $MnFe_2O_4$, the cation distribution within the spinel structure of oxides prepared this way exhibits a strong temperature dependence.[433]

In cases where a transition metal cation is either not soluble or not stable in aqueous solution, nanoparticles may be prepared by hydrolysis of a suitable precursor, very similar to the reactions used in the sol-gel method (section 3.1). TiO_2, for example, has been prepared from tetraisopropyl titanate:[434]

$$Ti(O^iPr)_4 + 2H_2O \rightarrow TiO_2 + 4(^iPr{-}OH) \quad (75)$$

In this case, the reverse micelles containing the precursor were prepared in the absence of water; hydrolysis occurred when a second water-containing reverse micelle solution was added. Proper adjustment of the reactant concentrations resulted in either amorphous TiO_2 ([H_2O]/[AOT] ≤ 6) or anatase ([H_2O]/[AOT] ≥ 10).

In some instances, as with coprecipitation reactions, microemulsions are used to prepare precursors that are decomposed to the desired phase by subsequent calcination, although this will inevitably result in some degree of agglomeration. Yener and Giesche

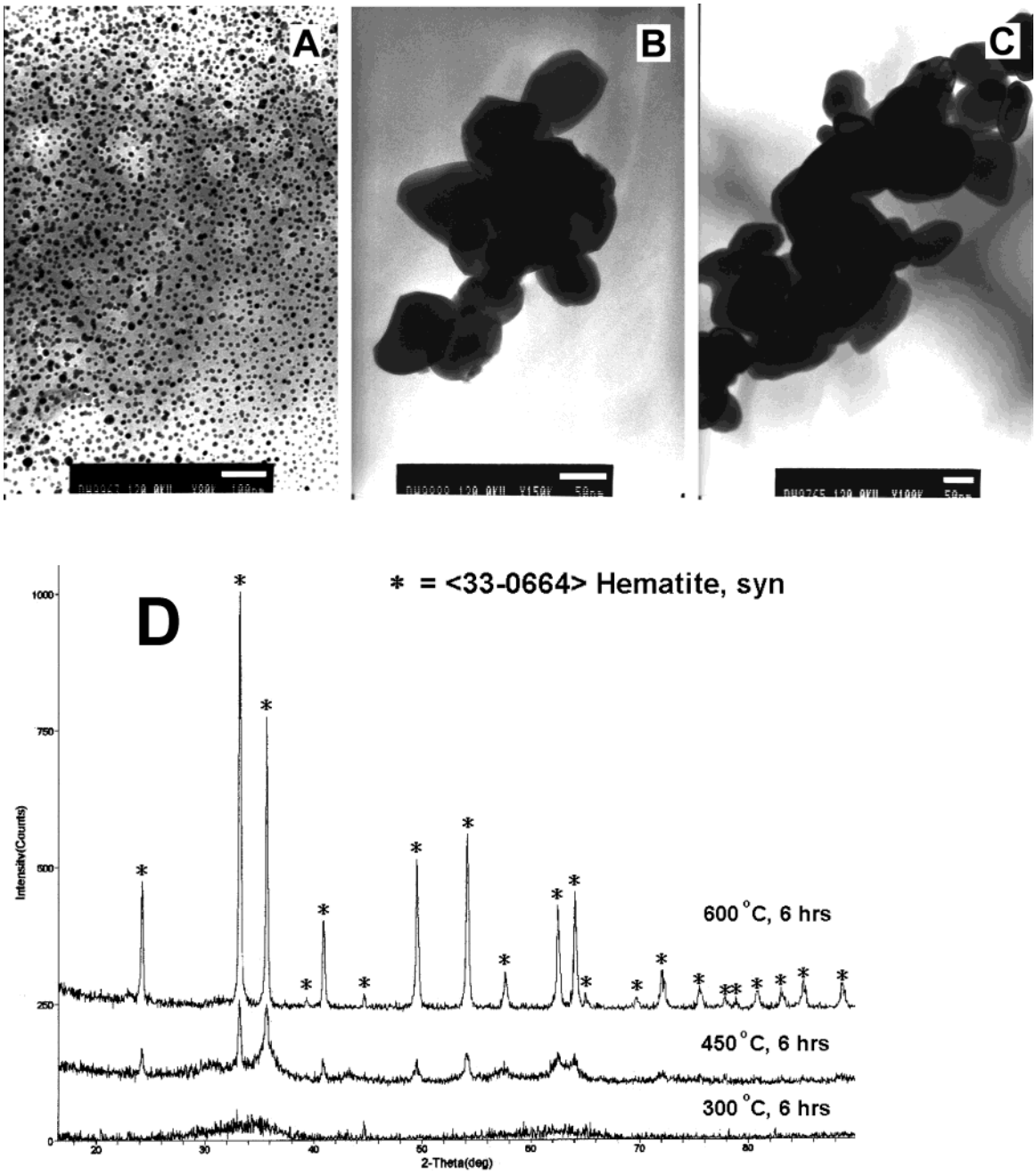

Figure 31. TEM images of Fe_2O_3 (hematite) particles prepared in an AOT microemulsion: (A) as-prepared (bar = 100 nm), (B) calcined at 450 °C (bar = 50 nm); (C) calcined at 600 °C (bar = 50 nm). The evolution of the crystalline hematite phase can be traced by powder X-ray diffraction (D). (Reprinted from ref 435 with permission from American Ceramic Society, www.ceramics.org. Copyright 1999. All rights reserved.)

prepared a series of mixed-metal ferrites by precipitating the precursors in a H_2O−AOT−isooctane system and calcining the products at 300−600 °C; the TEM images and powder X-ray patterns of one of their samples are reproduced in Figure 31.[435] Kumar et al. prepared 10 nm particles of the $YBa_2Cu_3O_{7-\delta}$ superconductor by combining a micellar solution of Y^{3+}, Ba^{2+}, and Cu^{2+} prepared in an Igepal CO-430−cyclohexane system with a second micellar solution containing oxalic acid in the aqueous cores.[436] The precipitate was collected by centrifugation and calcined at 800 °C to decompose the oxalate precursors. Nanoparticulate Al_2O_3,[437] $LaMnO_3$,[438] $BaFe_{12}O_{19}$,[439] $Cu_2L_2O_5$ (L = Ho, Er),[440] and $LiNi_{0.8}Co_{0.2}O_2$[441] are among the oxides that have recently been prepared by similar processes. The $BaFe_{12}O_{19}$ prepared in this way is noteworthy in that it exhibits a higher coercivity and saturation magnetization than samples prepared by a traditional coprecipitation route.[442] A representative sampling of various oxides prepared by coprecipitation in microemulsions is given in Table 7.

4.2.4. Syntheses of Other Inorganics

Many of the earliest microemulsion-based syntheses reported in the literature involved the coprecipitation of transition-metal halides or sulfides. Similar to the precipitation of hydroxides, two micelle solutions containing the desired ions are prepared sepa-

Table 7. Survey from the Literature of Oxides Prepared from Microemulsions

oxide	starting material	surfactant	precipitating agent	reaction conditions	product size (nm)	ref
$LiNi_{0.8}Co_{0.2}O_2$	$LiNO_3$ $Ni(NO_3)_2$ $Co(NO_3)_2$	NP-10	kerosene	calcined 400−800 °C	19−100	441
Al_2O_3	$AlCl_3$	Triton X-114	NH_4OH	calcined 600−900 °C	50−60	437
TiO_2	$Ti(O^iPr)_4$	AOT	H_2O		20−200	434
$Mn_{1-x}Zn_xFe_2O_4$	$Mn(NO_3)_2$ $Zn(NO_3)_2$ $Fe(NO_3)_3$	AOT	NH_4OH	calcined 300−600 °C	5−37	435
Fe_3O_4	$FeCl_2$ $FeCl_3$	AOT	NH_4OH		∼2	443
Fe_3O_4	$FeSO_4$	AOT	NH_4OH		10	431
$CoCrFeO_4$	$CoCl_2$ $CrCl_3$ $Fe(NO_3)_3$	SDS	CH_3NH_2	calcined 600 °C	6−16	444
$CoFe_2O_4$	$CoCl_2$ $FeCl_3$	SDS	CH_3NH_2	dried 100 °C	6−9	445
$Ni_{1-x}Zn_xFe_2O_4$	$Ni(NO_3)_2$ $Zn(NO_3)_2$ $Fe(NO_3)_3$	AOT	NH_4OH	calcined 300−600 °C	5−30	435
CuM_2O_5 (M = Ho, Er)	$Cu(NO_3)_2$ $NO(NO_3)_3$ $Er(NO_3)_3$	CTAB	$(NH_4)_2CO_3$	calcined 900 °C	25−30	440
$Y_3Fe_5O_{12}$	$Y(NO_3)_3$ $Fe(NO_3)_3$	Igepal CA-520	NH_4OH + $(NH_4)_2CO_3$	calcined 600−1000 °C	3	446
$YBa_2Cu_3O_{7-\delta}$	$Y(OAc)_3$ $BaCO_3$ $Cu(OAc)_2$	Igepal CA-430	oxalic acid		3−12	436
SnO_2	$SnCl_4$	AOT	NH_4OH	calcined 600 °C	30−70	447
$BaFe_{12}O_{19}$	$Ba(NO_3)_2$ $Fe(NO_3)_3$	CTAB	$(NH_4)_2CO_3$	calcined 950 °C	5−25	439, 442
CeO_2	$Ce(NO_3)_3$	CTAB	NH_4OH	calcined 500−700 °C	6−10	448

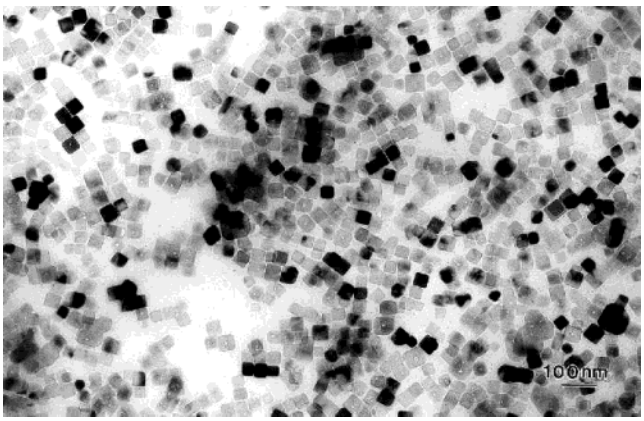

Figure 32. TEM image of nanocrystalline $KMnF_3$. (Reprinted with permission from ref 422. Copyright 1999 Everett E. Carpenter.)

rately and then rapidly mixed. Initially used to prepare simple binary halides such as AgCl,[449] the method was later adapted to more complicated ternary systems, like the cubic, perovskite-structured nanocrystals of $KMnF_3$ depicted in Figure 32, prepared by[422]

$$MnCl_2(aq) + KF(aq) \rightarrow KMnF_3(s) + 2KCl(aq) \quad (76)$$

This is an example of a reaction in which both the starting materials and the surfactant must be carefully chosen; when attempted in AOT, the above reaction produced $NaMnF_3$.

Metal chalcogenides can likewise be precipitated using a reverse micelle solution containing dissolved Na_2S, Na_2Se, or similar salts as the precipitating agent. Hirai et al., for example, recently prepared 2−4 nm diameter PbS particles from micellar solutions of $Pb(NO_3)_2$ and Na_2S.[450] Due to the high solubility of PbS relative to those of most metal chalcogenides, the authors found that using a large excess of one of the reactants tended to reduce the particle size of the products; the excess of either Pb^{2+} or S^{2-} is thought to minimize the effects of Ostwald ripening.

Similarly, Gan et al. have prepared ∼5 nm particles of Mn-doped ZnS in a microemulsion system consisting of NP-5 and NP-9 surfactants and petroleum ether as the oil phase.[451] Precipitation was induced by adding a micellar solution of Na_2S to a micellar solution of $MnCl_2$ and $ZnCl_2$. Subsequent hydrothermal treatment of the products increased the average diameter to ∼12 nm but substantially broadened the size distribution.

Vaucher et al. recently reported a microemulsion-based route to nanocrystalline Prussian blue, $[AFe^{III}\{Fe^{II}(CN)_6\}]$ ($A = Li^+$, Na^+, K^+, NH_4^+).[452] AOT−isooctane microemulsions containing aqueous $(NH_4)_3[Fe(C_2O_4)_3]$ and $(NH_4)_3[Fe(CN)_6]$ with ω = 5−20 were combined and exposed to UV light. Stable suspensions of Prussian blue particles appeared after a few days. The cubic 16 nm particles with very narrow size distributions (σ = 2.5 nm) self-assembled into highly ordered 2-D (or 3-D) superlattices containing 60−100 nanoparticles. The same authors have reported the synthesis of $Co_3[Fe(CN)_6]_2$.[453] Others have reported $Cu_2[Fe(CN)_6]$ nanoparticles prepared by a similar route, though no self-assembly was observed in this system.[454]

4.2.5. Synthesis of Core–Shell and Onion-Structured Nanoparticles

Many metallic nanoparticles, particularly Fe, are susceptible to rapid oxidation to the point of pyrophoricity. This problem can be largely circumvented, however, by coating the nanoparticles with gold or other inert metals. Gold coatings are of particular interest because the nanoparticles' surfaces can be subsequently functionalized with various organic species by taking advantage of the very strong Au−S bond, as described in section 2.1.4.

The technique for applying gold coatings on metal nanoparticles is reasonably straightforward and simply adds an additional step to the reverse micelle synthesis. A water-soluble gold salt ($HAuCl_4$) is dissolved and dispersed in a separate reverse micelle solution that is then added to the metal-containing reverse micelle solution that has already been reduced with an excess of BH_4^-. The aqueous $AuCl_4^-$ ions encapsulate the metal particles and are subsequently reduced by

$$8AuCl_4^- + 3BH_4^- + 9H_2O \leftrightarrows 8Au + 3B(OH)_3 + 21H^+ + 32Cl^- \quad (77)$$

forming a metallic gold shell around the metal particles.[455,456] $AuCl_4^-$ is sufficiently oxidizing for $N_2H_5^+$ to achieve the same result. Probability dictates, however, that some gold-containing reverse micelles will be reduced before coalescing with a metal-containing nanoparticle. As a result, the final product will typically contain some gold particles and possibly some uncoated transition metal particles. In any event, it should be noted that recent results by Ravel et al., who performed X-ray absorption spectroscopy (XAS) on gold-coated iron particles, indicate that the iron cores of such particles are still susceptible to oxidation.[457]

Taking the above process one step further, the synthesis can begin with Au nanoparticles, followed by a coating with Fe and followed again with a coating of Au, creating an Au−Fe−Au onion type structure (Figure 33).[430,458]

The preparation of core−shell type structures is not limited to metals as the core or shell materials. Combinations of precipitation, reduction, and hydrolysis reactions can be performed sequentially to produce oxides coated with metals, oxides coated with oxides, and so forth. Fe_3O_4, for example, can be coated with another oxide, such as MnO, with strict control of shell thickness.[431] In this case, reverse micelles containing 10 nm diameter Fe_3O_4 core particles, formed by precipitation and auto-oxidation of Fe^{2+}, were combined with a reverse micelle solution containing aqueous $KMnO_4$ with $\omega = 15$. The permanganate was subsequently reduced by addition of another 15 nm reverse micelle solution containing hydrazine. The product thus consisted of nanoparticles with 10 nm diameter Fe_3O_4 cores and 2.5 nm thick MnO shells.

Santra et al. recently reported a similar method for producing SiO_2-coated iron oxides in a nonionic surfactant system.[459] The authors precipitated 1−2 nm Fe_2O_3 or Fe_3O_4 by combining a reverse micelle solution containing Fe^{2+} and Fe^{3+} with one containing NH_4OH. Silica coatings with thicknesses as low as 1 nm were applied by adding tetraethyl orthosilicate (TEOS) to the NH_4OH reverse micelles prior to mixing. In this case, NH_4OH plays a dual role as both precipitating agent for the iron ions and catalyst for the hydrolysis of TEOS. Tago et al. prepared SiO_2-coated $Co_xFe_{3-x}O_4$ by a similar method (Figure 34).[460]

Gan et al. used nonionic surfactant micellar systems to coat $BaSO_4$ particles with polyaniline.[461] A micellar solution containing $BaCl_2$, HCl, and aniline was combined with a second solution containing

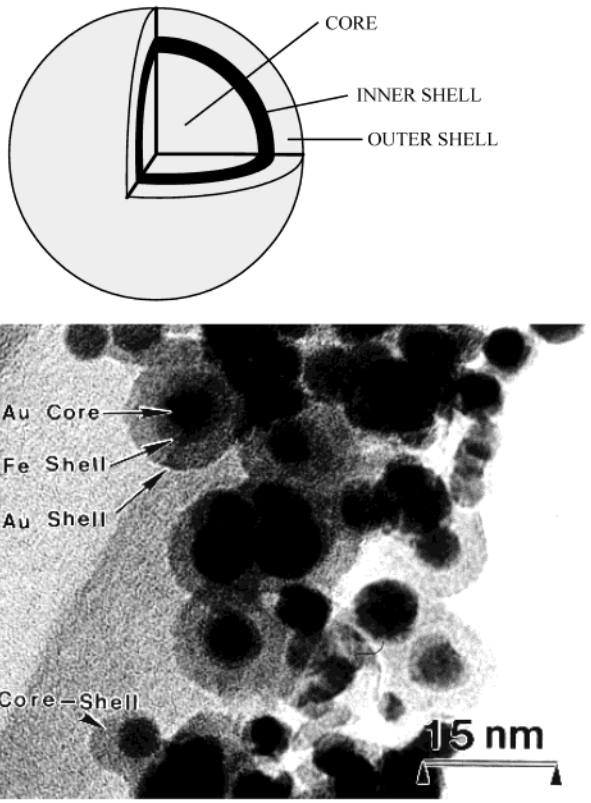

Figure 33. TEM image and schematic of an onion structure. (Reprinted with permission from ref 458. Copyright 1999 Materials Research Society.)

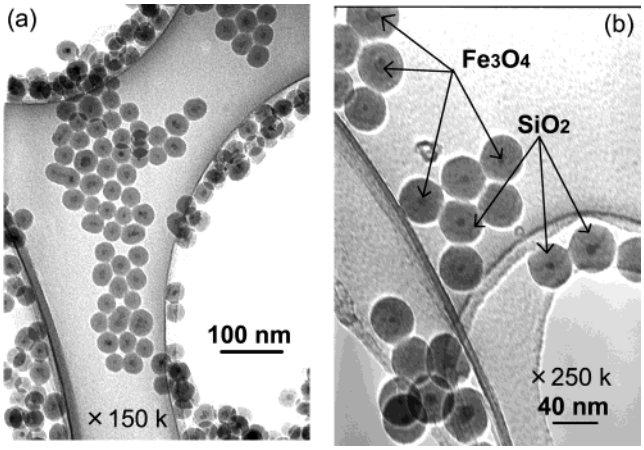

Figure 34. TEM images of SiO_2-coated Fe_3O_4 nanoparticles prepared in water-in-oil microemulsions. (Reprinted from ref 460 with permission from the American Ceramic Society, www.ceramics.org. Copyright 1999. All rights reserved.)

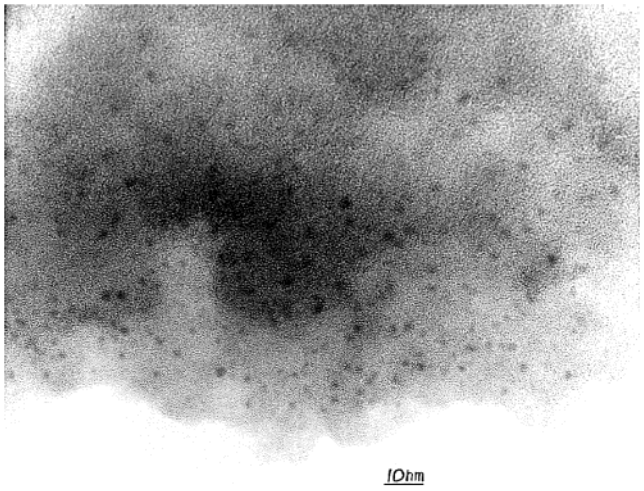

Figure 35. TEM image of Au clusters embedded in a silica matrix. The particles are 5.7 nm in diameter and highly dispersed. Particle size is independent of gel precursor type, drying procedure, and the H_2O/Si ratio. (Reprinted with permission from ref 462. Copyright 1997 American Chemical Society.)

$K_2S_2O_8$ and H_2SO_4. Precipitation of $BaSO_4$ within the micelles was immediate whereas the formation of the polyaniline required up to 24 h.

Martino et al. combined the reverse micelle method with sol-gel processing to encapsulate Au nanoclusters in silica matrixes.[462] The Au was precipitated by injecting a solution of $LiBH_4$ into a micellar solution containing $HAuCl_4$ and TEOS. Gelation of the TEOS was induced by raising the pH, and the gel was transformed into a xerogel by drying or into an aerogel by supercritical CO_2 extraction. The product consisted of 5−7 nm Au particles imbedded in a porous silica matrix (Figure 35).

4.2.6. Microemulsion Syntheses in Supercritical CO_2

Recently, a number of researchers have reported syntheses of nanoparticulate metals and chalcogenides using microemulsions in which supercritical CO_2 ($scCO_2$) serves as the solvent (oil phase).[463] The surfactant systems discussed in section 4.1 are not, by themselves, suitable for use in $scCO_2$ because the intermicellar van der Waals attractions are too strong. Ji et al. recently reported the synthesis of Ag nanoparticles in a system consisting of water, AOT, and perfluoropolyether-phosphate ether (PFPE-PO_4) as a cosurfactant in $scCO_2$ at 35 °C and 367 bar.[464] Two micellar solutions, one containing $AgNO_3$ and the other containing $NaBH(OAc)_3$ as the reducing agent, were prepared and mixed. The 5−15 nm products were polydispersed with slight agglomeration (Figure 36). The method was later adapted to the synthesis of Cu, CdS, and ZnS nanoparticles.[465,466] Others have used this method to prepare nanoparticulate silver halides.[467]

4.2.7. The Germ-Growth Method

Lin et al. have developed a variation of the microemulsion process in which seed crystals are first precipitated in the micellar cores and subsequently grown by further addition of reactant.[468] This is essentially the seed-mediated growth method discussed in section 2, adapted to a microemulsion to help restrict the size distribution of the particles. The method was developed specifically for the preparation of nanoparticulate Co, which tends to form Co_2B when reduced with borohydride in the presence of high concentrations of water.[39] In this modified method, the [water]/[surfactant] ratio was kept low and constant. After small Co seeds were precipated in the reverse micelle cores, additional microemulsions containing aqueous Co^{2+} or BH_4^- were added sequentially, and the process could be repeated several times. With each addition of reactant, the Co was preferentially precipated on the existing Co seeds rather than nucleating as new crystallites. The size of the resulting nanocrystals could be controlled in the range 3.8−8.8 nm with a relatively narrow size distribution. This method should be adaptable to other metals.

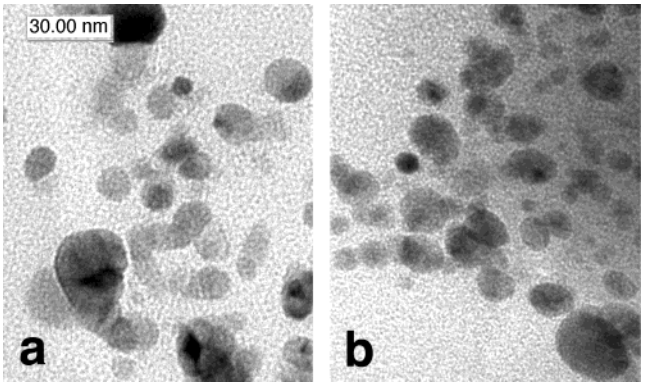

Figure 36. TEM images of Ag nanoparticles synthesized in microemulsions containing (a) liquid CO_2 (25 °C and 300 bar) and (b) supercritical CO_2 (35 °C and 367 bar). (Reprinted with permission from ref 464. Copyright 1999 American Chemical Society.)

5. Hydrothermal/Solvothermal Processing of Nanoparticles and Nanocomposites

5.1. Principles of Hydrothermal and Solvothermal Processing

In a sealed vessel (bomb, autoclave, etc.), solvents can be brought to temperatures well above their boiling points by the increase in autogenous pressures resulting from heating. Performing a chemical reaction under such conditions is referred to as *solvothermal processing* or, in the case of water as solvent, *hydrothermal processing*. Review articles devoted specifically to these methods appear frequently in the literature.[469−474]

The critical point for water lies at 374 °C and 218 atm. Above this temperature and pressure, water is said to be *supercritical*. Supercritical fluids exhibit characteristics of both a liquid and a gas: the interfaces of solids and supercritical fluids lack surface tension, yet supercritical fluids exhibit high viscosities and easily dissolve chemical compounds that would otherwise exhibit very low solubilities under ambient conditions.

Some solvothermal processes indeed involve supercritical solvents. Most, however, simply take advantage of the increased solubility and reactivity of metal

salts and complexes at elevated temperatures and pressures without bringing the solvent to its critical point. In any event, solvothermal processing allows many inorganic materials to be prepared at temperatures substantially below those required by traditional solid-state reactions. Unlike the cases of coprecipitation and sol-gel methods, which also allow for substantially reduced reaction temperatures, the products of solvothermal reactions are usually crystalline and do not require postannealing treatments.

As a matter of safety, the pressures generated in a sealed vessel should always be estimated beforehand. The equations necessary for doing so go far beyond the ideal gas law and are outlined in the review by Rajamathi and Seshadri.[471]

5.2. Hydrothermal and Solvothermal Methods

5.2.1. Solvothermal Processing of Nanocrystalline Oxides

The synthesis of nanocrystalline TiO_2, which is an important photocatalyst for the decomposition of toxic chemicals, is one of the more thoroughly investigated solvothermal/hydrothermal reactions. Oguri et al. reported in 1988 the preparation of anatase by hydrothermally processing hydrous titania prepared by the controlled hydrolysis of $Ti(OEt)_4$ in ethanol.[475] The reaction conditions leading to monodispersed anatase nanoparticles by this approach were elucidated by others.[476] The extension of the method to the preparation of lanthanide-doped titania particles has also been reported.[477]

More recently, Cheng et al. developed a method for preparing nanoparticulate, phase-pure rutile and anatase from aqueous $TiCl_4$ by a hydrothermal process.[478] They found that acidic conditions favored rutile while basic conditions favored anatase. Interestingly, they discovered that higher temperatures favor more highly dispersed products and that mineralizers such as $SnCl_4$ and NaCl tended to reduce the average grain size, while NH_4Cl led to agglomeration.

Research on the synthesis of nanophase TiO_2 still continues. Expanding the work of Cheng et al., others have determined that the phase purity of the products from hydrothermally processed aqueous $TiCl_4$ depends primarily on concentration, with higher concentrations of $TiCl_4$ favoring the rutile phase, while particle size depends primarily on reaction time.[479] Yin et al. modified the process to produce 2−10 nm crystallites of monodispersed, phase-pure anatase by adding citric acid to stabilize the TiO_2 nanoparticles and hydrothermally heating the precursors in the presence of KCl or NaCl mineralizers.[480]

The hydrothermal synthesis of nanocrystalline, monodispersed CeO_2 with a very narrow size distribution was recently reported by Masui et al.[481] The authors combined $CeCl_3 \cdot 6H_2O$ and aqueous ammonia with a citric acid stabilizer and heated the solution in a sealed Teflon container at 80 °C. The CeO_2 nanoparticles exhibited a 3.1 nm average diameter. The ceria particles were subsequently coated with BN by combining them with a mixture of boric acid and 2,2′-iminodiethanol, evaporating the solvent, and heating at 800 °C under flowing ammonia (Figure 37).

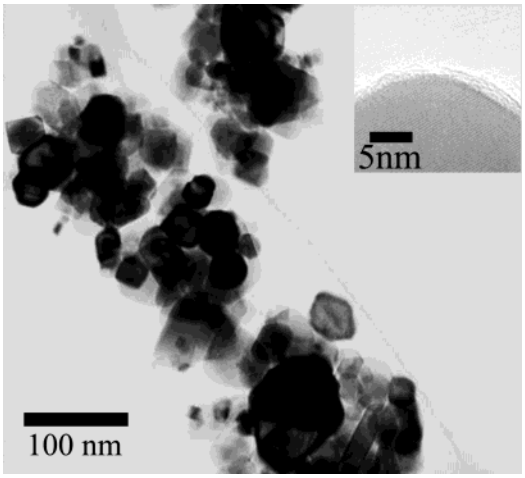

Figure 37. (top) TEM image of CeO_2 nanoparticles coated with turbostratic boron nitride and (bottom) the size distribution of the sample. (Reprinted with permission from ref 481. Copyright 2003 Royal Society of Chemistry.)

Inoue et al. were able to reduce the particle size of hydrothermally prepared colloidal CeO_2 to 2 nm by autoclaving a mixture of cerium metal and 2-methoxyethanol at 250 °C.[482] In this case, the autoclave was purged with nitrogen prior to heating and the colloidal particles were coagulated after heating with methanol and ammonia. The authors noted that higher reaction temperatures tended to increase particle size.

The solvothermal syntheses of some transition metal oxides can be achieved by the decomposition of metal−Cupferron complexes, M^xCup_x (Cup = $C_6H_5N(NO)O^-$), based on the method of Rockenberger et al.[184] discussed in section 2.2.9. Thimmaiah et al. were able to replace the amine-based solvents used by Rockenberger with toluene and prepared ∼10 nm diameter γ-Fe_2O_3 and ∼7 nm $CoFe_2O_4$ by hydrothermal heating of the reaction mixtures.[483] The authors noted, however, that the presence of at least trace quantities of a strongly coordinating amine was necessary to act as a capping agent and prevent aggregation and that longer-chain amines tended to reduce the average particle size of γ-Fe_2O_3. The same group has reported the synthesis of nanoparticulate $ZnFe_2O_4$ by an identical method.[472]

In many cases, anhydrous metal oxides have been prepared by solvothermal treatments of sol-gel or microemulsion-based precursors. Wu et al. prepared anatase and rutile TiO_2 by hydrothermal treatment of acidified $Ti(OBu)_4$ in a Triton X-100−*n*-hexanol−cyclohexane microemulsion.[484] The microemulsion was heated to 120−200 °C in a stainless steel autoclave. Microemulsions acidified with HNO_3 produced monodispersed anatase nanoparticles while those acidified with HCl produced rutile nanorods. Rutile-structured TiO_2 prepared this way has been shown to be active toward the photocatalytic oxidation of phenol.[485]

5.2.2. Synthesis of Nanocrystalline Nitrides and Chalcogenides

Yang et al. prepared a series of MSe_2 (M = Ni, Co, Fe) nanoparticles by a solvothermal reduction process.[486] The starting materials in this case were the

appropriate metal chloride, elemental Se, hydrazine, and a strongly coordinating solvent such as pyridine, DMF, or ethylenediamine. The reaction was initiated under ambient conditions before the mixture was transferred to an autoclave and heated to 80−200 °C. By varying the solvent and reaction temperatures, the authors were able to vary the sizes and morphologies of the products from filament-like to octahedral to spherical.

Although the presence of water can sometimes cause problems with the synthesis of non-oxidic species in hydrothermal reactions, the literature nonetheless contains numerous examples of successful syntheses of nanoparticulate metal chalcogenides.[487] Peng et al. developed a method for the hydrothermal synthesis of ZnSe and CdSe.[488] The starting materials in this case were powdered Zn or Cd metal and Se powder that were heated to 180 °C in an autoclave filled to 70% capacity with water. The products, while nanoparticulate, were agglomerated due to the absence of a stabilizer or capping agent. Gautam et al. were able to solvothermally prepare monodispersed ~3 nm CdSe particles using trioctyl phosphine oxide (TOPO) as a capping agent.[489]

Chen et al. prepared a series of MS_2 (M = Ni, Co, Fe, Ni, Mo) sulfides and MSe_2 (M = Ni, Mo) selenides hydrothermally using metal chlorides and $Na_2S_2O_3$ or Na_2SeSO_3 as starting materials, or in the case of the molybdenum-containing products, Na_2MoO_4 was used and hydrazine was added.[490] The average crystallite size of the agglomerated products ranged from ~4 nm for MoS_2 to ~85 nm for FeS_2.

While most hydrothermal syntheses of chalcogenides involve the preparation of binary systems, more complicated ternary compounds have also been reported. A series of $M^IM^{III}S_2$ ($M^I = Ag^+$, Cu^+; $M^{III} = Ga^{3+}$, In^{3+}) semiconductors have been prepared by Liu et al. from the combination of MCl salts with elemental Ga or In (M′) and S:[491,492]

$$3MCl + 4M' + 6S \rightarrow 3MM'S_2 + M'Cl_3 \quad (78)$$

The reactions were carried out in autoclaves heated to 180−230 °C with ethylenediamine as solvent. The products ranged from 5 to 12 nm but exhibited some signs of agglomeration.

Xiao et al. were able to take the previously mentioned process one step further, preparing the $CuIn(Se_xS_{1-x})_2$ quaternary semiconductors over the full $0 \le x \le 1$ compositional range.[493] In this case, the starting materials were $InCl_3 \cdot 4H_2O$, $CuCl_2 \cdot 2H_2O$, Se, and S, and ethylenediamine was the preferred solvent. Particle sizes were typically on the order of 15 nm.

Metal nitrides such as GaN can be prepared by similar reactions involving Li_3N:[494,495]

$$GaCl_3 + Li_3N \rightarrow GaN + 3LiCl \quad (79)$$

The reactions were typically carried out in nonpolar, aprotic solvents such as benzene at ~280 °C.

5.2.3. New Developments in Hydrothermal/Solvothermal Methods

In the past few years, two new developments have emerged in solvothermal/hydrothermal syntheses, namely the design and operation of "continuous flow" hydrothermal reactors and microwave-assisted solvothermal processing. Continuous flow reactors are particularly relevant given their suitability to large-scale production.[496]

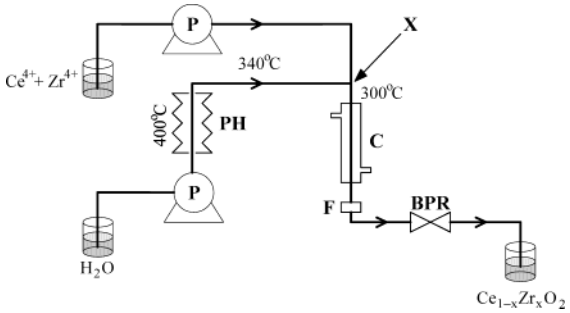

Figure 38. Schematic of a continuous-flow hydrothermal reactor for the production of nanoparticles. See text for a detailed description of the apparatus. (Reprinted with permission from ref 497. Copyright 2000 Royal Society of Chemistry.)

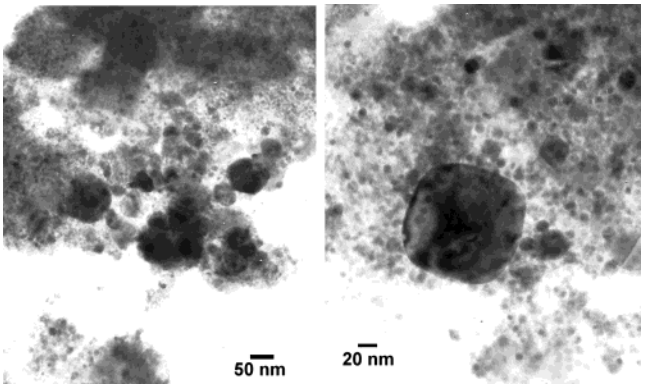

Figure 39. TEM micrographs showing the decomposition product of $Fe(OAc)_2$ in a hydrothermal flow reactor at 300 °C and 25 MPa. (Reprinted with permission from ref 504. Copyright 2001 Royal Society of Chemistry.)

Continuous flow reactors, such as that depicted in Figure 38 for the synthesis of $Ce_{1-x}Zr_xO_2$ nanoparticles in near-critical water,[497,498] should be distinguished from the aerosol- and vapor-phase flow reactors that have been used for some time for the synthesis of nanoparticles,[499−503] and from the microwave flow reactors discussed previously (section 2.2.8). From the diagram in Figure 35, a mixture of aqueous $(NH_4)_2Ce(NO_3)_6$ and $Zr(OAc)_4$ was combined at the mixing point (X) with a stream of near-critical water heated to 400 °C in a preheater (PH); the liquids were transported with pumps (P). The mixture was then cooled immediately with a water cooler (C) and passed through a filter (F). The final product was collected as a colloidal suspension. The pressure in the system was controlled with the back-pressure regulator (BPR). This arrangement produced 5 nm colloidal particles at rates up to 10 g/h. The composition of the $Ce_{1-x}Zr_xO_2$ nanoparticles could be varied over the entire $0 \le x \le 1$ compositional range by adjusting the ratios of Ce^{4+} and Zr^{4+} in the starting solution.[498] The same authors have reported the syntheses of a series of ferrite nanoparticles by a similar method, including the Fe_3O_4 particles depicted in Figure 39, produced by decomposition of

$Fe(OAc)_2$.[504] Others have successfully adapted the method to the synthesis of TiO_2[505] and $BaTiO_3$.[506]

Microwave-assisted solvothermal methods are somewhat less commonly encountered in the literature. Nonetheless, microwave-hydrothermal processing has been used since 1992 for the synthesis of various oxides[507] and zeolites,[508] although these methods were originally developed in the interest of reducing reaction times rather than particle sizes. Komarneni et al., in particular, made extensive use of this method to synthesize a wide variety of compounds and composite materials.[507,509−514] More recently, they have adapted their method specifically toward the synthesis of nanoparticles, including the MFe_2O_4 (M = Zn, Ni, Mn, Co) ferrites,[515] $BaTiO_3$,[516] and monodispersed α-Fe_2O_3.[517] Komarneni and Katsuki have recently reviewed this work.[518] Other recently reported nanophase compounds prepared by the microwave-hydrothermal technique include Fe_3O_4,[519,520] colloidal, anatase-structured TiO_2,[521] ZrO_2,[522] and $Ce_{0.75}Zr_{0.25}O_2$.[523]

One of the primary uses of the microwave-hydrothermal method is in the preparation of nanostructured mesoporous materials.[524−526] This is, however, an extremely broad topic and is beyond the scope of this review. The interested reader is referred to any of several excellent review articles addressing the synthesis of mesoporous materials.[527−529]

6. Templated Syntheses

The synthesis of nanoparticles on templates has garnered an increasing amount of attention in the past few years. As will be discussed here, this approach encompasses a broad array of synthetic strategies and frequently involves methods that are best described as hybrids between previously discussed techniques.

The technique of heterogeneous nucleation discussed in section 2, in which "seed" crystals serve as nucleation sites for further deposition and growth of crystallites, can essentially be considered one of the simpler forms of a templated synthesis. This technique can be used to increase the average particle size of nanoparticles, such as when aqueous Au^{3+} is deposited on colloidal Au, or Ag^+ is deposited on colloidal Ag.[530,531] The method can also be used for the synthesis of core−shell and onion structures, such as the deposition Pd, Bi, Sn, or In on colloidal Au,[532,533] Au on TiO_2,[534] CeO_2 on carbon nanotubes,[535] Ni on Al_2O_3 particles,[536] ZnO on Al_2O_3,[537] Ni on Pd or Pt,[538] or CdS on HgTe.[539] Pileni has recently reviewed these methods.[540] Pradhan et al. have written a more general review of seed-mediated methods for nanoparticle syntheses.[541]

To maintain the narrow size distribution of the nanoparticles, care must be taken to ensure that smaller particles do not nucleate from solution during the deposition process. Several new techniques have recently emerged to prevent this occurrence. Brown et al. used hydroxylamine (NH_2OH) for the seed-mediated growth of colloidal Au, increasing the average diameter from 12 nm up to 50 nm.[542] The use of hydroxylamine is critical to this process. While hydroxylamine can theoretically reduce $AuCl_4^-$ to Au^0, the reduction kinetics of this process are greatly enhanced in the presence of the colloidal Au seed particles, in which the Au surfaces serve as catalysts. The reduction of $AuCl_4^-$ therefore preferentially occurs at the Au surfaces, as opposed to leading to the nucleation of new, smaller Au particles from solution. This process can therefore be described as *electroless plating*.[543] Taking the process one step further, Schmid et al. deposited ~9 nm thick Pt and Pd shells on 18 nm colloidal Au particles from solutions of $HtPtCl_2$ or H_2PdCl_4 using hydroxylamine hydrochloride ($NH_2OH{\cdot}HCl$) as the reducing agent and p-$H_2NC_6H_5SO_3^-Na^+$ as a stabilizer (Figure 40).[532]

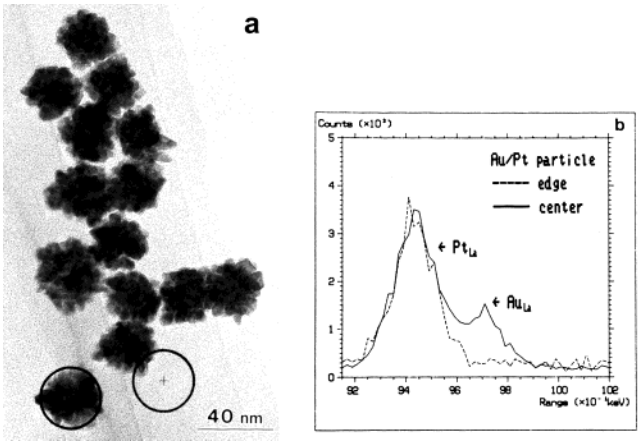

Figure 40. (a) High-resolution TEM image of Au@Pt particles prepared from a seed-mediated growth process. The EDX spectra of the circled areas are presented in part b. (Reprinted with permission from ref 532. Copyright 1991 Wiley-VCH.)

In recent years, a great deal of interest has developed in the synthesis of metal and metal oxide nanoparticles on polymer templates. Initially, these reactions consisted simply of the reduction of transition metals, the decomposition of metal carbonyls, or precipitation of metal oxides in polymer matrixes. Platonova et al. prepared 1 nm Co in a polystyrene (PS)−PVP copolymer this way.[544] The syntheses of nanoparticulate $CoFe_2O_4$[545] and Fe_3O_4[546] have recently been achieved by similar methods. In recent years, various researchers have developed increasingly complex variations of these syntheses. Bronstein et al. prepared 1−2 nm Au, Pd, and Pt using poly(octadecylsiloxane), which formed a bilayer structure of opposing Si−O−Si chains with water intercalated between the layers.[547] Metal cations were inserted into the aqueous layers prior to reduction with borohydride ion. Liang et al. have reported a process by which Au was deposited on spherical particles of polystyrene (PS) by first coating the PS with a positively charged polymer like poly(allylamine hydrochloride) and combining it with colloidal Au stabilized with 4-(dimethylamino)pyridine (DMAP).[548] The capping ligands of the colloidal Au particles were consequently electrostatically attached to the coated PS particles. The gold particles could then be enlarged by the hydroxylamine method described previously. The polymers were subsequently removed either by calcination of the products at 310 °C under oxygen or by washing with THF, resulting in the formation of 500 nm diameter hollow gold spheres.

In an inverse approach to the above process, Marinakos et al. used colloidal Au particles as templates for the formation of hollow polymer spheres.[549] They deposited the colloidal Au (prepared by the citrate method discussed in section 2.2.1) into the spheres of a porous alumina membrane and applied one or more layers of a polymer, such as polypyrrole, to the Au by diffusing pyrrole vapor through the membrane in the presence of a polymerization initiator. Au was subsequently dissolved by washing with a cyanide solution, and the alumina membrane could be removed by treatment with dilute KOH. The polymer coating could be varied from 5 to 100 nm thick, depending on the time allowed for vapor deposition. The sizes of the cores were controlled by varying the diameters of Au particles in the colloids from 5 to 200 nm. Nair et al. have similarly prepared hollow ZrO_2 nanoparticles by leaching Ag from Ag@ZrO_2 particles with CCl_4.[550]

Crooks et al. have encapsulated Pd and Pt nanoparticles as small as 1 nm with dendrimers such as poly(amidoamine) by absorbing the respective metal cations into the dendrimer structure prior to chemical reduction.[551] The authors have extended this process to the encapsulation of Cu, Ni, Fe, Au, and Ru and have recently reviewed this work in detail.[552]

The synthesis and deposition of nanoparticles inside the pores of mesoporous materials, such as MCM-41, have become rather commonplace, and the topic has been extensively reviewed.[553−556] Mesoporous alumina exhibits rather unusual surface properties and has been shown to be an effective adsorbent for ions from aqueous solutions.[557] The ions, once adsorbed into the pores, can be subsequently oxidized or reduced to nanoparticulate oxides or metals. Such composite materials are particularly attractive as supported catalysts.[558−560] The methods of preparing these composite materials extend well beyond simple adsorption and include vapor phase methods[561] as well as electrodeposition.[554,562] The discussion here, however, will be limited to wet-chemical methods.

The synthesis of metal−SiO_2 composites discussion in section 3.2.3 can be viewed as a primitive version of this template approach, but in the case of the sol-gel methods, the metal or metal oxide nanoparticles are not necessarily contained within the SiO_2 pores. Bronstein et al., however, were able to incorporate Pd and Pt into the pores of SiO_2 monoliths by submerging the preprepared monoliths in solutions of $PdCl_4^{2-}$, $PtCl_4^{2-}$, or $PtCl_6^{2-}$ for periods up to 72 h followed by reduction with either aqueous $NaBH_4$ or gaseous H_2.[563] The Pd and Pt particles so-prepared appear to have diameters below 1 nm (Figure 41).

Lensveld et al. similarly deposited <10 nm particles of NiO inside the pore structure MCM-41 by impregnating the mesoporous material with aqueous solutions of a nickel citrate complex followed by calcination of the composites at 450 °C in air.[564] This, in effect, can be viewed as the synthesis of NiO by the Pechini method (section 3.3) inside a mesoporous material. Lakshmi et al. have likewise reported the synthesis of nanostructured TiO_2, WO_3, and ZnO in porous alumina using a modified sol-gel process in which Al_2O_3 membranes were dipped in the appropriate sols and heated to 400 °C.[565] Others have similarly deposited 30 nm Eu_2O_3 particles in amorphous alumina.[566]

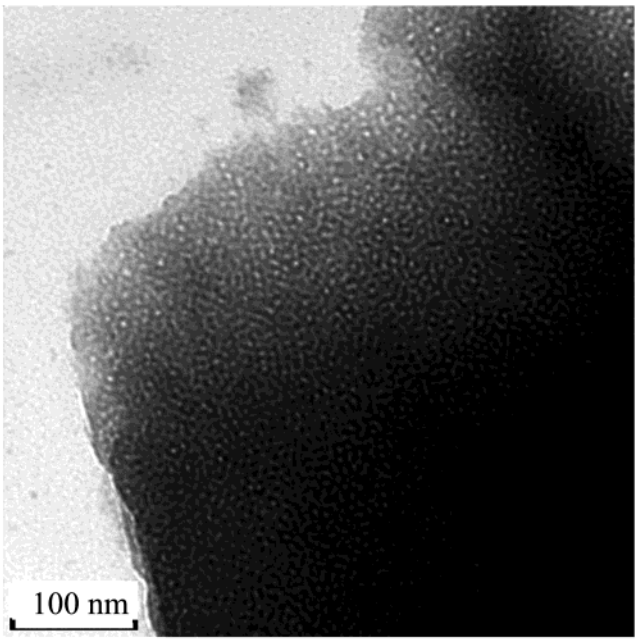

Figure 41. TEM image of <1 nm Pd nanoparticles in a silica monolith. (Reprinted with permission from ref 563. Copyright 2001 Wiley-VCH.)

In a rather unique approach, Hoh et al. were able to precipitate 1−7 nm $CoFe_2O_4$ within the pores of Dowex, a common ion exchange resin with sulfonic acid functional groups.[567] In this case, aqueous solutions containing Co^{2+} and Fe^{3+} were combined with the resin, followed by addition of NaOH to initiate precipitation. Ding and Gin, in contrast, prepared 4−7 nm Pd in the channels of a lyotropic liquid crystal polymer by an ion exchange reaction, followed by reduction under hydrogen, although the ordered pore structure appears to collapse during the reduction process.[568]

Kim et al. prepared Au nanoparticles in mesoporous carbon by first encapsulating colloidal Au with SiO_2 shells formed by the hydrolysis of aminopropyltrimethoxysilane in the presence of sodium silicate.[569] The Au@SiO_2 particles were subsequently encapsulated in mesoporous silica by initiating a second hydrolysis reaction of TEOS and octadecyltrimethoxysilane. After calcination, the particles containing Au@SiO_2 cores and porous silica shells were saturated with phenol and a polymerization initiator and heated under vacuum, resulting in the formation of an amorphous carbon−silica composite. The silica could be subsequently removed by etching with an HF solution. The final product consisted of 13 nm Au cores surrounded by 15−25 nm thick carbon shells with hollow cores. Because the interiors of the carbon shells are larger than the 13 nm Au particles, the resulting product is referred to as a *nanorattle* (Figure 42). The subject of carbon-encapsulated metal nanoparticles, including their various methods of syntheses, has recently been reviewed.[570]

Morley et al. deposited 10−100 nm Ag particles within the pores of poly(styrene-divinylbenzene) beads

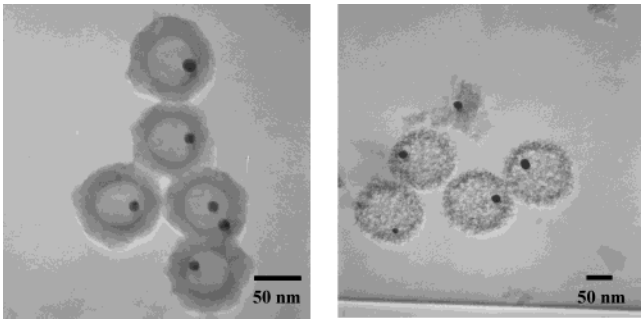

Figure 42. TEM images of Au@HCMS polymer capsules (left) and Au@HCMS carbon capsules. (Reprinted with permission from ref 569. Copyright 2002 American Chemical Society.)

and silica aerogels by solvothermal treatment in supercritical CO_2.[323] The silver precursor, in the form of Ag(hfpd)(tetraamine) or Ag(hfpd)(tetraglyme) (hfpd = 1,1,1,5,5,5-hexafluoropentane-2,4-dione), was combined with the host material and CO_2 in an autoclave and heated to 40 °C (4000 psi). Subsequent decomposition of the complexes to Ag metal was performed in a second step, in which the autoclave was filled with H_2 and heated to 60 °C (1000 psi).

Last, although carbon nanotubes cannot be classified as a mesoporous material, Wu et al. were able to deposit CuO and Fe−Ni alloy nanorods inside carbon nanotubes with 3−10 nm interior diameters by combining acid-washed nanotubes with saturated solutions of the appropriate metal nitrates and calcining at 450 °C under inert atmosphere or H_2.[571,572] In the case of CuO, the nanotube templates could subsequently be removed by calcination at 750 °C in air. Others have deposited Ni and CoNiFe alloy nanoparticles on the surfaces of carbon nanotubes electrochemically.[573]

7. Biomimetic Syntheses

Interest in biotemplated nanoparticle syntheses was spurred dramatically when Meldrum et al. reported the synthesis of nanometric iron sulfide and amorphous manganese and uranyl oxides within protein cages.[574] The ferritin-containing protein cages were, in effect, serving as nanoreactors to constrain particle growth. Douglas and Young later reported the similar host−guest encapsulation of paratungstate and decavanadate inside the protein cage of a virus.[575] Research along these lines continues, now involving the protein engineering of viral cages as tailored nanoreactors.[576]

Much of the recent interest in biological nanoparticle syntheses is based on the molecular self-assembly of nanoparticles. Most of this work stems from the 1996 report by Mirkin et al., who demonstrated that functionalized DNA is capable of directing the self-assembly of Au nanostructures into regularly spaced 2-D arrays.[577] This line of research continues at a rapid pace,[578−581] and review articles appear frequently.[582−584]

Seidel et al. were recently able to induce the nucleation and growth of Pt nanoparticles at single DNA molecules.[585] In this case, λ-DNA was aged in a K_2PtCl_4 solution, followed by the addition of dimethylammine borane as a reducing agent. The DNA molecules effectively served as a heterogeneous nucleating agent and template for the formation of nanoparticulate Pt chains. Through an impressive application of scanning force microscopy (SFM), the researchers were able to observe the formation of the Pt particles on the biomolecules in situ (Figure 43). Similarly, Dujardin et al. used the tobacco mosaic virus as a template for the growth of <10 nm Pt, Au, and Ag nanoparticles into cylindrical aggregates.[586]

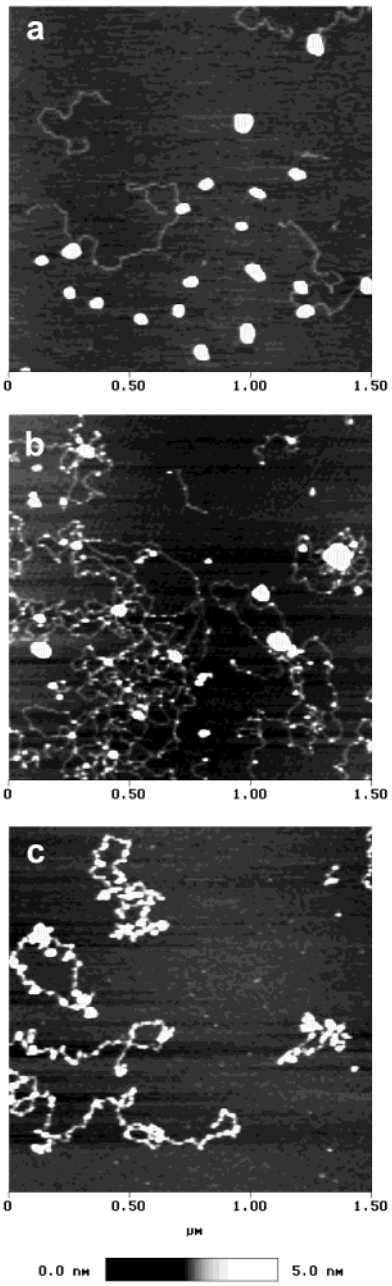

Figure 43. Scanning force microscopy (SFM) images of the different routes of cluster synthesis in the presence of DNA: (a) DNA was added 5 min after clusters were prepared; (b) clusters were prepared in the presence of nonactivated native DNA—that is, the reducing agent and DNA were added to the $[PtCl_4]^{2-}$ solution at the same time; and (c) clusters were prepared in the presence of activated DNA. (Reprinted with permission from ref 585. Copyright 2002 Wiley Europe.)

At the cutting edge of these types of syntheses, nanoparticles have recently been encapsulated in

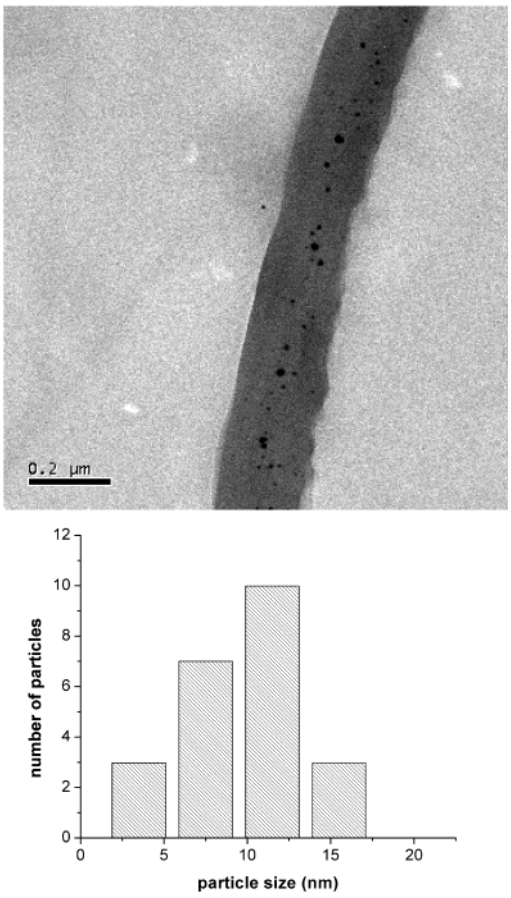

Figure 44. Low-magnification TEM image of an alfalfa shoot showing aggregates of gold nanoparticles and the particle size distribution in a typical sample. The plant actively uptakes metallic Au from solid media, after which nucleation and growth of the Au particles continues inside the roots and shoots. (Reprinted with permission from ref 595. Copyright 2002 American Chemical Society.)

engineered viral cages. Douglas et al. have recently engineered a cowpea chlorotic mottle virus devoid of nucleic acid and with a functionality mimicking that of ferritin.[576] Approximately 8 nm diameter γ-FeOOH particles were subsequently grown inside the 18−24 nm viral cages by the addition of aqueous Fe^{2+} solutions in the presence of air. A detailed description of the fundamentals of such processes is available in an excellent review by Douglas.[584]

Some microorganisms exhibit the ability to reduce metals, particularly those exhibiting high reduction potentials, such as Fe(III), Cr(VI), Mn(IV), and Co(III).[587−590] Roh et al. have recently published reports detailing the microbial synthesis of magnetites in which suspensions of FeOOH, solvated metal cations, and appropriate buffers were combined with glucose or lactate in the presence of *Thermoanaerobacter ethanolicus*, an iron(III)-reducing bacterium, and incubated at 65 °C.[591,592] Although the reduction and mineralization mechanisms are not well understood,[587,593] this method resulted in nanocrystalline $(Fe^{II}_{1-x}M^{II}_x)Fe^{III}_2O_4$ (M^{II} = Mn^{2+}, Ni^{2+}, Co^{2+}) and $Fe^{II}(Fe^{III}_{2-x}Cr^{III}_x)O_4$ ferrites in large yields.

The ability of some plants to uptake gold from soil is well-known, as mining companies take advantage of this phenomenon to aid in the exploration process.[594] Gardea-Torresday et al. were able to induce the uptake of gold into live alfalfa plants by adding aqueous $KAuCl_4$ to the nutrient solution used to grow the plants.[595] The gold was apparently reduced to metallic Au prior to uptake. Transport of the Au particles through the roots to the shoots resulted in aggregation of the 4−5 nm Au particles into clusters (Figure 44). While this technique is not practical as a synthetic method, the potential applications for the reclamation (bioremediation) of former mining sites are obvious.

Table 8. Colloidal Nanoparticles Stabilized by Solvated Ions

nanocrystalline core	core size (nm)	stabilizing ions, solvent	ref
ScOOH		2-ethoxyethanol, acetylacetone	597
TiO_2	10−20	Cl^-, H_3O^+, H_2O, poly(vinyl alcohol), eosin	598
TiO_2		$CH_3CO_2^-$, ClO_4^-, Br^-, NO_3^-, OH^-, propanol	28
MnO_x	2−8	NMe_4^+, OH^-, H_2O	599
$MnFe_2O_4$		Cl^-, H_3O^+, H_2O	600
α-Fe_2O_3	4−5	Cl^-, H_3O^+, H_2O	601
γ-Fe_2O_3	2−15 (broad)	(1) NMe_4^+, OH^-, H_2O; (2) oleic acid + sodium dodecylbenzene sulfonate; (3) polystyrene	602
γ-Fe_2O_3	(4−6) × (20−50) (rods)	H_3O^+, H_2O, Cl^-	603
Fe_2O_3, Fe_3O_4	5−15	NMe_4^+, OH^-, H_2O	604
Fe_3O_4	5.7	NMe_4^+, OH^-, H_2O	605
Fe_3O_4	6, 12	H_3O^+, H_2O, Cl^-	606
Fe_3O_4	7	citrate, OH^-, H_2O	607
Fe_3O_4	8.5	H_3O^+, H_2O, Cl^-	603
$NiFe_2O_4$		NO_3^-, H_3O^+, H_2O	608
$CuFe_2O_4$		NO_3^-, H_3O^+, H_2O	608
ZnO		$CH_3CO_2^-$, ClO_4^-, Br^-, NO_3^-, OH^-, propanol	28
ZnO	<7	ethanol	609
$ZnFe_2O_4$		NO_3^-, H_3O^+, H_2O	608
ZrO_2	10−20	Cl^-, H_3O^+, H_2O, poly(vinyl alcohol), eosin	598
Pd, Pd−Au, Pd−Au−Ag		citrate, H_2O	114
CdSe, CdSe/CdS		citrate, OH^-, H_2O	610
SnO_2		Cl^-, H_2O, ethanol, acetylacetone	611
Au	17 × (39−730) (spheres, rods)	citrate, H_2O, poly(vinylpyrrolidone)	612
CeO_2	7	NO_3^-, H_3O^+, H_2O	613

Table 9. Capping Ligands and Coordinating Polymers

donor atom	neutral	anionic	polymeric
C	RNC		
N	R_3N, R_2HN, RH_2N, aromatic amines		$[-CH_2CH_2NH-]_n$ polyvinylpyridine
O	ROH, R_2O, $RC(O)NR_2$, R_3PO	RCO_2^-, RSO_3^-, RPO_3^{2-}, RO^-	$[-CH(OH)CH_2-]_n$ $[-CH_2CH_2O-]_n$ $[-CH(CO_2H)CH_2-]_n$ poly(vinylpyrrolidone) starch (dextran) cyclodextrine alginic acid
P	PR_3		
S	R_2S	RS^-, RCS_2^-, $RCOS^-$	polythiophene

Table 10. Nanoparticles Stabilized with Lipophilic Capping Ligands with O-Donor Atoms

nanocrystalline core	core size (nm)	capping ligand	ref
TiO_2	5.5−10	trioctylphosphine oxide	614
$MnFe_2O_4$	5.3, 6.6	oleic acid, myristic acid	182
FePt	3, ..., 10	oleic acid	91
Fe−Co		oleic acid	183
Fe−FeO_x		oleic acid	183
Fe_2O_3	5−16	octylphosphonic acid 11-undecenoic acid dodecylphosphonic acid	615
γ-Fe_2O_3	4, ..., 16	oleic acid	616
γ-Fe_2O_3	4	caprylic acid	617
γ-Fe_2O_3	10	(1) 2-bromo-2-methylpropionic acid; (2) styrene; (3) polymerization	618
γ-Fe_2O_3	4−10	dodecanol, 2,2′-didodecyl-1,3-dihydroxypropane, 2-dodecyl-1,3-dihydroxypropane, tridodecylcarbinol, didodecylcarbinol	619
Fe_3O_4	4, 8−16	oleic acid	181
Fe_3O_4	6, 12	oleic acid	620
Fe_3O_4	4.2, 6.6	oleic acid, myristic acid	182
Co	3−13	oleic acid	89, 91
Co	2.2−6.4	oleic acid	129
Co	4 × (25−75) disks 8 (spheres)	oleic acid	126, 108
$CoFe_2O_4$	3.3, 4.2	oleic acid, myristic acid	182
Co−Ni		oleic acid	183
CoPt	1.9	oleic acid	129
$CoPt_3$	1.8	oleic acid	129
Ni		oleic acid	183
$NiFe_2O_4$	3.6, 5.1	oleic acid, myristic acid	182
ZnO		octadecylphosphonic acid	621
$ZnFe_2O_4$	5.1, 5.6	oleic acid, myristic acid	182
CdS	1.2, ..., 11.5	trioctylphosphine oxide	197, 199
CdS	various sizes	hexylphosphonic, tetradecylphosphonic acid	208
CdSe	1.5, ..., 10	trioctylphosphine oxide	203
CdSe	1.5, ..., 10	tributylphosphine oxide	199
CdSe	various sizes and shapes	hexylphosphonic acid	206, 207
CdSe	various sizes	hexylphosphonic, tetradecylphosphonic acid	208
CdSe	1.5, ..., 10	hexadecyl phosphate	199
CdSe	1.5, ..., 25	stearic acid or dodecylamine	209, 622
CdSe	4	penta(3-hexylthiophene) phosphonic acid, tri(3-hexylthiophene) phosphonic acid	623
CdSe·ZnS	ZnS shell various sizes	trioctylphosphine oxide + trioctylphosphine + hexadecylamine	204
CdTe	various sizes	hexylphosphonic, tetradecylphosphonic acid	208
CdTe	1.2, ..., 11.5	trioctylphosphine oxide	197, 199
InP	20−50	trioctylphosphine oxide	202
$BaTiO_3$	4−12	oleic acid	606
$Pb_{1-x}Mn_xSe$	10.5	oleic acid	212
PbSe	3.5, ..., 15	oleic acid	210
Eu_2O_3	2−40	trioctylphosphine oxide	624
Gd_2O_3		lauric acid−liposome	625

Table 11. Nanoparticles Stabilized with Lipophilic Capping Ligands with C-Donor Atoms

nanocrystalline core	core size (nm)	capping ligand	ref
Co@Pt core−shell	6.27	dodecylisocyanide	129

Table 12. Nanoparticles Stabilized with Lipophilic Capping Ligands with N-Donor Atoms

nanocrystalline core	core size (nm)	capping ligand	ref
Mn_3O_4		trioctylamine	184
γ-Fe_2O_3		trioctylamine	184
γ-Fe_2O_3	5	octylamine	626
γ-Fe_2O_3	7.2, 10.4	octylamine, dodecylamine	483
$CoFe_2O_4$	7.3	octylamine, dodecylamine	483
Ni	3.7	hexadecylamine	80
Cu_2O	4−10	hexadecylamine	184
Ru	2−3	rnh_2 (r = octyl, dodecyl, hexadecyl)	146
CdS	1.2, ..., 11.5	pyridine	197
CdSe	1.2, ..., 11.5	pyridine	197
CdSe	various sizes	hexadecylamine (trioctylphosphine + trioctylphosphine oxide)	204
CdSe@ZnS (core−shell)	various sizes	hexadecylamine (trioctylphosphine + trioctylphosphine oxide)	204
CdTe	1.2, ..., 11.5	pyridine	197
In_2O_3	4, 6, 8	oleylamine	627

Table 13. Nanoparticles Stabilized with Lipophilic Capping Ligands with S-Donor Atoms

nanocrystalline core	core size (nm)	capping ligand	ref
ZnO		octanethiol, dodecanethiol	621
Ru	2−3	RSH (R = octyl, dodecyl, hexadecyl)	146
Ru	1.6, ..., 6	dodecanethiol	78
Pd	1−5	hexanethiol	628
Pd	1.8, ..., 6.0	RSH (R = C_4−C_{16} *n*-alkyls)	629
$Cd_{32}S_{14}(SC_6H_5)_{36}(DMF)_4$		thiophenol	630
Au	2	RSH (R = butyl, decyl, dodecyl, octadecyl)	631, 632
Au	1−3	dodecanethiol	57
Au@Ag		RSH (R = butyl, decyl, dodecyl, octadecyl)	631, 632
Au@Pt	3.5	RSH (R = butyl, decyl, dodecyl, octadecyl)	631, 632

Table 14. Nanoparticles Capped with P-Donor Atoms

nanocrystalline core	core size (nm)	capping ligand	ref
$Cu_{146}Se_{73}(PPh_3)_{30}$		triphenylphosphine	633
CdS	3−4	tributylphosphine	634
CdS	1.2, ..., 11.5	trioctylphosphine	197
CdSe	1.2, ..., 11.5	trioctylphosphine	197
CdTe	1.2, ..., 11.5	trioctylphosphine	197
CdTe@CdS		tributylphosphine	634

8. Surface-Derivatized Nanoparticles

This section focuses on the basic issues related to nanoparticles with chemically modified surfaces; however, topics dealing with design and application of the specific functional nanocomposites are not considered here. As was outlined in the previous sections, the most common methods of synthesizing nanocrystalline inorganic substances are based on reactions performed in solutions. Solution techniques allow maintainance of the desired composition of the reaction mixtures while eliminating the diffusion restrictions; such methods therefore permit accurate control of the stoichiometry. Solution techniques also allow management of the reaction kinetics and the course of crystallization of the insoluble target product. Solution reactions facilitate tuning the equilibrium between the reagents, products, and solvent and, therefore, provide the opportunity for controlling the interaction of growing crystals with the environment. One of the familiar examples of a system where these interactions are tuned to the desired extent is the synthesis of aqueous colloids (sols) of metals, metal oxides, sulfides, and so forth. Stability of these colloids is optimized as the interaction of the nanocrystals with the solvent and solvated ions is maintained to overcome the van der Waals interaction between the nanocrystals that otherwise leads to agglomeration. The mechanism of sol stabilization involves the adsorption of multiple layers of solvent molecules and solvated ions on the nanocrystals' surfaces, forming electric double layers (EDLs). The resulting highly dynamic assemblies possess excessive electrical charges at their peripherals that cause electrostatic repulsion between them. Details of modern DLVO theory that explain the dynamics in such systems are beyond the scope of this article, and the interested reader is referred to the literature.[596]

Application of the EDL-stabilization method to the synthesis of colloidal inorganics is limited primarily to aqueous solutions, although it may be used with other polar protic solvents as well. The dynamic nature of EDLs and their sensitivity to their environment impose a significant limitation to the stability of the corresponding colloids, but they also open up exceptional possibilities for further chemical steps

Table 15. Nanoparticles Stabilized with Functionalized Polymers

nanocrystalline core	core size (nm)	polymeric molecule	ref
FeOOH		alginic acid	635−637
γ-Fe_2O_3		alginic acid	638−640
Fe_3O_4	10	poly(vinyl alcohol)	641, 642
Fe_3O_4	6, 12	poly(ethylene oxide) (glycol)	114
Fe_3O_4	5.7	poly(meth)acrylic acid	605
Fe_3O_4	5.7	poly(hydroxymethyl)methacrylate	605
Fe_3O_4	6, 12	starch (dextran)	606
Fe_3O_4		starch (dextran)	643, 644, 645
Co	5	poly(dimethylphenylene oxide)	141
Co	1.4	poly(vinylpyrrolidone)	144
Co	1.6	poly(vinylpyrrolidone)	141
Co	4.2	polyphenylene oxide	646
Co·CoO	7.5	poly(dimethylphenylene oxide)	141
CoO		poly(vinylpyrrolidone)	141
$CoPt_{0.9}$	1	poly(vinylpyrrolidone)	143
$CoPt_{2.7}$	1.5	poly(vinylpyrrolidone)	143
Co_3O_4	2	poly(vinylpyrrolidone)	141
$Co_{3.2}Pt$		poly(vinylpyrrolidone)	143
Ni	3−5, 20−30 nm agglomerates	poly(vinylpyrrolidone)	143
ZnO	3.7	poly(vinylpyrrolidone)	647
ZnO	2.6, 2.8, 3.6, 4.0	poly(vinylpyrrolidone)	648
Ru	1.7	cellulose acetate	146
Ru	1.1	poly(vinylpyrrolidone)	646
Ru	1.1	poly(vinylpyrrolidone)	146
Pd	2.5	poly(vinylpyrrolidone)	649
Pd·Ni		poly(vinylpyrrolidone)	649
CdTe		alginic acid	650
$Cd_xHg_{1-x}Te$		alginic acid	650
Pt	1.6	poly(vinylpyrrolidone)	646
Pt·Ru *fcc* → *hcp*		poly(vinylpyrrolidone)	646
HgTe		alginic acid	650

toward the modification of the nanoparticles' surfaces, such as depositing a layer of another inorganic substance (inorganic core−inorganic shell composites), attaching certain organic capping ligands (inorganic core−organic shell composites), depositing/assembling the surfactant-free nanoparticles on the preferred substrate, covalent binding to the desired (bio)molecular systems, and so forth. The most recent developments that utilize colloidal inorganic nanoparticles stabilized by solvated ions are summarized in Table 8.

According to an alternative method, van der Waals interparticle attractions that lead to agglomeration are compensated by surrounding the nanocrystals with bulky organic shells that help keep them apart from each other. This organic interface possessing either hydrophilic or lipophilic properties efficiently stabilizes colloids in aqueous or nonpolar solvent media. There are different types of substances used as components of organic shells, the most common being ionic surfactants, coordinating polymers, and capping ligands. All these compounds possess polar groups that can be attached to the nanoparticle surface and a bulky component within the molecule that provides spatial isolation of the nanocrystal from the environment and provides the solubility properties.

The term "surfactant" is used here for the substances commonly used for preparation of water−oil microemulsions, such as AOT, sodium dodecyl sulfate, CTAB, DDAB, DPB, and TOAB, and for other similar compounds with amphiphilic properties. The AOT and sodium dodecyl sulfate surfactants have an anionic sulfate ester group with a bulky lipophilic substituent. Stabilization of colloids is achieved when the polar group ("head") of these compounds adsorbs on the surfaces of nanocrystals and the organic nonpolar "tail" faces the peripherals of the resulting assembly, thereby providing steric repulsion. In the case of quarternary ammonium halides (CTAB, DDAB, DPB, TOAB, etc.), halide anions surround the nanoparticle surface while their bulky cationic partners form the external protecting shell. The nanoparticle−surfactant assemblies can be viewed as water-free surfactant micelles bodied with the nanocrystals. Details of the application of surfactant-stabilized microemulsions for the synthesis of nanocrystalline materials are described in section 4.1 of this review.

The term "capping ligand" is used for organic molecules that contain a donor group with substituents of varying steric bulk. The main distinction between capping ligands and surfactants lies in the differences of the strength of their binding to metal atoms at the nanocrystal surface, which is greater in the case of capping ligands. These molecules usually closely relate to complexing agents, whose binding to metal atoms or ions has a pronounced covalent character. Generally, colloids containing surfactants have only limited stability, while nanocrystals surrounded by capping ligands are similar to giant metal−cluster complexes that are described as individual substances. To reach the same stability, a smaller mass of capping ligand per unit mass of nanocrystals is required than if surfactant (or polymeric) stabilizer is used. In many cases a monolayer of the molecules of capping ligand around the nanocrystal is sufficient to attain stability against agglomeration with the possibility of isolating and redissolving the solute. The borderline between cap-

Table 16. Nanoparticles Stabilized with Tetraalkylammonium Salts

nanocryst core	core size (nm)	tetraalkylammonium salt	ref
Co	2.5	$Oc_4N^+Cl^-$	651
Ni	4.5	Oc_4N^+: glycolate, lactate, tartrate, gluconate, acetate, dichloroacetate, pivalate, pyruvate, formate, nitrate, bromide	652
Cu	5−10	Oc_4N^+, Br^-	653
Pd	3.6	Oc_4N^+: glycolate, lactate, tartrate, gluconate, acetate, dichloroacetate, pivalate, pyruvate, formate, nitrate, bromide	652
Pd	2.75, 2.0	Oc_4N^+, Bu_4N^+, Cl^-	654
PtRu	1.2	Oc_4N^+, Cl^-	655
Pt_3Sn	1.3	Oc_4N^+, Cl^-	656

Table 17. Nanoparticles Stabilized with Hydrophilic Capping Ligands with O-Donor Atoms

nanocryst core	core size (nm)	capping ligand	ref
FeO_x	5	phosphorylcholine	657, 658
FeO_x		bis- and trisphosphonates, carboxylates, sulfonates	658
γ-Fe_2O_3	4	betaine chloride, 2,5-dihydroxybenzoic acid	659
Fe_3O_4	8.5−11	carboxylated poly(aminoamide) dendrimer	660

Table 18. Nanoparticles Stabilized with Functionalized and Hydrophilic S-Donor Capping Ligands

nanocrystalline core	core size (nm)	capping ligand	ref
$Cd_{17}S_4(SCH_2CH_2OH)_{26}$		mercaptoethanol	661
$Cd_{32}S_{14}(SCH_2CH(OH)CH_3)_{36}\cdot 4H_2O$		mercapto-2-propanol	662
CdSe		1-mercapto-2,3-propanediol, 3-mercaptopropyltrimethoxysilane	610
CdSe@CdS		1-mercapto-2,3-propanediol, 3-mercaptopropyltrimethoxysilane	610
CdTe	nanocrystals, nanowires	mercaptoacetic acid	663
Pt	1.2	1,3-propanedithiol, 1,8-octanedithiol, *p*-hydroxythiophenol, *p*-aminothiophenol, *p*-mercaptobenzoic acid	147
Au	4.6 nm; 30 nm spherical aggregates	mercaptoacetic acid	664
Au	2.8 ± 1	mercaptopoly(ethylene glycol)	665
Au	1.8	$HS(CH_2CH_2O)_xCH_3$; $x = 2, 3, 4$	666
Au	5	4-mercaptophenol	667
Au	1.02, 1.08, 1.28, 1.94, 3.36	mercaptosuccinic acid	74
Au	~145 atoms	$3\text{-}Br(CH_2)_3SH$, $8\text{-}Br(CH_2)_8SH$, $12\text{-}Br(CH_2)_{12}SH$	668

ping ligands and surfactants, however, is not always clearly defined.

In some methods of synthesizing nanoparticles, the passivating agents are introduced into the reaction solution at the initial step. If capping ligands are used, they interact with metal ions in solution and therefore affect the reaction equilibrium and the rates of crystal nucleation and growth, thus influencing the entire course of the precipitation reaction. Adjustment of the complexing properties of reaction solutions allows tuning not only of the nanocrystal size but also of the shape—from spheres to polygons, rods, and wires (see sections 2.2.5 and 2.2.8 of this review).

The importance of capping ligands is not only in providing suitable synthesis conditions and the ability to tune the nanocrystals' sizes and shapes. Due to differences in electronic and binding properties, capping ligands influence the optoelectronic and magnetic properties of functional nanocrystalline inorganic materials. For this reason, it seems useful to classify capping ligands on the basis of their donor group. This general classification is shown in Table 9.

Typical capping ligands can be classified as anionic and neutral. The most common anionic ligands are O- and S-donor type carboxylates, phosphonates, sulfonates, alkoxides, and thiolates. Among common neutral ligands are amines (aliphatic and aromatic), phosphines, phosphine oxides, alcohols, amides, ethers, and sulfides. The nature of the substituents in capping ligands is variable, depending on the specific application of the nanocomposite. Hydrocarbon chains are used for oil-soluble particles, but polar functional groups are preferred when an application requires solubility in water or other polar solvents and a certain reactivity is required for obtaining more complex molecular assemblies. The classification of the recently studied systems on the basis of type of donor groups and type of substituent (determining hydrophilic or lipophilic properties) is given in Tables 10−18.

9. Acknowledgments

We wish to extend our thanks to those authors cited in this work who graciously provided us with TEM, SEM, and AFM images and so forth. Financial support from the Defense Advanced Research Projects Agency (Grant No. MDA972-03-C-0100) is also gratefully acknowledged.

10. References

(1) Feynman, R. P. *Eng. Sci.* **1960**, *23*, 22.
(2) Rouvray, D. *Chem. Br.* **2000**, *36*, 46.
(3) Lawton, G. *Chem. Ind. (London)* **2001**, 174.
(4) Havancsak, K. *Mater. Sci. Forum* **2003**, *414−415*, 85.
(5) Presting, H.; Konig, U. *Mater. Sci. Eng., C: Biomim. Supramol. Syst.* **2003**, *C23*, 737.
(6) Roco, M. C. *Curr. Opin. Biotechnol.* **2003**, *14*, 337.
(7) Orive, G.; Hernandez, R. M.; Rodriguez Gascon, A.; Dominguez-Gil, A.; Pedraz, J. L. *Curr. Opin. Biotechnol.* **2003**, *14*, 659.
(8) Guetens, G.; Van Cauwenberghe, K.; De Boeck, G.; Maes, R.; Tjaden, U. R.; van der Greef, J.; Highley, M.; van Oosterom, A. T.; de Bruijn, E. A. *J. Chromatogr., B: Biomed. Sci. Appl.* **2000**, *739*, 139.
(9) Hochella, M. F. *Earth Planet. Sci. Lett.* **2002**, *203*, 593.
(10) Lieber, C. M. *MRS Bull.* **2003**, *28*, 486.
(11) Buchachenko, A. L. *Russ. Chem. Rev.* **2003**, *72*, 375.
(12) Klabunde, K. J. In *Nanoscale Materials in Chemistry*; Klabunde, K. J., Ed.; Wiley-Interscience: New York, 2001.
(13) Ring, T. A. *Fundamentals of Ceramic Powder Processing and Synthesis*; Academic Press: San Diego, CA, 1996.
(14) Nielsen, A. E. *Kinetics of Precipitation*; Pergamon Press: Oxford, 1964.
(15) Dirksen, J. A.; Ring, T. A. *Chem. Eng. Sci.* **1991**, *46*, 2389.
(16) Tromp, R. M.; Hannon, J. B. *Surf. Rev. Lett.* **2002**, *9*, 1565.
(17) Karpinski, P. H.; Wey, J. S. In *Handbook of Industrial Crystallization*, 2nd ed.; Myerson, A. S., Ed.; Butterworth-Heinemann: Stoneham, MA, 2001.
(18) Blackadder, D. A. *Chem. Eng.* **1964**, CE303.
(19) Füredi-Milhofer, H. *Pure Appl. Chem.* **1981**, *53*, 2041.
(20) Lifshitz, I. M.; Slyozov, V. V. *J. Phys. Chem. Solids* **1961**, *19*, 35.
(21) Wagner, C. *Z. Elektrochem.* **1961**, *65*, 581.
(22) Sugimoto, T. *Adv. Colloid Interface Sci.* **1987**, *28*, 65.
(23) Marqusee, J. A.; Ross, J. *J. Chem. Phys.* **1983**, *79*, 373.
(24) Madras, G.; McCoy, B. J. *J. Chem. Phys.* **2002**, *117*, 8042.
(25) Sugimoto, S. *J. Colloid Interface Sci.* **1978**, *63*, 16.
(26) Sugimoto, S. *J. Colloid Interface Sci.* **1978**, *63*, 369.
(27) Tokuyama, M.; Kawasaki, K.; Enomoto, Y. *Physica A* **1986**, *134A*, 323.
(28) Oskam, G.; Hu, Z.; Penn, R. L.; Pesika, N.; Searson, P. C. *Phys. Rev. E* **2002**, *66*, 011403.
(29) Dadyburjor, D. B.; Ruckenstein, E. *J. Cryst. Growth* **1977**, *40*, 279.
(30) Kahlweit, M. *Ber. Bunsen-Ges. Phys. Chem.* **1974**, *78*, 997.
(31) Park, J.; Privman, V.; Matijevic, E. *J. Phys. Chem. B* **2001**, *105*, 11630.
(32) Bramley, A. S.; Hounslow, M. J.; Ryall, R. L. *J. Colloid Interface Sci.* **1996**, *183*, 155.
(33) Reetz, M. T.; Helbig, W.; Quaiser, S. A.; Stimming, U.; Breuer, N.; Vogel, R. *Science* **1995**, *267*, 367.
(34) Roucoux, A.; Schulz, J.; Patin, H. *Chem. Rev.* **2002**, *102*, 3757.
(35) Klabunde, K. J.; Mulukutla, R. S. In *Nanoscale Materials in Chemistry*; Klabunde, K. J., Ed.; Wiley-Interscience: New York, 2001.
(36) Johnson, B. F. G. *Top. Catal.* **2003**, *24*, 147.
(37) Burkin, A. R.; Richardson, F. D. *Powder Metall.* **1967**, *10*, 33.
(38) Schaufelberger, F. A. *J. Metals* **1956**, *8*, 695.
(39) Glavee, G. N.; Klabunde, K. J.; Sorensen, C. M.; Hadjipanayis, G. C. *Langmuir* **1993**, *9*, 162.
(40) Glavee, G. N.; Klabunde, K. J.; Sorensen, C. M.; Hadjipanayis, G. C. *Inorg. Chem.* **1995**, *34*, 28.
(41) Glavee, G. N.; Klabunde, K. J.; Sorensen, C. M.; Hadjipanayis, G. C.; Tang, Z. X.; Yiping, L. *Nanostruct. Mater.* **1993**, *3*, 391.
(42) Glavee, G. N.; Klabunde, K. J.; Sorensen, C. M.; Hadjipanayis, G. C. *Langmuir* **1994**, *10*, 4726.
(43) Dragieva, I. D.; Stoynov, Z. B.; Klabunde, K. J. *Scr. Mater.* **2001**, *44*, 2187.
(44) Gui, Z.; Fan, R.; Mo, W.; Chen, X.; Yang, L.; Hu, Y. *Mater. Res. Bull.* **2003**, *38*, 169.
(45) Chen, D.-H.; Hsieh, C.-H. *J. Mater. Chem.* **2002**, *12*, 2412.
(46) Sondi, I.; Goia, D. V.; Matijevic, E. *J. Colloid Interface Sci.* **2003**, *260*, 75.
(47) Yonezawa, T.; Onoue, S.; Kimizuka, N. *Langmuir* **2000**, *16*, 5218.
(48) Tan, Y.; Dai, X.; Li, Y.; Zhu, D. *J. Mater. Chem.* **2003**, *13*, 1069.
(49) Yonezawa, T.; Sutoh, M.; Kunitake, T. *Chem. Lett.* **1997**, 619.
(50) Boutonnet, M.; Kizling, J.; Stenius, P.; Maire, G. *Colloids Surf.* **1982**, *5*, 209.
(51) Enüstün, B. V.; Turkevich, J. *J. Am. Chem. Soc.* **1963**, *85*, 3317.
(52) Turkevich, J.; Stevenson, P. S.; Hillier, J. *Discuss. Faraday Soc.* **1951**, *11*, 58.
(53) Keating, C. D.; Musick, M. D.; Keefe, M. H.; Natan, M. J. *J. Chem. Educ.* **1999**, *76*, 949.
(54) Chow, G. M.; Ambrose, T.; Xiao, J. Q.; Twigg, M. E.; Baral, S.; Ervin, A. M.; Quadri, S. B.; Feng, C. R. *Nanostruct. Mater.* **1992**, *1*, 361.
(55) van Wonterghem, J.; Mørup, S.; Koch, C. J. W.; Charles, S. W.; Wells, S. *Nature* **1986**, *322*, 622.
(56) Harris, V. G.; Kaatz, F. H.; Browning, V.; Gillespie, D. J.; Everett, R. K.; Ervin, A. M.; Elam, W. T.; Edelstein, A. S. *J. Appl. Phys.* **1994**, *75*, 6610.
(57) Brust, M.; Walker, M.; Bethell, D.; Schiffrin, D. J.; Whyman, R. *Chem. Commun.* **1994**, 801.
(58) Brust, M.; Fink, J.; Bethell, D.; Schiffrin, J.; Kiely, C. *Chem. Commun.* **1995**, 1655.
(59) Weisbecker, C. S.; Merritt, M. V.; Whitesides, G. M. *Langmuir* **1996**, *12*, 3763.
(60) Porter, L. A., Jr.; Ji, D.; Westcott, S. L.; Graupe, M.; Czernuszewicz, R. S.; Halas, N. J.; Lee, T. R. *Langmuir* **1998**, *14*, 7378.
(61) Thomas, P. J.; Saravanan, P.; Kulkarni, G. U.; Rao, C. N. R. *Pramana−J. Phys.* **2002**, *58*, 371.
(62) Yonezawa, T.; Kunitake, T. *Colloids Surf., A* **1999**, *149*, 193.
(63) Green, M.; O'Brien, P. *Chem. Commun.* **2000**, 183.
(64) Xu, W.; Liu, W.; Zhang, D.; Xu, Y.; Wang, T.; Zhu, W. *Colloids Surf., A* **2002**, *204*, 201.
(65) Corbierre, M. K.; Cameron, N. S.; Sutton, M.; Mochrie, S. G. J.; Lurio, L. B.; Ruhm, A.; Lennox, R. B. *J. Am. Chem. Soc.* **2001**, *123*, 10411.
(66) Prasad, B. L. V.; Stoeva, S. I.; Sorensen, C. M.; Klabunde, K. J. *Chem. Mater.* **2003**, *15*, 935.
(67) Brown, L. O.; Hutchison, J. E. *J. Am. Chem. Soc.* **1997**, *119*, 12384.
(68) Ingram, R. S.; Hostetler, M. J.; Murray, R. W. *J. Am. Chem. Soc.* **1997**, *119*, 9175.
(69) Hostetler, M. J.; Green, S. J.; Stokes, J. J.; Murray, R. W. *J. Am. Chem. Soc.* **1996**, *118*, 4212.
(70) Nuss, S.; Böttcher, H.; Wurm, H.; Hallensleben, M. L. *Angew. Chem., Int. Ed.* **2001**, *40*, 4016.
(71) Tour, J. M.; Jones, L., II; Pearson, D. L.; Lambda, J. J. S.; Burgin, T. P.; Whitesides, G. M.; Allara, D. L.; Parikh, A. N.; Atre, S. V. *J. Am. Chem. Soc.* **1995**, *117*, 9529.
(72) Andres, R. P.; Bielefeld, J. D.; Henderson, J. I.; Janes, D. B.; Kolagunta, V. R.; Kubiak, C. P.; Mahoney, W. J.; Osifchin, R. G. *Science* **1996**, *273*, 1690.
(73) Stoeva, S. I.; Klabunde, K. J.; Sorensen, C. M.; Dragieva, I. *J. Am. Chem. Soc.* **2002**, *124*, 2305.
(74) Chen, S.; Kimura, K. *Langmuir* **1999**, *15*, 1075.
(75) Chen, S.; Kimura, K. *Chem. Lett.* **1999**, 1169.
(76) Han, M. Y.; Quek, C. H.; Huang, W.; Chew, C. H.; Gan, L. H. *Chem. Mater.* **1999**, *11*, 1144.
(77) Pastoriza-Santos, I.; Liz-Marzán, L. M. *Langmuir* **1999**, *15*, 948.
(78) Viau, G.; Brayner, R.; Poul, L.; Chakroune, N.; Lacaze, E.; Fievet-Vincent, F.; Fievet, F. *Chem. Mater.* **2003**, *15*, 486.
(79) Wu, S.-H.; Chen, D.-H. *J. Colloid Interface Sci.* **2003**, *259*, 282.
(80) Hou, Y.; Gao, S. *J. Mater. Chem.* **2003**, *13*, 1510.
(81) Cotton, F. A.; Wilkinson, G. *Advanced Inorganic Chemistry*, 5th ed.; Wiley: New York, 1988.
(82) Tsai, K.-L.; Dye, J. L. *J. Am. Chem. Soc.* **1991**, *113*, 1650.
(83) Tsai, E. H.; Dye, J. L. *Chem. Mater.* **1993**, *5*, 540.
(84) Kirkpatrick, E. M.; Leslie-Pelecky, D. L.; Kim, S.-H.; Rieke, R. D. *J. Appl. Phys.* **1999**, *85*, 5375.
(85) Bönnemann, H.; Brijoux, W.; Joussen, T. *Angew. Chem., Int. Ed.* **1990**, *29*, 273.
(86) Bönnemann, H.; Brijoux, W.; Brinkmann, R.; Dinjus, E.; Jouben, T.; Korall, B. *Angew. Chem., Int. Ed. Engl.* **1991**, *30*, 1312.
(87) Bönnemann, H.; Bogdanovic, B.; Brinkmann, R.; Spliethoff, B.; He, D.-W. *J. Organomet. Chem.* **1993**, *451*, 23.
(88) Zeng, D.; Hampden-Smith, M. J. *Chem. Mater.* **1993**, *5*, 681.
(89) Sun, S.; Murray, C. B.; Doyle, H. *Mater. Res. Soc. Symp. Proc.* **1999**, *577*, 385.
(90) Sun, S.; Murray, C. B. *J. Appl. Phys.* **1999**, *85*, 4325.
(91) Murray, C. B.; Sun, S.; Doyle, H.; Betley, T. *MRS Bull.* **2001**, 985.
(92) Bönnemann, H.; Brijoux, W.; Hofstadt, H.-W.; Ould-Ely, T.; Schmidt, W.; Wassmuth, B.; Weidenthaler, C. *Angew. Chem., Int. Ed.* **2002**, *41*, 599.
(93) Angermund, K.; Bühl, M.; Dinjus, E.; Endruschat, U.; Gassner, F.; Haubold, H.-G.; Hormes, J.; Köhl, G.; Mauschick, F. T.; Modrow, H.; Mörtel, R.; Mynott, R.; Tesche, B.; Vad, T.; Waldöfner, N.; Bönnemann, H. *Angew. Chem., Int. Ed.* **2002**, *41*, 4041.
(94) Bönnemann, H.; Waldöfner, N.; Haubold, H.-G.; Vad, T. *Chem. Mater.* **2002**, *14*, 1115.
(95) Haubold, H.-G.; Vad, T.; Waldöfner, N.; Bönnemann, H. *J. Appl. Crystallogr.* **2003**, *36*, 617.
(96) Angermund, K.; Bühl, M.; Endruschat, U.; Mauschick, F. T.; Mörtel, R.; Mynott, R.; Tesche, B.; Waldöfner, N.; Bönnemann, H.; Köhl, G.; Modrow, H.; Hormes, J.; Dinjus, E.; Gassner, F.; Haubold, H.-G.; Vad, T.; Kaupp, M. *J. Phys. Chem. B* **2003**, *107*, 7507.
(97) Bönnemann, H.; Brijoux, W.; Brinkmann, R.; Matoussevitch, N.; Waldöfner, N.; Palina, N.; Modrow, H. *Inorg. Chim. Acta* **2003**, *350*, 617.
(98) Viau, G.; Fievet-Vincent, F.; Fievet, F. *Solid State Ionics* **1996**, *84*, 259.
(99) Reetz, M. T.; Helbig, W. *J. Am. Chem. Soc.* **1994**, *116*, 7401.

(100) Rodriguez-Sanchez, L.; Blanco, M. C.; Lopez-Quintela, M. A. *J. Phys. Chem. B* **2000**, *104*, 9683.
(101) Mohamed, M. B.; Wang, Z. L.; El-Sayed, M. A. *J. Phys. Chem. A* **1999**, *103*, 10255.
(102) Asenjo, J.; Amigo, R.; Krotenko, E.; Torres, F.; Tejada, J.; Brillas, E.; Sardin, G. *J. Nanosci. Nanotechnol.* **2001**, *1*, 441.
(103) Huang, H. H.; Ni, X. P.; Loy, G. L.; Chew, C. H.; Tan, K. L.; Loh, F. C.; Deng, J. F.; Xu, G. Q. *Langmuir* **1996**, *12*, 909.
(104) Draganic, I. G.; Draganic, Z. D. *The Radiolysis of Water*; Academic Press: New York, 1971.
(105) Henglein, A. *Langmuir* **1999**, *15*, 6738.
(106) Ershov, B. G.; Sukhov, N. L.; Janata, E. *J. Phys. Chem. B* **2000**, *104*, 6138.
(107) Henglein, A. *J. Phys. Chem. B* **2000**, *104*, 1206.
(108) Wang, S.; Zin, H. *J. Phys. Chem. B* **2000**, *104*, 5681.
(109) Henglein, A.; Meisel, D. *Langmuir* **1998**, *14*, 7392.
(110) Hodak, J. H.; Henglein, A.; Hartland, G. V. *J. Phys. Chem. B* **2000**, *104*, 9954.
(111) Henglein, A. *J. Phys. Chem. B* **2000**, *104*, 2201.
(112) Henglein, A.; Giersig, M. *J. Phys. Chem. B* **2000**, *104*, 5056.
(113) Mulvaney, P.; Giersig, M.; Henglein, A. *J. Phys. Chem.* **1992**, *96*, 10419.
(114) Henglein, A. *J. Phys. Chem. B* **2000**, *104*, 6683.
(115) Lee, H. J.; Je, J. H.; Hwu, Y.; Tsai, W. L. *Nucl. Instr. Methods Phys. Res. B* **2003**, *199*, 342.
(116) Chen, Y. H.; Yeh, C. S. *Chem. Commun.* **2001**, 371.
(117) Chen, Y. H.; Tseng, Y. H.; Yeh, C.-S. *J. Mater. Chem.* **2002**, *12*, 1419.
(118) Tsai, S.-H.; Liu, Y.-H.; Wu, P.-L.; Yeh, C.-S. *J. Mater. Chem.* **2003**, *13*, 978.
(119) Kato, Y.; Sugimoto, S.; Shinohara, K.; Tezuka, N.; Kagotani, T.; Inomata, K. *Mater. Trans., JIM* **2002**, *43*, 406.
(120) Hess, P. H.; Parker, H., Jr. *J. Appl. Polym. Sci.* **1966**, *10*, 1915.
(121) Smith, T. W.; Wychick, D. *J. Phys. Chem.* **1980**, *84*, 1621.
(122) Charles, S. W.; Wells, S.; Villadsen, J. *Hyperfine Interact.* **1986**, *27*, 333.
(123) van Wonterghem, J.; Mørup, S.; Charles, S. W.; Wells, S.; Villadsen, J. *Phys. Rev. Lett.* **1985**, *55*, 410.
(124) Ge, F.; Chen, L.; Ku, W.; Zhu, J. *Nanostruct. Mater.* **1997**, *8*, 703.
(125) Dinega, D.; Bawendi, M. G. *Angew. Chem., Int. Ed. Engl.* **1999**, *38*, 1788.
(126) Puntes, V. F.; Krishnan, K. M.; Alivisatos, A. P. *Science* **2001**, *291*, 2115.
(127) Puntes, V. F.; Zanchet, D.; Erdonmez, C. K.; Alivisatos, A. P. *J. Am. Chem. Soc.* **2002**, *124*, 12874.
(128) Sun, S.; Murray, C. B.; Weller, D.; Folks, L.; Moser, A. *Science* **2000**, *287*, 1989.
(129) Park, J.-I.; Cheon, J. *J. Am. Chem. Soc.* **2001**, *123*, 5743.
(130) Amiens, C.; de Caro, D.; Chaudret, B.; Bradley, J. S.; Mazel, R.; Roucau, C. *J. Am. Chem. Soc.* **1993**, *115*, 11638.
(131) Duteil, A.; Queau, R.; Chaudret, B.; Mazel, R.; Roucau, C.; Bradley, J. S. *Chem. Mater.* **1993**, *5*, 341.
(132) Rodriguez, A.; Amiens, C.; Chaudret, B.; Casanove, M.-J.; Lecante, P.; Bradley, J. S. *Chem. Mater.* **1996**, *8*, 1978.
(133) Osuna, J.; de Caro, D.; Amiens, C.; Chaudret, B.; Snoeck, E.; Respaud, M.; Broto, J.-M.; Fert, A. *J. Phys. Chem.* **1996**, *100*, 14571.
(134) Bardaji, M.; Vidoni, O.; Rodriguez, A.; Amiens, C.; Chaudret, B.; Casanove, M.-J.; Lecante, P. *New J. Chem.* **1997**, *21*, 1243.
(135) Zitoun, D.; Amiens, C.; Chaudret, B.; Fromen, M. C.; Lecante, P.; Casanove, M. J.; Respaud, M. *J. Phys. Chem. B* **2003**, *107*, 6997.
(136) Pellegatta, J.-L.; Blandy, C.; Choukroun, R.; Lorber, C.; Chaudret, B.; Lecante, P.; Snoeck, E. *New J. Chem.* **2003**, *17*, 1528.
(137) Pelzer, K.; Vidoni, O.; Philippot, K.; Chaudret, B.; Colliere, V. *Adv. Funct. Mater.* **2003**, *13*, 118.
(138) Gomez, M.; Philippot, K.; Colliere, V.; Lecante, P.; Muller, G.; Chaudret, B. *New J. Chem.* **2003**, *27*, 114.
(139) Dassenoy, F.; Philippot, K.; Ely, T. O.; Amiens, C.; Lecante, P.; Snoeck, E.; Mosset, A.; Casanove, M.-J.; Chaudret, B. *New J. Chem.* **1998**, *22*, 703.
(140) Ely, T. O.; Amiens, C.; Chaudret, B. *Chem. Mater.* **1999**, *11*, 526.
(141) Verelst, M.; Ely, T. O.; Amiens, C.; Snoeck, E.; Lecante, P.; Mosset, A.; Respaud, M.; Broto, J. M.; Chaudret, B. *Chem. Mater.* **1999**, *11*, 2702.
(142) Pan, C.; Dassenoy, F.; Casanove, M.-J.; Philippot, K.; Amiens, C.; Lecante, P.; Mosset, A.; Chaudret, B. *J. Phys. Chem. B* **1999**, *103*, 10098.
(143) Ely, T. O.; Pan, C.; Amiens, C.; Chaudret, B.; Dassenoy, F.; Lecante, P.; Casanove, M.-J.; Mosset, A.; Respaud, M.; Broto, J. M. *J. Phys. Chem. B* **2000**, *104*, 695.
(144) Dassenoy, F.; Casanove, M.-J.; Lecante, P.; Verelst, M.; Snoeck, E.; Mosset, A.; Ely, T. O.; Amiens, C.; Chaudret, B. *J. Chem. Phys.* **2000**, *112*, 8137.
(145) Choukroun, R.; de Caro, D.; Chaudret, B.; Lecante, P.; Snoeck, E. *New J. Chem.* **2001**, *25*, 525.
(146) Pan, C.; Pelzer, K.; Philippot, K.; Chaudret, B.; Dassenoy, F.; Lecante, P.; Casanove, M.-J. *J. Am. Chem. Soc.* **2001**, *123*, 7584.
(147) Gomez, S.; Erades, L.; Philippot, K.; Chaudret, B.; Colliere, V.; Balmes, O.; Bovin, J.-O. *Chem. Commun.* **2001**, 1474.
(148) Zitoun, D.; Respaud, M.; Fromen, M.-C.; Casanove, M.-J.; Lecante, P.; Amiens, C.; Chaudret, B. *Phys. Rev. Lett.* **2002**, *89*, 037203/1.
(149) Casanove, M.-J.; Lecante, P.; Fromen, M.-C.; Respaud, M.; Zitoun, D.; Pan, C.; Philippot, K.; Amiens, C.; Chaudret, B.; Dassenoy, F. *Mater. Res. Soc. Symp. Proc.* **2002**, *704*, 349.
(150) Cordente, N.; Respaud, M.; Senocq, F.; Casanove, M.-J.; Amiens, C.; Chaudret, B. *Nano Lett.* **2001**, *1*, 565.
(151) Dumestre, F.; Chaudret, B.; Amiens, C.; Fromen, M.-C.; Casanove, M.-J.; Renaud, P.; Zurcher, P. *Angew. Chem., Int. Ed.* **2002**, *41*, 4286.
(152) Scheeren, C. W.; Machado, G.; Dupont, J.; Fichtner, P. F. P.; Texeira, S. R. *Inorg. Chem.* **2003**, *42*, 4738.
(153) Soulantica, K.; Maisonnat, A.; Fromen, M.-C.; Casanove, M.-J.; Lecante, P.; Chaudret, B. *Angew. Chem., Int. Ed.* **2001**, *40*, 448.
(154) Soulantica, K.; Erades, L.; Sauvan, M.; Senocq, F.; Maisonnat, A.; Chaudret, B. *Adv. Funct. Mater.* **2003**, *13*, 553.
(155) Soulantica, K.; Maisonnat, A.; Senocq, F.; Fromen, M.-C.; Casanove, M.-J.; Chaudret, B. *Angew. Chem., Int. Ed.* **2001**, *40*, 2984.
(156) de Caro, D.; Agelou, V.; Duteil, A.; Chaudret, B.; Mazel, R.; Roucau, C.; Bradley, J. S. *New J. Chem.* **1995**, *19*, 1265.
(157) Albuquerque, A. S.; Ardisson, J. D.; Macedo, W. A. *J. Appl. Phys.* **2000**, *87*, 4352.
(158) Chen, Q.; Rondinone, A. J.; Chakoumakos, B. C.; Zhang, Z. J. *J. Magn. Magn. Mater.* **1999**, *194*, 1.
(159) Wang, J. F.; Ponton, C. B.; Harris, I. R. *J. Magn. Magn. Mater.* **2002**, *242*−*245*, 1464.
(160) Gu, Y.; Li, G.-Z.; Meng, G.; Peng, D. *Mater. Res. Bull.* **2000**, *35*, 297.
(161) Li, J.-G.; Ikegami, T.; Wang, Y.; Mori, T. *J. Am. Ceram. Soc.* **2002**, *85*, 2376.
(162) Xiang, L.; Deng, X. Y.; Jin, Y. *Scr. Mater.* **2002**, *47*, 219.
(163) Du, Y.; Fang, J.; Zhang, M.; Hong, J.; Yin, Z.; Zhang, Q. *Mater. Lett.* **2002**, *57*, 802.
(164) Borse, P. H.; Kankate, L. S.; Dassenoy, F.; Vogel, W.; Urban, J.; Kulkarni, S. K. *J. Mater. Sci., Mater. Electron.* **2002**, *13*, 553.
(165) Kuo, P. C.; Tsai, T. S. *J. Appl. Phys.* **1989**, *65*, 4349.
(166) Tang, Z. X.; Sorensen, C. M.; Klabunde, K. J.; Hadjipanayis, G. C. *J. Colloid Interface Sci.* **1991**, *146*, 38.
(167) Rojas, T. C.; Ocana, M. *Scr. Mater.* **2002**, *46*, 655.
(168) Chinnasamy, C. N.; Jeyadevan, B.; Perales-Perez, O.; Shinoda, K.; Tohji, K.; Kasuya, A. *IEEE Trans. Magn.* **2002**, *38*, 2640.
(169) Li, J.; Dai, D.; Zhao, B.; Lin, Y.; Liu, C. *J. Nanopart. Res.* **2002**, *4*, 261.
(170) Wu, K. T.; Kuo, P. C.; Yao, Y. D.; Tsai, E. H. *IEEE Trans. Magn.* **2001**, *37*, 2651.
(171) Voit, W.; Kim, D. K.; Zapka, W.; Muhammed, M.; Rao, K. V. 2001; p Y7.8.1.
(172) Tang, Z. X.; Sorensen, C. M.; Klabunde, K. J.; Hadjipanayis, G. C. *Phys. Rev. Lett.* **1991**, *67*, 3602.
(173) Liu, Z. L.; Liu, Y. J.; Yao, K. L.; Ding, Z. H.; Tao, J.; Wang, X. *J. Mater. Synth. Process.* **2002**, *10*, 83.
(174) Wang, Y.; Ma, C.; Sun, X.; Li, H. *Inorg. Chem. Commun.* **2002**, *5*, 751.
(175) Zhang, Z.; Guo, L.; Wang, W. *J. Mater. Res.* **2001**, *16*, 803.
(176) Mizushima, K.; Jones, P. C.; Wiseman, P. J.; Goodenough, J. B. *Mater. Res. Bull.* **1980**, *15*, 783.
(177) Chen, H.; Qiu, X.; Zhu, W.; Hagenmuller, P. *Electrochem. Commun.* **2002**, *4*, 488.
(178) Music, S.; Popovic, S.; Maljkovic, M.; Furic, K.; Gajovic, A. *Mater. Lett.* **2002**, *56*, 806.
(179) Deb, P.; Biswas, T.; Sen, D.; Basumallick, A.; Mazumder, S. *J. Nanopart. Res.* **2002**, *4*, 91.
(180) Ennas, G.; Marongiu, G.; Musinu, A.; Falqui, A.; Ballirano, P.; Caminiti, R. *J. Mater. Res.* **1999**, *14*, 1570.
(181) O'Brien, S.; Brus, L.; Murray, C. B. *J. Am. Chem. Soc.* **2001**, *123*, 12085.
(182) Caruntu, D.; Remond, Y.; Chou, N. H.; Jun, M.-J.; Caruntu, G.; He, J.; Goloverda, G.; O'Connor, C.; Kolesnichenko, V. *Inorg. Chem.* **2002**, *41*, 6137.
(183) Sun, S.; Zeng, H. *J. Am. Chem. Soc.* **2002**, *124*, 8204.
(184) Rockenberger, J.; Scher, E. C.; Alivisatos, A. P. *J. Am. Chem. Soc.* **1999**, *121*, 11595.
(185) Rosetti, R.; Hull, R.; Gibson, J. M.; Brus, L. E. *J. Chem. Phys.* **1985**, *83*.
(186) Dannhauser, T.; O'Neill, M.; Johansson, K. R.; Whitten, D.; McLendon, G. *J. Phys. Chem.* **1953**, *57*, 670.
(187) Berry, C. R. *Phys. Rev.* **1967**, *161*, 848.
(188) Trindade, T.; O'Brien, P.; Pickett, N. L. *Chem. Mater.* **2001**, *13*, 3843.
(189) Dushkin, C. D.; Saita, S.; Yoshie, K.; Yamaguchi, Y. *Adv. Colloid Interface Sci.* **2000**, *88*, 37.
(190) Steigerwald, M. L.; Sprinkle, C. R. *Organometallics* **1988**, *7*, 245.
(191) Stuczynski, S. M.; Brennan, J. G.; Steigerwald, M. L. *Inorg. Chem.* **1989**, *28*, 4431.
(192) Steigerwald, M. L. *Mater. Res. Soc. Symp. Proc.* **1989**, *131*, 37.

(193) Brennan, J. G.; Siegrist, T.; Carroll, P. J.; Stuczynski, S. M.; Brus, L. E.; Steigerwald, M. L. *J. Am. Chem. Soc.* **1989**, *111*, 4141.
(194) Brennan, J. G.; Siegrist, T.; Carroll, P. J.; Stuczynski, S. M.; Reynders, P.; Brus, L. E.; Steigerwald, M. L. *Chem. Mater.* **1990**, *2*, 403.
(195) Stuczynski, S. M.; Opila, R. L.; Marsh, P.; Brennan, J. G.; Steigerwald, M. L. *Chem. Mater.* **1991**, *3*, 379.
(196) Marcus, M. A.; Brus, L. E.; Murray, C.; Bawendi, M. G.; Prasad, A.; Alivisatos, A. P. *Nanostruct. Mater.* **1992**, *1*, 323.
(197) Murray, C. B.; Norris, D. J.; Bawendi, M. G. *J. Am. Chem. Soc.* **1993**, *115*, 8706.
(198) Becerra, L. R.; Murray, C. B.; Griffin, R. G.; Bawendi, M. G. *J. Chem. Phys.* **1994**, *100*, 3297.
(199) Murray, C. B.; Kagan, C. R.; Bawendi, M. G. *Science* **1995**, *270*, 1335.
(200) Danek, M.; Jensen, K. F.; Murray, C. B.; Bawendi, M. G. *Chem. Mater.* **1996**, *8*, 173.
(201) Guzelian, A. A.; Banin, U.; Kadavanich, A. V.; Peng, X.; Alivisatos, A. P. *Appl. Phys. Lett.* **1996**, *69*, 1432.
(202) Guzelian, A. A.; Katari, J. E. B.; Kadavanich, A. V.; Banin, U.; Hamad, K.; Juban, E.; Alivisatos, A. P.; Wolters, R. H.; Arnold, C. C.; Heath, J. R. *J. Phys. Chem.* **1996**, *100*, 7212.
(203) Peng, X.; Wickham, J.; Alivisatos, A. P. *J. Am. Chem. Soc.* **1998**, *120*, 5343.
(204) Talapin, D. V.; Rogach, A. L.; Kornowski, A.; Haase, M.; Weller, H. *Nano Lett.* **2001**, *1*, 207.
(205) Peng, X.; Manna, L.; Yang, W.; Wickham, J.; Scher, E.; Kadavanich, A. *Nature* **2000**, *404*, 59.
(206) Manna, L.; Scher, E. C.; Alivisatos, A. P. *J. Am. Chem. Soc.* **2000**, *122*, 12700.
(207) Peng, Z. A.; Peng, X. *J. Am. Chem. Soc.* **2001**, *123*, 1389.
(208) Peng, Z. A.; Peng, X. *J. Am. Chem. Soc.* **2001**, *123*, 183.
(209) Qu, L.; Peng, Z. A.; Peng, X. *Nano Lett.* **2001**, *1*, 333.
(210) Murray, C. B.; Sun, S.; Gaschler, W.; Doyle, H.; Betley, T. A.; Kagan, C. R. *IBM J. Res. Dev.* **2001**, *45*, 47.
(211) Mikulec, F. V.; Kuno, M.; Bennati, M.; Hall, D. A.; Griffin, R. G.; Bawendi, M. G. *J. Am. Chem. Soc.* **2000**, *122*, 2532.
(212) Ji, T.; Jian, W.-B.; Fang, J. *J. Am. Chem. Soc.* **2003**, *125*, 8448.
(213) Pastoriza-Santos, I.; Liz-Marzán, L. M. *Langmuir* **2002**, *18*, 2888.
(214) Fiévet, F.; Lagier, J. P.; Figlarz, M. *MRS Bull.* **1989**, *24*, 29.
(215) Yu, W.; Tu, W.; Liu, H. *Langmuir* **1999**, *15*, 6.
(216) Tsuji, M.; Hashimoto, M.; Tsuji, T. *Chem. Lett.* **2002**, 1232.
(217) Tu, W.; Liu, H. *Chem. Mater.* **2000**, *12*, 564.
(218) Palchik, O.; Avivi, S.; Pinkert, D.; Gedanken, A. *Nanostruct. Mater.* **1999**, *11*, 415.
(219) Zhu, J.; Palchik, O.; Chen, S.; Gedanken, A. *J. Phys. Chem. B* **2000**, *104*, 7344.
(220) Palchik, O.; Zhu, J.; Gedanken, A. *J. Mater. Chem.* **2000**, *10*, 1251.
(221) Palchik, O.; Kerner, R.; Gedanken, A.; Weiss, A. M.; Slifkin, M. A.; Palchik, V. *J. Mater. Chem.* **2001**, *11*, 874.
(222) Grisaru, H.; Palchik, O.; Gedanken, A.; Palchik, V.; Slifkin, M. A.; Weiss, A. M. *J. Mater. Chem.* **2002**, *12*, 339.
(223) Kerner, R.; Palchik, O.; Gedanken, A. *Chem. Mater.* **2001**, *13*, 1413.
(224) Li, Q.; Wei, Y. *Mater. Res. Bull.* **1998**, *33*, 779.
(225) Wada, Y.; Kuramoto, H.; Sakata, T.; Mori, H.; Sumida, T.; Kitamura, T.; Yanagida, S. *Chem. Lett.* **1999**, 607.
(226) Liao, X.-H.; Wang, H.-C.; Zhu, J.-J.; Chen, H.-Y. *Mater. Res. Bull.* **2001**, *36*, 2339.
(227) Suslick, K. S. *Science* **1990**, *247*, 1439.
(228) Flint, E. B.; Suslick, K. S. *Science* **1991**, *253*, 1397.
(229) Atchley, A. A.; Crum, L. A. In *Ultrasound*; Suslick, K. S., Ed.; VCH: New York, 1988.
(230) Suslick, K. S.; Hammerton, D. A.; Cline, R. E. *J. Am. Chem. Soc.* **1986**, *108*, 5641.
(231) Suslick, K. S.; Choe, S.-B.; Cichowlas, A. A.; Grinstaff, M. W. *Nature* **1991**, *353*, 414.
(232) Suslick, K. S.; Fang, M.; Hyeon, T. *J. Am. Chem. Soc.* **1996**, *118*, 11960.
(233) Grinstaff, M. W.; Salmon, M. B.; Suslick, K. S. *Phys. Rev. B* **1993**, *48*, 269.
(234) Gonsalves, K. E.; Rangarajan, S. P.; Garcia-Ruiz, A.; Law, C. C. *J. Mater. Sci. Lett.* **1996**, *15*, 1261.
(235) Shafi, K. V. P. M.; Koltypin, Y.; Gedanken, A.; Prozorov, R.; Balogh, J.; Lendavi, J.; Felner, I. *J. Phys. Chem. B* **1997**, *101*, 6409.
(236) Liang, J.; Jiang, X.; Liu, G.; Deng, Z.; Zhuang, J.; Li, F.; Li, Y. *Mater. Res. Bull.* **2003**, *38*, 161.
(237) Pang, G.; Xu, X.; Markovich, V.; Avivi, S.; Palchik, O.; Koltypin, Y.; Gorodetsky, G.; Yeshurun, Y.; Buchkremer, H. P.; Gedanken, A. *Mater. Res. Bull.* **2003**, *38*, 11.
(238) Zheng, X.; Xie, Y.; Zhu, L.; Jiang, X.; Yan, A. *Ultrason. Sonochem.* **2002**, *9*, 311.
(239) Ebelmen, M. *Ann. Chim. Phys.* **1846**, *16*, 129.
(240) Geffcken, W.; Berger, E. German Patent 736,411, May, 1939.
(241) Hench, L. L.; West, J. K. *Chem. Rev.* **1990**, *90*, 33.
(242) Roy, R. *Chem. Process. Adv. Mater.* **1992**, 1022.
(243) Brinker, C. J.; Scherer, G. W. *Sol−Gel Science: The Physics and Chemistry of Sol−Gel Processing*; Academic Press: San Diego, CA, 1990.
(244) Wright, J. D.; Sommerdijk, N. A. J. M. *Sol−Gel Materials: Chemistry and Applications*; Taylor and Francis: London, 2001.
(245) Pierre, A. C. *Introduction to Sol−Gel Processing*; Kluwer: Boston, 1998.
(246) Sakka, S. *Sol−Gel Science and Technology: Topics in Fundamental Research and Applications: Sol Gel Prepared Ferroelectrics and Related Materials*; Kluwer: Boston, 2002.
(247) Yan, C.; Sun, L.; Cheng, F. *Handbook of Nanophase and Nanostructured Materials*; 2003; p 72.
(248) Shukla, S.; Seal, S. In *Synthesis, Functionalization and Surface Treatment of Nanoparticles*; Baraton, M.-I., Ed.; American Scientific Publishers: Stevenson Ranch, CA, 2003.
(249) Kumta, P. N.; Kim, J. Y.; Sriram, M. A. *Ceram. Trans.* **1999**, *94*, 163.
(250) Bradley, D. C.; Mehrotra, R. C.; Gaur, D. P. *Metal Alkoxides*; Academic Press: London, 1978.
(251) Brinker, C. J. *J. Non-Cryst. Solids* **1988**, *100*, 31.
(252) Gallagher, D.; Ring, T. A. *Chimia* **1989**, *43*, 298.
(253) Diao, Y.; Walawender, W. P.; Sorensen, C. M.; Klabunde, K. J.; Ricker, T. *Chem. Mater.* **2002**, *14*, 362.
(254) Kepert, D. L. *The Early Transition Metals*; Academic Press: London, 1972.
(255) Smith, D. M.; Glaves, C. L.; Davis, P. J.; Brinker, C. J. *Mater. Res. Soc. Symp. Proc.* **1988**, *121*, 657.
(256) Scherer, G. W. *J. Am. Ceram. Soc.* **1984**, *67*, 709.
(257) Scherer, G. W.; Brinker, C. J.; Roth, E. P. *J. Non-Cryst. Solids* **1985**, *72*, 369.
(258) Tokumoto, M. S.; Pulcinelli, S. H.; Santilli, C. V.; Briois, V. *J. Phys. Chem. B* **2003**, *107*, 568.
(259) Livage, J.; Beteille, F.; Roux, C.; Chatry, M.; Davidson, P. *Acta Mater.* **1998**, *46*, 743.
(260) Livage, J.; Henry, M.; Sanchez, C. *Prog. Solid State Chem.* **1988**, *18*, 259.341.
(261) Cao, Y.; Hu, J.-C.; Hong, Z.-S.; Deng, J.-F.; Fan, K.-N. *Catal. Lett.* **2002**, *81*, 107.
(262) Wu, Z. G.; Zhao, Y. X.; Xu, L. P.; Liu, D. S. *J. Non-Cryst. Solids* **2003**, *330*, 274.
(263) Hamdeh, H. H.; Barghout, K.; Ho, J. C.; Willey, R. J.; O'Shea, M. J.; Chaudhuri, J. *J. Magn. Magn. Mater.* **2000**, *212*, 112.
(264) Niederberger, M.; Bartl, M. H.; Stucky, G. D. *Chem. Mater.* **2002**, *14*, 4364.
(265) Niederberger, M.; Bartl, M. H.; Stucky, G. D. *J. Am. Chem. Soc.* **2002**, *124*, 13642.
(266) Nishiwaki, K.; Kakuta, N.; Ueno, A.; Nakabayashi, H. *J. Catal.* **1989**, *118*, 498.
(267) Bischoff, B. L.; Anderson, M. A. *Chem. Mater.* **1995**, *7*, 1772.
(268) Zhu, Z.; Tsung, L. Y.; Tomkiewicz, M. *J. Phys. Chem.* **1995**, *99*, 15945.
(269) Zhu, Z.; Lin, M.; Dagan, G.; Tomkiewicz, M. *J. Phys. Chem.* **1995**, *99*, 15950.
(270) Hsu, J.-P.; Nacu, A. *Langmuir* **2003**, *19*, 4448.
(271) Liu, H.; Yang, W.; Ma, Y.; Cao, Y.; Yao, J.; Zhang, J.; Hu, T. *Langmuir* **2003**, *19*, 3001.
(272) Oliveira, M. M.; Schnitzler, D. C.; Zarbin, A. J. G. *Chem. Mater.* **2003**, *15*, 1903.
(273) Yu, D. S.; Han, J. C.; Ba, L. *Am. Ceram. Soc. Bull.* **2002**, *81*, 38.
(274) Gun'ko, Y. K.; Pillai, S. C.; McInerney, D. *J. Mater. Sci., Mater. Electron.* **2001**, *12*, 299.
(275) Cerda, J.; Arbiol, J.; Diaz, R.; Dezanneau, G.; Morante, J. R. *Mater. Lett.* **2002**, *56*, 131.
(276) Araki, B.; Mailhé, C.; Baffier, N.; Livage, J.; Vedel, J. *Solid State Ionics* **1983**, *9/10*, 439.
(277) West, K.; Zachau-Christiansen, B.; Jacobsen, T.; Skaarup, S. *Electrochim. Acta* **1993**, *38*, 1215.
(278) Park, H.-K.; Smyrl, W. H.; Ward, M. D. *J. Electrochem. Soc.* **1995**, *142*, 1068.
(279) Harreld, J. H.; Dong, W.; Dunn, B. *Mater. Res. Bull.* **1998**, *33*, 561.
(280) Dong, W.; Rolison, D. R.; Dunn, B. *Electrochem. Solid State Lett.* **2000**, *3*, 457.
(281) Dong, W.; Dunn, B. *J. Non-Cryst. Solids* **1998**, *225*, 135.
(282) Long, J. W.; Swider, K. E.; Stroud, R. M.; Rolison, D. R. *Electrochem. Solid State Lett.* **2000**, *3*, 453.
(283) Long, J. W.; Young, A. L.; Rolison, D. R. *J. Electrochem. Soc.* **2003**, *150*, A1161.
(284) Swider, K. E.; Hagans, P. L.; Merzbacher, C. I.; Rolison, D. R. *Chem. Mater.* **1997**, *9*, 1248.
(285) Rolison, D. R. *Science* **2003**, *299*, 1698.
(286) Rolison, D. R.; Dunn, B. *J. Mater. Chem.* **2001**, *11*, 963.
(287) Kim, I.; Kumta, P. N. *J. Mater. Chem.* **2003**, *13*, 2028.
(288) Kim, J. Y.; Kumta, P. N.; Phillips, B. L.; Risbud, S. H. *J. Phys. Chem. B* **2000**, *104*, 7895.
(289) Kim, J. Y.; Sriram, M. A.; Kumta, P. N.; Phillips, B. L.; Risbud, S. *Ceram. Trans.* **1997**, *85*, 167.
(290) Sriram, M. A.; Kumta, P. N. *J. Mater. Chem.* **1998**, *8*, 2441.

(291) Claus, P.; Brueckner, A.; Mohr, C.; Hofmeister, H. *J. Am. Chem. Soc.* **2000**, *122*, 11430.
(292) Rath, A.; Aceves, E.; Mitome, J.; Liu, J.; Ozkan, U. S.; Shore, S. G. *J. Mol. Catal., A* **2001**, *165*, 103.
(293) Pajonk, G. M. *Catal. Today* **1999**, *52*, 3.
(294) Yu, K. M. K.; Yeung, C. M. Y.; Thompsett, D.; Tsang, S. C. *J. Phys. Chem. B* **2003**, *107*, 4515.
(295) Bharathi, S.; Nogami, M. *Analyst* **2001**, *126*, 1919.
(296) Lee, Y.-H.; Farquharson, S.; Kwon, H.; Shahriari, M.; Rainey, P. *Proc. SPIE—Int. Soc. Opt. Eng.* **1999**, *3537*, 252.
(297) Lev, O.; Tsionsky, M.; Rabinovich, L.; Glezer, V.; Sampath, S.; Pankratov, I.; Gun, J. *Anal. Chem.* **1995**, *67*, 22A.
(298) Smith, D. D.; Snow, L. A.; Sibille, L.; Ignont, E. *J. Non-Cryst. Solids* **2001**, *285*, 256.
(299) Jain, R. K.; Lind, R. C. *J. Opt. Soc. Am.* **1983**, *73*, 647.
(300) Ricard, D.; Roussignol, P.; Flytzanis, C. *Opt. Lett.* **1985**, *10*, 511.
(301) Bronstein, L. M.; Svergun, D. I.; Khokhlov, A. R. In *Polymer Gels and Networks*; Osada, Y., Khokhlov, A. R., Eds.; Dekker: New York, 2002.
(302) Anderson, M. L.; Morris, C. A.; Stroud, R. M.; Merzbacher, C. I.; Rolison, D. R. *Langmuir* **1999**, *15*, 674.
(303) Tai, Y.; Watanabe, M.; Kaneko, K.; Tanemura, S.; Miki, T.; Murakami, J.; Tajiri, K. *Adv. Mater. (Weinheim, Ger.)* **2001**, *13*, 1611.
(304) Wallace, J. M.; Rice, J. K.; Pietron, J. J.; Stroud, R. M.; Long, J. W.; Rolison, D. R. *Nano Lett.* **2003**, *2003*, 1463.
(305) Morris, C. A.; Anderson, M. L.; Stroud, R. M.; Merzbacher, C. I.; Rolison, D. R. *Science* **1999**, *284*, 622.
(306) Richard-Plouet, M.; Guille, J.-L.; Frere, Y.; Danicher, L. *J. Sol-Gel Sci. Technol.* **2002**, *25*, 207.
(307) Zhang, L.; Coffer, J.; Xu, W.; Zerda, T. W. *Chem. Mater.* **1997**, *9*, 2249.
(308) Kozuka, H.; Sakka, S. *Chem. Mater.* **1993**, *5*, 222.
(309) Liz-Marzan, L. M.; Giersig, M.; Mulvaney, P. *Langmuir* **1996**, *12*, 4329.
(310) Lu, Y.; Yin, Y.; Li, Z.-Y.; Xia, Y. *Nano Lett.* **2002**, *2*, 785.
(311) Hardikar, V. V.; Matijevic, E. *J. Colloid Interface Sci.* **2000**, *221*, 133.
(312) Han, Y.-S.; Yoon, S.-M.; Kim, D.-K. *Bull. Korean Chem. Soc.* **2000**, *21*, 1193.
(313) Ma, M.; Zhang, Y.; Yu, W.; Shen, H.; Zhang, H.; Gu, N. *Colloids Surf., A* **2003**, *212*, 219.
(314) Schroedter, A.; Weller, H.; Eritja, R.; Ford, W. E.; Wessels, J. M. *Nano Lett.* **2002**, *2*, 1363.
(315) Cheng, S.; Wei, Y.; Feng, Q.; Quiu, K.-Y.; Pang, J.-B.; Jansen, S. A.; Yin, R.; Ong, K. *Chem. Mater.* **2003**, *15*, 1560.
(316) Epifani, M.; Carlino, E.; Blasi, C.; Giannini, C.; Tapfer, L.; Vasanelli, L. *Chem. Mater.* **2001**, *13*, 1533.
(317) Fonseca, F. C.; Goya, G. F.; Jardim, R. F.; Carreno, N. L. V.; Longo, E.; Leite, E. R.; Muccillo, R. *Appl. Phys. A* **2003**, *76*, 621.
(318) Corrias, A.; Casula, M. F.; Ennas, G.; Marras, S.; Navarra, G.; Mountjoy, G. *J. Phys. Chem. B* **2003**, *107*, 3030.
(319) Casula, M. F.; Corrias, A.; Paschina, G. *J. Sol-Gel Sci. Technol.* **2003**, *26*, 667.
(320) Casula, M. F.; Corrias, A.; Paschina, G. *J. Mater. Chem.* **2002**, *12*, 1505.
(321) Ennas, G.; Casula, M. F.; Falqui, A.; Gatteschi, D.; Marongiu, G.; Piccaluga, G.; Sangregorio, C.; Pinna, G. *J. Non-Cryst. Solids* **2001**, *293—295*, 1.
(322) Wu, P.-W.; Dunn, B.; Doan, V.; Schwartz, B. J.; Yablonovitch, E.; Yamane, M. *J. Sol-Gel Sci. Technol.* **2000**, *19*, 249.
(323) Morley, K. S.; Marr, P. C.; Webb, P. B.; Berry, A. R.; Allison, F. J.; Moldovan, G.; Brown, P. D.; Howdle, S. M. *J. Mater. Chem.* **2002**, *12*, 1898.
(324) Casas, L.; Roig, A.; Molins, E.; Grenèche, J. M.; Tejada, J. *Appl. Phys. A* **2002**, *74*, 591.
(325) Casula, M. F.; Corrias, A.; Paschina, G. *Mater. Res. Soc. Symp. Proc.* **2000**, *581*, 363.
(326) Casula, M. F.; Corrias, A.; Paschina, G. *J. Mater. Res.* **2000**, *15*, 2187.
(327) Bharathi, S.; Lev, O. *Chem. Commun.* **1997**, 2303.
(328) Bharathi, S.; Fishelson, N.; Lev, O. *Langmuir* **1999**, *15*, 1929.
(329) Kobayashi, Y.; Correa-Duarte, M. A.; Liz-Marzan, L. M. *Langmuir* **2001**, *17*, 6375.
(330) Vacassy, R.; Lemaire, L.; Valmalette, J.-C.; Dutta, J.; Hofmann, H. *J. Mater. Sci. Lett.* **1998**, *17*, 1665.
(331) Caizer, C.; Popovici, M.; Savii, C. *Acta Mater.* **2003**, *51*, 3607.
(332) Piccaluga, G.; Corrias, A.; Ennas, G.; Musinu, A. *Mater. Sci. Found.* **2000**, *13*, 1.
(333) Xing, G.; Chen, G.; Song, X.; Yuan, X.; Yao, W.; Yan, H. *Microelectron. Eng.* **2003**, *66*, 70.
(334) Pechini, M. P. U.S. Patent 3,330,697, July 11, 1967.
(335) Fang, T.-T.; Wu, M.-S.; Tsai, J.-D. *J. Am. Ceram. Soc.* **2002**, *85*, 2984.
(336) Li, X.; Agarwal, V.; Liu, M.; Rees, W. S. *J. Mater. Res.* **2000**, *15*, 2393.
(337) Zhou, Z.-H.; Deng, Y.-F.; Jiang, Y.-Q.; Wan, H.-L.; Ng, S.-W. *Dalton Trans.* **2003**, 2636.
(338) Lessing, P. A. *Ceram. Bull.* **1989**, *68*, 1002.
(339) Kakihana, M.; Yoshimura, M. *Bull. Chem. Soc. Jpn.* **1999**, *72*, 1427.
(340) Hodgson, S. N. B.; Shen, X.; Sale, F. R. *J. Mater. Sci.* **2000**, *35*, 5275.
(341) Xu, Y.; He, Y.; Wang, L. *J. Mater. Res.* **2001**, *16*, 1195.
(342) Chiang, C.; Shei, C. Y.; Wu, S. F.; Huang, Y. T. *Appl. Phys. Lett.* **1991**, *58*, 2435.
(343) Zhang, L.; Xue, D. *J. Mater. Sci. Lett.* **2002**, *21*, 1931.
(344) Low, K. O.; Sale, F. R. *J. Magn. Magn. Mater.* **2003**, *256*, 221.
(345) Hui, Z.; Michele, P. *J. Mater. Chem.* **2002**, *12*, 3787.
(346) Anderton, D. J.; Sale, F. R. *Powder Metall.* **1979**, *22*, 14.
(347) Lamas, D. G.; Lascalea, G. E.; Walsoe de Reca, N. E. *J. Eur. Ceram. Soc.* **1998**, *18*, 1217.
(348) Chang, Y.-S.; Chang, Y.-H.; Chen, I.-G.; Chen, G.-J.; Chai, Y.-L. *J. Cryst. Growth* **2002**, *243*, 319.
(349) Peschke, S. L.; Ciftcioglu, M.; Doughty, D. H.; Voigt, J. A. *Mater. Res. Soc. Symp. Proc.* **1992**, *271*, 101.
(350) Moure, C.; Gutierrez, D.; Tartaj, J.; Duran, P. *J. Eur. Ceram. Soc.* **2003**, *23*, 729.
(351) Falter, L. M.; Payne, D. A.; Friedmann, T. A.; Wright, W. H.; Ginsberg, D. M. *Br. Ceram. Proc.* **1989**, *41*, 261.
(352) Laberty-Robert, C.; Ansart, F.; Deloget, C.; Gaudon, M.; Rousset, A. *Ceram. Int.* **2003**, *29*, 151.
(353) Lamas, D. G.; Juarez, R. E.; Lascalea, G. E.; Walsoe de Reca, N. E. *J. Mater. Sci. Lett.* **2001**, *20*, 1447.
(354) Kumar, S.; Messing, G. L. *Mater. Res. Soc. Symp. Proc.* **1992**, *271*, 95.
(355) Lee, D. W.; Won, J. H.; Shim, K. B. *Mater. Lett.* **2003**, *57*, 3346.
(356) Armaleo, L.; Bandoli, G.; Barreca, D.; Bettinelli, M.; Bottaro, G.; Caneschi, A. *Surf. Interface Anal.* **2002**, *34*, 112.
(357) Popa, M.; Kakihana, M. *Catal. Today* **2003**, *78*, 519.
(358) Anderson, H. U.; Pennell, M. J.; Guha, J. P. *Adv. Ceram.* **1987**, *21*, 91.
(359) Gholinia, A.; Sale, F. R. *J. Therm. Anal.* **1994**, *42*.
(360) Roy, S.; Sigmund, W.; Aldinger, F. *J. Mater. Res.* **1999**, *14*, 1524.
(361) Kahoul, A.; Nkeng, P.; Hammouche, A.; Naamoune, F.; Poillerat, G. *J. Solid State Chem.* **2001**, *161*, 379.
(362) Zhang, J.-J.; Ning, J.-W.; Liu, X.-J.; Pan, Y.-B.; Huang, L.-P. *Mater. Res. Bull.* **2003**, *38*, 1249.
(363) Hwang, B. J.; Santhanam, R.; Liu, D. G. *J. Power Sources* **2001**, *97—98*, 443.
(364) Huang, J.; Zhuang, H.; Li, W. *Mater. Res. Bull.* **2003**, *38*, 149.
(365) Popa, M.; Kakihana, M. *Solid State Ionics* **2002**, *151*, 251.
(366) Fuentes, A. F.; Hernandez-Ibarra, O.; Mendoza-Suarez, G.; Escalante-Garcia, J. I.; Boulahya, K.; Amador, U. *J. Solid State Chem.* **2003**, *173*, 319.
(367) Sen, A.; Pramanik, P. *Mater. Lett.* **2001**, *50*, 287.
(368) Lu, C.-H.; Lin, Y.; Wang, H.-C. *J. Mater. Sci. Lett.* **2003**, *22*, 615.
(369) Jiu, J.; Ge, Y.; Li, X.; Nie, L. *Mater. Lett.* **2002**, *54*, 260.
(370) Chen, D.-H.; Wu, S.-H. *Chem. Mater.* **2000**, *12*, 1354.
(371) Tan, R.; Zhu, Y.; Feng, J.; Ji, S.; Cao, L. *J. Alloys Compd.* **2002**, *337*, 282.
(372) Hoar, T. P.; Schulman, J. H. *Nature* **1943**, *152*, 102.
(373) Schulman, J. H.; Riley, D. P. *J. Colloid Sci.* **1948**, *3*, 383.
(374) Gillberg, G.; Lehtinen, H.; Friberg, S. *J. Colloid Interface Sci.* **1970**, *33*, 40.
(375) Prince, L. M. *J. Soc. Cosmet. Chem.* **1970**, *21*, 193.
(376) Zana, R. *Heterog. Chem. Rev.* **1994**, *1*, 145.
(377) Shinoda, K.; Friberg, S. *Adv. Colloid Interface Sci.* **1975**, *4*, 281.
(378) Wennerstrom, H.; Soderman, O.; Olsson, U.; Lindman, B. *Colloids Surf., A* **1997**, *123—124*, 13.
(379) Fendler, J. H. *Acc. Chem. Res.* **1976**, *9*, 153.
(380) Liveri, V. T. In *Nano-Surface Chemistry*; Rosoff, M., Ed.; Dekker: New York, 2001.
(381) Meguro, K.; Ueno, M.; Esumi, K. In *Nonionic Surfactants: Physical Chemistry*; Schick, M. J., Ed.; Dekker: New York, 1987.
(382) Langevin, D. In *Structure and Reactivity in Reverse Micelles*; Pileni, M. P., Ed.; Elsevier: Amsterdam, 1989.
(383) Pillai, V.; Shah, D. O. In *Surfactant Science Series*; Kunieda, H., Solans, C., Eds.; Dekker: New York, 1997; Vol. 66.
(384) John, V. T.; Simmon, B.; McPherson, G. L.; Bose, A. *Curr. Opin. Colloid Interface Sci.* **2002**, *7*, 288.
(385) Pileni, M. P.; Lisiecki, I.; Motte, L.; Petit, C. *Res. Chem. Intermed.* **1992**, *17*, 101.
(386) Eastoe, J.; Warne, B. *Curr. Opin. Colloid Interface Sci.* **1996**, *1*, 800.
(387) Pileni, M. P.; Duxin, N. *Chem. Innovation* **2000**, *30*, 25.
(388) Nagy, J. B.; Jeunieau, L.; Debuigne, F.; Ravet-Bodart, I. *Surf. Sci. Ser.* **2003**, *109*, 343.
(389) Winsor, P. A. *Chem. Rev.* **1968**, *68*, 1.
(390) Silber, J. J.; Biasutti, A.; Abuin, E.; Lissi, E. *Adv. Colloid Interface Sci.* **1999**, *82*, 189.
(391) Li, F.; Li, G.-Z.; Wang, H.-Q.; Xue, A.-J. *Colloids Surf., A* **1997**, *127*, 89.
(392) Chang, G. X.; Shen, F.; Yang, L. F.; Ma, L. R.; Tang, Y.; Yao, K. D.; Sun, P. C. *Mater. Chem. Phys.* **1998**, *56*, 97.
(393) Kunieda, H.; Shinoda, K. *J. Colloid Interface Sci.* **1979**, *70*, 577.
(394) Frank, S. G.; Shaw, Y.-H.; Li, N. C. *J. Phys. Chem.* **1973**, *77*, 238.

(395) Zulauf, M.; Eicke, H.-F. *J. Phys. Chem.* **1979**, *83*, 480.
(396) Robinson, B. H.; Toprakcioglu, C.; Dore, J. C.; Chieux, P. J. *J. Chem. Soc., Faraday Trans.* **1984**, *80*, 13.
(397) Day, R. A.; Robinson, B. H.; Clarke, J. H. R.; Doherty, J. V. *J. Chem. Soc., Faraday Trans. 1* **1979**, *75*, 132.
(398) Toprakcioglu, C.; Dore, J. C.; Robinson, B. H.; Howe, A.; Chieux, P. *J. Chem. Soc., Faraday Trans. 1* **1984**, *80*, 413.
(399) Bedwell, B.; Gulari, E. *J. Colloid Interface Sci.* **1984**, *102*, 88.
(400) Clarke, J. H. R.; Nicholson, J. D.; Regan, K. N. *J. Chem. Soc., Faraday Trans. 1* **1985**, *81*, 1173.
(401) Howe, A. M.; Toprakcioglu, C.; Dore, J. C.; Robinson, B. H. *J. Chem. Soc., Faraday Trans. 1* **1986**, *82*, 2411.
(402) D'Aprano, A.; Lizzio, A.; Liveri, V. T. *J. Phys. Chem.* **1987**, *91*, 4749.
(403) D'Aprano, A.; Lizzio, A.; Liveri, V. T.; Aliotta, F.; Vasi, C.; Migliardo, P. *J. Phys. Chem.* **1988**, *92*, 4436.
(404) Goffredi, M.; Liveri, V. T.; Vassallo, G. *J. Solution Chem.* **1993**, *22*, 941.
(405) Moran, P. D.; Bowmaker, G. A.; Cooney, R. P.; Bartlett, J. R.; Woolfrey, J. L. *Langmuir* **1995**, *11*, 738.
(406) Riter, R. E.; Undiks, E. P.; Levinger, N. E. *J. Am. Chem. Soc.* **1998**, *120*, 6062.
(407) Grand, D. *J. Phys. Chem. B* **1998**, *102*, 4322.
(408) Arcoleo, V.; Goffredi, M.; Liveri, V. T. *J. Colloid Interface Sci.* **1998**, *198*, 216.
(409) Cheng, G. X.; Shen, F.; Yang, L. F.; Ma, L. R.; Tang, Y.; Yao, K. D.; Sun, P. C. *Mater. Chem. Phys.* **1998**, *56*, 97.
(410) Maugey, M.; Bellocq, A.-M. *Langmuir* **1999**, *15*, 8602.
(411) Caragheorgheopol, A.; Bandula, R.; Caldararu, H.; Joela, H. *J. Mol. Liq.* **1997**, *72*, 105.
(412) Kumar, C.; Balasubramanian, D. *J. Phys. Chem.* **1980**, *84*, 1895.
(413) Mackay, R. A. In *Nonionic Surfactants: Physical Chemistry*; Schick, M. J., Ed.; Dekker: New York, 1987; Vol. 23.
(414) Sjöblom, J.; Stenius, P. In *Nonionic Surfactants: Physical Chemistry*; Schick, M. J., Ed.; Dekker: New York, 1987; Vol. 23.
(415) D'Aprano, D.; Lizzio, A.; Liveri, V. T. *J. Phys. Chem.* **1987**, *91*, 4749.
(416) Eicke, H.-F.; Kubik, R. *Faraday Discuss. Chem. Soc.* **1983**, 305.
(417) Fletcher, P. D. I.; Howe, A. M.; Robinson, B. H. *J. Chem. Soc., Faraday Trans. 1* **1987**, *83*, 985.
(418) Mangey, M.; Bellocq, A.-M. *Langmuir* **1999**, *15*, 8602.
(419) Sunamoto, J.; Hamada, T. *Bull. Chem. Soc. Jpn.* **1978**, *51*, 3130.
(420) Soma, J.; Papadopoulos, K. D. *J. Colloid Interface Sci.* **1996**, *181*, 225.
(421) Barnickel, P.; Wokaun, A.; Sager, W.; Eicke, H.-F. *J. Colloid Interface Sci.* **1992**, *148*, 80.
(422) Carpenter, E. E. Ph.D. Thesis, University of New Orleans, New Orleans, LA, 1999.
(423) Petit, C.; Lixon, P.; Pileni, M. P. *Langmuir* **1991**, *7*, 2620.
(424) Chen, J. P.; Lee, K. M.; Sorensen, C. M.; Klabunde, K. J.; Hadjipanayis, G. C. *J. Appl. Phys.* **1994**, *75*, 5876.
(425) Lisiecki, I.; Pileni, M. P. *J. Am. Chem. Soc.* **1993**, *115*, 3887.
(426) Lisiecki, I.; Pileni, M. P. *J. Phys. Chem.* **1995**, *99*, 5077.
(427) Johnson, J. A.; Saboungi, M.-L.; Thiyagarajan, P.; Csencsits, R.; Meisel, D. *J. Phys. Chem. B* **1999**, *103*, 59.
(428) Foos, E. E.; Stroud, R. M.; Berry, A. D.; Snow, A. W.; Armistead, J. P. *J. Am. Chem. Soc.* **2000**, *122*, 7114.
(429) Carpenter, E. E.; Sims, J. A.; Wienmann, J. A.; Zhou, W. L.; O'Connor, C. J. *J. Appl. Phys.* **2000**, *87*, 5615.
(430) Carpenter, E. E.; Kumbhar, A.; Wiemann, J. A.; Srikanth, H.; Wiggins, J.; Zhou, W.; O'Connor, C. J. *Mater. Sci. Eng., A* **2000**, *286*, 81.
(431) O'Connor, C. J.; Seip, C. T.; Carpenter, E. E.; Li, S.; John, V. T. *Nanostruct. Mater.* **1999**, *12*, 65.
(432) Yener, D. O.; Giesche, H. *J. Am. Ceram. Soc.* **2001**, *84*, 1987.
(433) Zhang, Z. J.; Wang, Z. L.; Chakoumakos, B. C.; Yin, J. S. *J. Am. Chem. Soc.* **1998**, *120*, 1800.
(434) Moran, P. D.; Bartlett, J. R.; Bowmaker, G. A.; Woolfrey, J. L.; Cooney, R. P. *J. Sol-Gel Sci. Technol.* **1999**, *15*, 251.
(435) Yener, D. O.; Giesche, H. *Ceram. Trans.* **1999**, *94*, 407.
(436) Kumar, P.; Pillai, V.; Bates, S. R.; Shah, D. O. *Mater. Lett.* **1993**, *16*, 68.
(437) Pang, Y.-X.; Bao, X. *J. Mater. Chem.* **2002**, *12*, 3699.
(438) Hayashi, M.; Uemura, H.; Shimanoe, K.; Miura, N.; Yamazoe, N. *Electrochem. Solid State Lett.* **1998**, *1*, 268.
(439) Pillai, V.; Kumar, P.; Multani, M. S.; Shah, D. O. *Colloids Surf., A* **1993**, *80*, 69.
(440) Porta, F.; Bifulco, C.; Fermo, P.; Bianchi, C. L.; Fadoni, M.; Prati, L. *Colloids Surf., A* **1999**, *160*, 281.
(441) Lu, C.-H.; Wang, H.-C. *J. Mater. Chem.* **2003**, *13*, 428.
(442) Palla, B. J.; Shah, D. O.; Garcia-Casillas, P.; Matutes-Aquino, J. *J. Nanopart. Res.* **1999**, *1*, 215.
(443) Lee, H. S.; Lee, W. C.; Furubayashi, T. *J. Appl. Phys.* **1999**, *85*, 5231.
(444) Vestal, C. R.; Zhang, Z. J. *Chem. Mater.* **2002**, *14*, 3817.
(445) Liu, C.; Rondinone, A. J.; Zhang, Z. J. *Pure Appl. Chem.* **2000**, *72*, 37.
(446) Vaqueiro, P.; Lopez-Quintela, M. A.; Rivas, J. *J. Mater. Chem.* **1997**, *7*, 501.
(447) Song, K. C.; Kim, J. H. *Powder Technol.* **2000**, *107*, 268.
(448) Wu, Z.; Zhang, J.; Benfield, R. E.; Ding, Y.; Grandjean, D.; Zhang, Z.; Xin, J. *J. Phys. Chem. B* **2002**, *106*, 4569.
(449) Binnig, G.; Rohrer, H.; Gerber, C.; Weibel, G. *Appl. Phys. Lett.* **1982**, *40*, 178.
(450) Hirai, T.; Tsubaki, Y.; Sato, H.; Komasawa, I. *J. Chem. Eng. Jpn.* **1995**, *28*, 468.
(451) Gan, L. M.; Liu, B.; Chew, C. H.; Xu, S. J.; Chua, S. J.; Loy, G. L.; Xu, G. Q. *Langmuir* **1997**, *13*, 6427.
(452) Vaucher, S.; Li, M.; Mann, S. *Angew. Chem., Int. Ed.* **2000**, *39*, 1793.
(453) Vaucher, S.; Fielden, J.; Li, M.; Dujardin, E.; Mann, S. *Nano Lett.* **2002**, *2*, 225.
(454) Moulik, S. P.; De, G. C.; Panda, A. K.; Bhowmik, B. B.; Das, A. R. *Langmuir* **1999**, *15*, 8361.
(455) O'Connor, C. J.; Sims, J. A.; Kumbhar, A.; Kolesnichenko, V. L.; Zhou, W. L.; Wiemann, J. A. *J. Magn. Magn. Mater.* **2001**, *226−230*, 1915.
(456) Lin, J.; Zhou, W.; Kumbhar, A.; Wiemann, J.; Fang, J.; Carpenter, E. E.; O'Connor, C. J. *J. Solid State Chem.* **2001**, *159*, 26.
(457) Ravel, B.; Carpenter, E. E.; Harris, V. G. *J. Appl. Phys.* **2002**, *91*, 8195.
(458) Zhou, W. L.; Carpenter, E. E.; Sims, J.; Kumbhar, A.; O'Connor, C. J. *Mater. Res. Soc. Symp. Proc.* **2000**, *581*, 107.
(459) Santra, S.; Tapec, R.; Theodoropoulou, N.; Dobson, J.; Hebard, A.; Tan, W. *Langmuir* **2001**, *17*, 2900.
(460) Tago, T.; Hatsuta, T.; Miyajima, K.; Kishida, M.; Tashiro, S.; Wakabayashi, K. *J. Am. Ceram. Soc.* **2002**, *85*, 2188.
(461) Gan, L. M.; Zhang, L. H.; Chan, H. S. O.; Chew, C. H. *Mater. Chem. Phys.* **1995**, *40*, 94.
(462) Martino, A.; Yamanaka, S. A.; Kawola, J. S.; Loy, D. A. *Chem. Mater.* **1997**, *9*, 423.
(463) Cooper, A. I. *Adv. Mater. (Weinheim, Ger.)* **2001**, *13*, 1111.
(464) Ji, M.; Chen, X.; Wai, C. M.; Fulton, J. L. *J. Am. Chem. Soc.* **1999**, *121*, 2631.
(465) Ohde, H.; Hunt, F.; Wai, C. M. *Chem. Mater.* **2001**, *13*, 4130.
(466) Ohde, H.; Ohde, M.; Bailey, F.; Kim, H.; Wai, C. M. *Nano Lett.* **2002**, *2*, 721.
(467) Ohde, H.; Ye, X.-R.; Wai, C. M.; Rodriguez, J. M. *Chem. Commun.* **2000**, 2353.
(468) Lin, X. M.; Sorensen, C. M.; Klabunde, K. J.; Hajipanayis, G. C. *J. Mater. Res.* **1999**, *14*, 1542.
(469) Yu, S.-H. *J. Ceram. Soc. Jpn.* **2001**, *109*, S65.
(470) Cansell, F.; Chevalier, B.; Demourgues, A.; Etourneau, J.; Even, C.; Garrabos, Y.; Pessey, V.; Petit, S.; Tressaud, A.; Weill, F. *J. Mater. Chem.* **1999**, *9*, 67.
(471) Rajamathi, M.; Seshadri, R. *Curr. Opin. Solid State Mater. Sci.* **2002**, *6*, 337.
(472) Gautam, U. K.; Ghosh, M.; Rajamathi, M.; Seshadri, R. *Pure Appl. Chem.* **2002**, *74*, 1643.
(473) Demazeau, G. *J. Mater. Chem.* **1999**, *9*, 15.
(474) Li, J.; Chen, Z.; Wang, R.-J.; Proserpio, D. M. *Coord. Chem. Rev.* **1999**, *190−192*, 707.
(475) Oguri, Y.; Riman, R. E.; Bowen, H. K. *J. Mater. Sci.* **1988**, *23*, 2897.
(476) Kondo, M.; Kazuo, S.; Ooki, R.; Miztani, N. *J. Ceram. Soc. Jpn.* **1994**, *102*, 742.
(477) Jeon, S.; Braun, P. V. *Chem. Mater.* **2003**, *15*, 1256.
(478) Cheng, H.; Ma, J.; Zhao, Z.; Qi, L. *Chem. Mater.* **1995**, *7*, 663.
(479) Yanquing, Z.; Erwei, S.; Zhizhan, C.; Wenjun, L.; Xingfang, H. *J. Mater. Chem.* **2001**, *11*, 1547.
(480) Yin, H.; Wada, Y.; Kitamura, T.; Sumida, T.; Hasegawa, Y.; Yanagida, S. *J. Mater. Chem.* **2002**, *12*, 378.
(481) Masui, T.; Hirai, H.; Hamada, R.; Imanaka, N.; Adachi, G.; Sakata, T.; Mori, H. *J. Mater. Chem.* **2003**, *13*, 622.
(482) Inoue, M.; Kimura, M.; Inui, T. *Chem. Commun.* **1999**, 957.
(483) Thimmaiah, S.; Rajamathi, M.; Singh, N.; Bera, P.; Meldrum, F.; Chandrasekhar, N.; Seshadri, R. *J. Mater. Chem.* **2001**, *11*, 3215.
(484) Wu, M.; Long, J.; Huang, A.; Luo, Y.; Feng, S.; Xu, R. *Langmuir* **1999**, *15*, 8822.
(485) Andersson, M.; Österlund, L.; Ljungström, S.; Palmqvist, A. *J. Phys. Chem. B* **2002**, *106*, 10674.
(486) Yang, J.; Cheng, G.-H.; Zeng, J.-H.; Yu, S.-H.; Liu, X.-M.; Qian, Y.-T. *Chem. Mater.* **2001**, *13*, 848.
(487) Sheldrick, W. S.; Wachold, M. *Angew. Chem., Int. Ed. Engl.* **1997**, *36*, 206.
(488) Peng, Q.; Dong, Y.; Deng, Z.; Sun, X.; Li, Y. *Inorg. Chem.* **2001**, *40*, 3840.
(489) Gautam, U. K.; Rajamathi, M.; Meldrum, F.; Morgan, P.; Seshadri, R. *Chem. Commun.* **2001**, 629.
(490) Chen, X.; Fan, R. *Chem. Mater.* **2001**, *13*, 802.
(491) Hu, J.; Lu, Q.; Tang, K.; Qian, Y.; Zhou, G.; Liu, X. *Chem. Commun.* **1999**, 1093.
(492) Lu, Q.; Hu, J.; Tang, K.; Qian, Y.; Zhou, G.; Liu, X. *Inorg. Chem.* **2000**, *39*, 1606.

(493) Xiao, J.; Xie, Y.; Xiong, Y.; Tang, R.; Qian, Y. *J. Mater. Chem.* **2001**, *11*, 1417.
(494) Xie, Y.; Qian, Y.; Wang, W.; Zhang, S.; Zhang, Y. *Science* **1996**, *272*, 1926.
(495) Qian, Y. T. *Adv. Mater.* **1999**, *11*, 1101.
(496) Adschiri, T.; Hakuta, Y.; Arai, K. *Ind. Eng. Chem. Res.* **2000**, *39*, 4901.
(497) Cabanas, A.; Darr, J. A.; Lester, E.; Poliakoff, M. *Chem. Commun.* **2000**, 901.
(498) Cabanas, A.; Darr, J. A.; Lester, E.; Poliakoff, M. *J. Mater. Chem.* **2001**, *11*, 561.
(499) Balabanova, E. *Vacuum* **2002**, *69*, 207.
(500) Wegner, K.; Walker, B.; Tsantilis, S.; Pratsinis, S. E. *Chem. Eng. Sci.* **2002**, *57*, 1753.
(501) Yamamoto, T.; Adachi, M.; Kawabata, K.; Kimura, K.; Hahn, H. W. *Appl. Phys. Lett.* **1993**, *63*, 3020.
(502) Janzen, C.; Wiggers, H.; Knipping, J.; Roth, P. *J. Nanosci. Nanotechnol.* **2001**, *1*, 221.
(503) Borsella, E.; Botti, S.; Martelli, S.; Montereali, R. M.; Vogel, W.; Carlino, E. *Mater. Sci. Forum* **1997**, *235*−*238*, 967.
(504) Cabanas, A.; Poliakoff, M. *J. Mater. Chem.* **2001**, *11*, 1408.
(505) Courtecuisse, V. G.; Bocquet, J. F.; Chhor, K.; Pommier, C. *J. Supercrit. Fluids* **1996**, *9*, 222.
(506) Bocquet, J. F.; Chhor, K.; Pommier, C. *Mater. Chem. Phys.* **1999**, *57*, 273.
(507) Komarneni, S.; Roy, R.; Li, Q. H. *Mater. Res. Bull.* **1992**, *27*, 1393.
(508) Meng, X.; Xu, W.; Tang, S.; Pang, W. *Chin. Chem. Lett.* **1992**, *3*, 69.
(509) Komarneni, S.; Karin, Q. L.; Stefansson, M.; Roy, R. *J. Mater. Res.* **1993**, *8*, 3176.
(510) Komarneni, S.; Li, Q. H.; Roy, R. *J. Mater. Chem.* **1994**, *4*, 1903.
(511) Komarneni, S.; Pidugu, R.; Li, Q. H.; Roy, R. *J. Mater. Res.* **1995**, *10*, 1687.
(512) Komarneni, S.; Hussein, M. Z.; Liu, C.; Breval, E.; Malla, P. B. *Eur. J. Solid State Inorg. Chem.* **1995**, *32*, 837.
(513) Komarneni, S.; Menon, V. C.; Li, Q. H. *Ceram. Trans.* **1996**, *62*, 37.
(514) Komarneni, S.; Menon, V. C. *Mater. Lett.* **1996**, *27*, 313.
(515) Komarneni, S.; D'Arrigo, M. C.; Leionelli, C.; Pellacani, G. C.; Katsuki, H. *J. Am. Ceram. Soc.* **1998**, *81*, 3041.
(516) Newalkar, B. L.; Komarneni, S.; Katsuki, H. *Mater. Res. Bull.* **2001**, *36*, 2347.
(517) Katsuki, H.; Komarneni, S. *J. Am. Ceram. Soc.* **2001**, *84*, 2313.
(518) Komarneni, S.; Katsuki, H. *Pure Appl. Chem.* **2002**, *74*, 1537.
(519) Khollam, Y. B.; Dhage, S. R.; Potdar, H. S.; Deshpande, S. B.; Bakare, P. P.; Kulkarni, S. D.; Date, S. K. *Mater. Lett.* **2002**, *56*, 571.
(520) Caillot, T.; Aymes, D.; Stuerga, D.; Viart, N.; Pourroy, G. *J. Mater. Sci.* **2002**, *37*, 5153.
(521) Wilson, G. J.; Will, G. D.; Frost, R. L.; Montgomery, S. A. *J. Mater. Chem.* **2002**, *12*, 1787.
(522) Bellon, K.; Chaumont, D.; Stuerga, D. *J. Mater. Res.* **2001**, *16*, 2619.
(523) Potdar, H. S.; Deshpande, S. B.; Deshpande, A. S.; Gokhale, S. P.; Date, S. K.; Khollam, Y. B.; Patil, A. J. *Mater. Chem. Phys.* **2002**, *74*, 306.
(524) Komarneni, S.; Komarneni, J. S.; Newalkar, B.; Stout, S. *Mater. Res. Bull.* **2002**, *37*, 1025.
(525) Newalkar, B. L.; Komarneni, S. *Chem. Mater.* **2001**, *13*, 4573.
(526) Newalkar, B. L.; Olanrewaju, J.; Komarneni, S. *J. Phys. Chem. B* **2001**, *105*, 8356.
(527) Kumar, R. *Catalysis* **2002**, 71.
(528) Schuth, F.; Schmidt, W. *Adv. Mater.* **2002**, *14*, 629.
(529) He, X.; Antonelli, D. *Angew. Chem., Int. Ed.* **2002**, *41*, 214.
(530) Zhang, Z.; Han, M. *Chem. Phys. Lett.* **2003**, *374*, 91.
(531) Jana, N. R.; Gearheart, L.; Murphy, C. J. *Chem. Mater.* **2001**, *13*, 2313.
(532) Schmid, G.; Lehnert, A.; Malm, J.-O.; Bovin, J.-O. *Angew. Chem., Int. Ed. Engl.* **1991**, *30*, 874.
(533) Yu, H.; Gibbons, P. C.; Kelton, K. F.; Buhro, W. E. *J. Am. Chem. Soc.* **2001**, *123*, 9198.
(534) Zanella, R.; Giorgio, S.; Henry, C. R.; Louis, C. *J. Phys. Chem. B* **2002**, *106*, 7634.
(535) Li, Y.; Ding, J.; Chen, J.; Xu, C.; Wei, B.; Liang, J.; Wu, D. **2002**, *37*, 313.
(536) Michalski, J.; Konopka, K.; Trzaska, M. *Acta Phys. Pol., A* **2002**, *102*, 181.
(537) Fangli, Y.; Peng, H.; Chunlei, Y.; Shulan, H.; Jinlin, L. *J. Mater. Chem.* **2003**, *13*, 634.
(538) Lalla, N. P.; Hegde, M. S.; Dupont, L.; Tekaia-Elhsissen, K.; Tarascon, J.-M.; Srivastava, O. N. *Curr. Sci.* **2000**, *78*, 73.
(539) Harrison, M. T.; Kershaw, S. V.; Rogach, A. L.; Kornowski, A.; Eychmuller, A.; Weller, H. *Adv. Mater. (Weinheim, Ger.)* **2000**, *12*, 123.
(540) Pileni, M. P. *Cryst. Res. Technol.* **1998**, *33*, 1155.
(541) Pradhan, N.; Jana, N. R.; Mallick, K.; Pal, T. *J. Surf. Sci. Technol.* **2000**, *2000*, 188.
(542) Brown, K. R.; Natan, M. J. *Langmuir* **1998**, *14*, 726.
(543) Mallory, G. O.; Hajdu, J. B. *Electroless Plating: Fundamentals and Applications*; American Electroplaters and Surface Finishers Society: Orlando, FL, 1990.
(544) Platonova, O. A.; Bronstein, L. M.; Solodovnikov, S. P.; Yanovskaya, I. M.; Obolonkova, E. S.; Valetsky, P. M.; Wenz, E.; Antonietti, M. *Colloid Polym. Sci.* **1997**, *275*, 426.
(545) Ahmed, S. R.; Kofinas, P. *Macromolecules* **2002**, *35*, 3338.
(546) Rabelo, D.; Lima, E. C. D.; Reis, A. C.; Nunes, W. C.; Novak, M. A.; Garg, V. K.; Oliveira, A. C.; Morais, P. C. *Nano Lett.* **2001**, *1*, 105.
(547) Bronstein, L. M.; Chernyshov, D. M.; Valetsky, P. M.; Wilder, E. A.; Spontak, R. J. *Langmuir* **2000**, *16*, 8221.
(548) Liang, Z.; Susha, A.; Caruso, F. *Chem. Mater.* **2003**, *15*, 3176.
(549) Marinakos, S. M.; Novak, J. P.; Brousseau, L. C., III; House, A. B.; Edeki, E. M.; Feldhaus, J. C.; Feldheim, D. L. *J. Am. Chem. Soc.* **1999**, *121*, 8518.
(550) Nair, A. S.; Renjis, T. T.; Suryanarayanan, V.; Pradeep, T. *J. Mater. Chem.* **2003**, *13*, 297.
(551) Zhao, M.; Crooks, R. M. *Angew. Chem., Int. Ed. Engl.* **1999**, *38*, 364.
(552) Crooks, R. M.; Zhao, M.; Sun, L.; Chechik, V.; Yeung, L. K. *Acc. Chem. Res.* **2001**, *34*, 181.
(553) Hulteen, J. C.; Martin, C. R. In *Nanoparticles and Nanostructured Films: Preparation, Characterization and Applications*; Fendler, J. H., Ed.; Wiley: New York, 1998.
(554) Foss, C. A., Jr. In *Metal Nanoparticles: Synthesis, Characterization, and Applications*; Feldheim, D. L., Foss, C. A., Jr., Eds.; Dekker: New York, 2001.
(555) Bronstein, L. M. *Top. Curr. Chem.* **2003**, *226*, 55.
(556) Ichikawa, M. *Metal Clusters in Chemistry*; 1999; p 1273.
(557) Wang, Y.; Bryan, C.; Xu, H.; Pohl, P.; Yang, Y.; Brinker, C. J. *J. Colloid Interface Sci.* **2002**, *254*, 23.
(558) Ying, J. Y.; Mehert, C. P.; Wong, M. S. *Angew. Chem., Int. Ed. Engl.* **1999**, *38*, 56.
(559) Morey, M. S.; Bryan, J. D.; Schartz, S.; Stucky, G. D. *Chem. Mater.* **2000**, *12*, 3435.
(560) Moller, K.; Bein, T. *Chem. Mater.* **1998**, *10*, 2950.
(561) Mehnert, C. P.; Weaver, D. W.; Ying, J. Y. *J. Am. Chem. Soc.* **1998**, *120*, 12289.
(562) Cepak, V. M.; Martin, C. R. *J. Phys. Chem. B* **1998**, *102*, 9985.
(563) Bronstein, L. M.; Polarz, S.; Smarsly, B.; Antonietti, M. *Adv. Mater. (Weinheim, Ger.)* **2001**, *13*, 1333.
(564) Lensveld, D. J.; Mesu, J. G.; van Dillen, A. J.; de Jong, K. P. *Stud. Surf. Sci. Catal.* **2002**, *143*, 647.
(565) Lakshmi, B. B.; Dorhout, P. K.; Martin, C. R. *Chem. Mater.* **1997**, *9*, 857.
(566) Mohanty, P.; Ram, S. *J. Eur. Ceram. Soc.* **2002**, *22*, 933.
(567) Hoh, J. C.; Yaacob, I. I. *J. Mater. Res.* **2002**, *17*, 3105.
(568) Ding, J. H.; Gin, D. L. *Chem. Mater.* **2000**, *12*, 22.
(569) Kim, M.; Sohn, K.; Na, H. B.; Hyeon, T. *Nano Lett.* **2002**, *2*, 1383.
(570) McHenry, M. E.; Subramoney, S. In *Fullerenes: Chemistry, Physics, and Technology*; Kadish, K. M., Ruoff, R. S., Eds.; Wiley: New York, 2000.
(571) Wu, H.-Q.; Wei, X.-W.; Shao, M.-W.; Gu, J.-S.; Qu, M.-Z. *Chem. Phys. Lett.* **2002**, *364*, 152.
(572) Wu, H.-Q.; Wei, X.-W.; Shao, M.-W.; Gu, J.-S.; Qu, M.-Z. *J. Mater. Chem.* **2002**, *12*, 1919.
(573) Yang, B.; Wu, Y.; Zong, B.; Shen, Z. *Nano Lett.* **2002**, *2*, 751.
(574) Meldrum, F. C.; Wade, V. J.; Nimmo, D. L.; Heywood, B. R.; Mann, S. *Nature* **1991**, *349*, 684.
(575) Douglas, T.; Young, M. *Nature* **1998**, *393*, 152.
(576) Douglas, T.; Strable, E.; Willits, D.; Aitouchen, A.; Libera, M.; Young, M. *Adv. Mater. (Weinheim, Ger.)* **2002**, *14*, 415.
(577) Mirkin, C. A.; Letsinger, R. L.; Mucic, R. C.; Storhoff, J. J. *Nature* **1996**, *382*, 607.
(578) Loweth, C. J.; Caldwell, W. B.; Peng, X.; Alivisatos, A. P.; Schultz, P. G. *Angew. Chem., Int. Ed. Engl.* **1999**, *38*, 1808.
(579) Braun, E.; Eichen, Y.; Sivan, U.; Ben-Yoseph, G. *Nature* **1998**, *391*, 775.
(580) Lee, S.-W.; Mao, C.; Flynn, C. E.; Belcher, A. M. *Science* **2002**, *296*, 892.
(581) Mucic, R. C.; Storhoff, J. J.; Mirkin, C. A.; Letsinger, R. L. *J. Am. Chem. Soc.* **1998**, *120*, 12674.
(582) Bashir, R. *Superlattices Microstruct.* **2001**, *29*, 1.
(583) Storhoff, J. J.; Mirkin, C. A. *Chem. Rev.* **1999**, *99*, 1849.
(584) Douglas, T. In *Biomimetic Materials Chemistry*; Mann, S., Ed.; Wiley: New York, 1996.
(585) Seidel, R.; Michael, M.; Pompe, W. *Surf. Interface Anal.* **2002**, *33*, 151.
(586) Dujardin, E.; Peet, C.; Stubbs, G.; Culver, J. N.; Mann, S. *Nano Lett.* **2003**, *3*, 413.
(587) Zhang, C.; Vali, H.; Romanek, C. S.; Phelps, T. J.; Liu, S. *Am. Mineral.* **1998**, *83*, 1409.
(588) Zhang, C.; Liu, S.; Logan, J.; Mazumder, R.; Phelps, T. J. *Appl. Biochem. Biotechnol.* **1996**, *57*−*58*, 923.
(589) Zhang, C.; Liu, S.; Phelps, T. J.; Cole, D. R.; Horita, J.; Fortier, S. M.; Elless, M.; Valley, H. W. *Geochim. Cosmochim. Acta* **1997**, *61*, 4621.

(590) Roh, Y.; Liu, S. V.; Li, G.; Huang, H. H.; Phelps, T. J.; Zhou, J. *Appl. Environ. Microbiol.* **2002**, *68*, 6013.
(591) Roh, Y.; Lauf, R. J.; McMillan, A. D.; Zhang, C.; Rawn, C. J.; Bai, J.; Phelps, T. J. *Solid State Commun.* **2001**, *118*, 529.
(592) Lauf, R. J.; Phelps, T. J.; Zhang, C.; Roh, Y. Ut-Battelle, LLC: United States, 2002.
(593) Lovley, D. R. *Annu. Rev. Microbiol.* **1993**, *47*, 263.
(594) McInnes, B. I. A.; Dunn, C. E.; Cameron, E. M.; Kameko, L. *J. Geochem. Explor.* **1996**, *57*, 227.
(595) Gardea-Torresdey, J. L.; Parson, J. G.; Gomez, E.; Peralta-Videa; Troiani, H. E.; Santiago, P.; Yacaman, M. J. *Nano Lett.* **2002**, *2*, 397.
(596) Evans, D. F.; Wennerstrom, H. *The Colloidal Domain, where Physics, Chemistry and Biology Meet*; VCH: New York, 1999.
(597) Grosso, D.; Sermon, P. A. *J. Mater. Chem.* **2000**, *10*, 359.
(598) Pelet, S.; Gratzel, M.; Moser, J.-E. *J. Phys. Chem. B* **2003**, *107*, 3215.
(599) Marquez, M.; Robinson, J.; Van Nostrand, V.; Schaefer, D.; Ryzhkov, L. R.; Lowe, W.; Suib, S. L. *Chem. Mater.* **2002**, *14*, 1493.
(600) Aquino, R.; Tourinho, F. A.; Itri, R.; Lara, M. C. F. L.; Depeyrot, J. *J. Magn. Magn. Mater.* **2002**, *252*, 23.
(601) McKenzie, K. J.; Marken, F. *Pure Appl. Chem.* **2001**, *73*, 1885.
(602) Xu, X.; Friedman, G.; Humfeld, K. D.; Majetich, S. A.; Asher, S. A. *Chem. Mater.* **2002**, *14*, 1249.
(603) Kang, Y. S.; Risbud, S.; Rabolt, J. F.; Stroeve, P. *Chem. Mater.* **1996**, *8*, 2209.
(604) Babes, L.; Denizot, B.; Tanguy, G.; Le Jeune, J. J.; Jallet, P. *J. Colloid Interface Sci.* **1999**, *212*, 474.
(605) Zaitsev, V. S.; Filimonov, D. S.; Gambino, R. J.; Chu, B. *J. Colloid Interface Sci.* **1999**, *212*, 49.
(606) Kim, D.-K.; Mikhailova, M.; Zhang, Y.; Muhammed, M. *Chem. Mater.* **2003**, *15*, 1617.
(607) Sauzedde, F.; Elaissari, A.; Pichot, C. *Colloid Polym. Sci.* **1999**, *277*, 846.
(608) Sousa, M. H.; Tourinho, F. A.; Depeyrot, J.; da Silva, G. J.; Lara, M. C. F. L. *J. Phys. Chem. B* **2001**, *105*, 1168.
(609) Meulenkamp, E. A. *J. Phys. Chem. B* **1998**, *102*, 5566.
(610) Rogach, A. L.; Nagesha, D.; Ostrander, J. W.; Giersig, M.; Kotov, N. A. *Chem. Mater.* **2000**, *12*, 2676.
(611) Broussous, L.; Santilli, C. V.; Pulcinelli, S. H.; Craievich, A. F. *J. Phys. Chem. B* **2002**, *106*, 2855.
(612) Van der Zande, B. M. I.; Dhont, J. K. G.; Bohmer, M. R.; Philipse, A. P. *Langmuir* **2000**, *16*, 459.
(613) Spalla, O.; Kekicheff, P. *J. Colloid Interface Sci.* **1997**, *192*, 43.
(614) Trentler, T. J.; Denler, T. E.; Bertone, J. F.; Agrawal, A.; Colvin, V. L. *J. Am. Chem. Soc.* **1999**, *121*, 1613.
(615) Shafi, K. V. P. M.; Ulman, A.; Yan, X.; Yang, N.-L.; Estournes, C.; White, H.; Rafailovich, M. *Langmuir* **2001**, *17*, 5093.
(616) Hyeon, T.; Lee, S. S.; Park, J.; Chung, Y.; Na, H. B. *J. Am. Chem. Soc.* **2001**, *123*, 12798.
(617) Bourlinos, A. B.; Simopoulos, A.; Petridis, D. *Chem. Mater.* **2002**, *14*, 899.
(618) Wang, Y.; Teng, X.; Wang, J.-S.; Yang, H. *Nano Lett.* **2003**, *3*, 789.
(619) Boal, A. K.; Das, K.; Gray, M.; Rotello, V. M. *Chem. Mater.* **2002**, *14*, 2628.
(620) Perales-Perez, O.; Sasaki, H.; Kasuya, A.; Jeyadevan, B.; Tohji, K.; Hihara, T.; Sumiyama, K. *J. Appl. Phys.* **2002**, *91*.
(621) Wong, E. M.; Hoertz, P. G.; Liang, C. J.; Shi, B.-M.; Meyer, G. J.; Searson, P. C. *Langmuir* **2001**, *17*, 8362.
(622) Qu, L.; Peng, X. *J. Am. Chem. Soc.* **2002**, *124*, 2049.
(623) Milliron, D. J.; Alivisatos, A. P.; Pitois, C.; Edder, C.; Fréchet, M. J. *Adv. Mater. (Weinheim, Ger.)* **2003**, *15*, 58.
(624) Wakefield, G.; Keron, H. A.; Dobson, P. J.; Hitchison, J. L. *J. Colloid Interface Sci.* **1999**, *215*, 179.
(625) Roberts, D.; Zhu, W. L.; Frommen, C. M.; Rosenzweig, Z. *J. Appl. Phys.* **2000**, *87*, 6208.
(626) Rajamathi, M.; Ghosh, M.; Seshadri, R. *Chem. Commun.* **2002**, 1152.
(627) Seo, W. S.; Jo, H. H.; Lee, K. M.; Park, J. T. *Adv. Mater. (Weinheim, Ger.)* **2003**, *15*, 795.
(628) Chen, S.; Huang, K.-C.; Stearns, J. A. *Chem. Mater.* **2000**, *12*, 540.
(629) Thomas, P. J.; Kulkarni, G. U.; Rao, C. N. R. *J. Phys. Chem. B* **2000**, *104*, 8138.
(630) Herron, N.; Calabrese, J. C.; Farneth, W. e.; Wang, Y. *Science* **1993**, *259*, 1426.
(631) Maye, M. M.; Zheng, W.; Leibowitz, F. L.; Ly, N. K.; Zhong, C.-J. *Langmuir* **2000**, *16*, 490.
(632) Maye, M. M.; Zhong, C.-J. *J. Mater. Chem.* **2000**, *10*, 1895.
(633) Krautscheid, H.; Fenske, D.; Baum, G.; Semmelmann, M. *Angew. Chem., Int. Ed.* **1993**, *32*, 1303.
(634) Schreder, B.; Schmidt, T.; Ptatschek, V.; Winkler, U.; Materny, A.; Umbach, E.; Lerch, M.; Muller, G.; Kiefer, W.; Spanhel, L. *J. Phys. Chem. B* **2000**, *104*, 1677.
(635) Nesterova, M.; Moreau, J.; Banfield, J. F. *Geochim. Cosmochim. Acta* **2003**, *67*, 1177.
(636) Nesterova, M. V.; Walton, S. A.; Webb, J. *J. Inorg. Biochem.* **2000**, *79*, 109.
(637) Shen, F.; Poncet-Legrand, C.; Somers, S.; Slade, A.; Yip, C.; Duft, A. M.; Winnik, F. M.; Chang, P. L. *Biotechnol. Bioeng.* **2003**, *83*, 282.
(638) Kroll, E.; Winnik, F. M.; Ziolo, R. F. *Chem. Mater.* **1996**, *8*, 1594.
(639) del Barco, E.; Asenjo, J.; Zhang, X. X.; Pieczynksi, R.; Julia, A.; Tejada, J.; Ziolo, R. F.; Fiorani, D.; Testa, A. M. *Chem. Mater.* **2001**, *13*, 1487.
(640) Llanes, F.; Diaz, C.; Ryan, H.; Marchessault, R. H. *Int. J. Polym. Mater.* **2002**, *51*, 537.
(641) Yokoi, H.; Yagishita, K.; Nakanishi, Y. *Bull. Chem. Soc. Jpn.* **1990**, *63*, 746.
(642) Skoutelas, A. P.; Karakassides, M. A.; Petridis, D. *Chem. Mater.* **1999**, *11*, 2754.
(643) Mykhaylyk, O.; Cherchenko, A.; Ilkin, A.; Dudchenko, N.; Ruditsa, V.; Novoseletz, M.; Zozulya, Y. *J. Magn. Magn. Mater.* **2001**, *225*, 241.
(644) Alexiou, C.; Arnold, W.; Hulin, P.; Klein, R. J.; Renz, H.; Parak, F. G.; Bergemann, C.; Lubbe, A. S. *J. Magn. Magn. Mater.* **2001**, *225*, 187.
(645) Papisov, M. I.; Bogdanov, A., Jr.; Schaffer, B.; Nossiff, N.; Shen, T.; Weissleder, R. *J. Magn. Magn. Mater.* **1993**, *122*, 383.
(646) Dassenoy, F.; Casanove, M.-J.; Lecante, P.; Pan, C.; Philippot, K.; Amiens, C.; Chaudret, B. *Phys. Rev. B* **2001**, *63*, 235407.
(647) Guo, L.; Yang, S.; Yang, C.; Yu, P.; Wang, J.; Ge, W.; Wang, G. K. L. *Appl. Phys. Lett.* **2000**, *76*, 2901.
(648) Guo, L.; Yang, S.; Yang, C.; Yu, P.; Wang, J.; Ge, W.; Wang, G. K. L. *Chem. Mater.* **2000**, *12*, 2268.
(649) Teranishi, T.; Miyake, M. *Chem. Mater.* **1999**, *11*, 3414.
(650) Gaponik, N.; Radtchenko, I. L.; Gerstenberger, M. R.; Fedutik, Y. A.; Sukhorukov, G. B.; Rogach, A. L. *Nano Lett.* **2003**, *3*, 369.
(651) Modrow, H.; Bucher, S.; Hormes, J.; Brinkmann, R.; Bönnemann, H. *J. Phys. Chem. B* **2003**, *107*, 3684.
(652) Bradley, J. S.; Tesche, B.; Busser, W.; Maase, M.; Reetz, M. T. *J. Am. Chem. Soc.* **2000**, *122*, 4631.
(653) Rothe, J.; Hormes, J.; Bönnemann, H.; Brijoux, W.; Siepen, K. *J. Am. Chem. Soc.* **1998**, *120*, 6019.
(654) Bucher, S.; Hormes, J.; Modrow, H.; Brinkmann, R.; Waldofner, N.; Bönnemann, H.; Beuermann, L.; Krischok, S.; Maus-Friedrichs, W.; Kempter, V. *Surf. Sci. Ser.* **2002**, *497*, 321.
(655) Vogel, W.; Britz, P.; Bönnemann, H.; Rothe, J.; Hormes, J. *J. Phys. Chem. B* **1997**, *101*, 11029.
(656) Bönnemann, H.; Britz, P. *Langmuir* **1998**, *14*, 6654.
(657) Denizot, B.; Tanguy, G.; Hindre, F.; Remp, E.; Le Jeune, J. J.; Jallet, P. *J. Colloid Interface Sci.* **1999**, *209*, 66.
(658) Portet, D.; Denizot, B.; Rump, E.; Le Jeune, J. J.; Jallet, P. *J. Colloid Interface Sci.* **2001**, *238*, 37.
(659) Bourlinos, A. B.; Bakandritsos, A.; Georgakilas, V.; Petridis, D. *Chem. Mater.* **2002**, *14*, 3226.
(660) Strable, E.; Bulte, J. W. M.; Moskowitz, B.; Vivekanandan, K.; Allen, M.; Douglas, T. *Chem. Mater.* **2001**, *13*, 2201.
(661) Vossmeyer, T.; Reck, G.; Schulz, B.; Katsikas, L.; Weller, H. *J. Am. Chem. Soc.* **1995**, *117*, 12881.
(662) Vossmeyer, T.; Reck, G.; Katsikas, L.; Haupt, E. T. K.; Schulz, B.; Weller, H. *Science* **1995**, *267*, 1476.
(663) Tang, Z.; Kotov, N. A.; Giersig, M. *Science* **2002**, *297*, 237.
(664) Adachi, E. *Langmuir* **2000**, *16*, 6460.
(665) Wuelfing, W. P.; Gross, S. M.; Miles, D. T.; Murray, R. W. *J. Am. Chem. Soc.* **1998**, *120*, 12696.
(666) Foos, E. E.; Snow, A. W.; Twigg, M. E.; Ancona, M. G. *Chem. Mater.* **2002**, *14*, 2401.
(667) Brust, M.; Fink, J.; Bethell, D.; Schiffrin, D. J.; Kiely, C. *Chem. Commun.* **1995**, 1655.
(668) Templeton, A. C.; Hostetler, M. J.; Kraft, C. T.; Murray, R. W. *J. Am. Chem. Soc.* **1998**, *120*, 1906.

CR030027B